# JOURNAL OF APPLIED PHYSICS

Vol. 10, No. 5 MAY, 1939

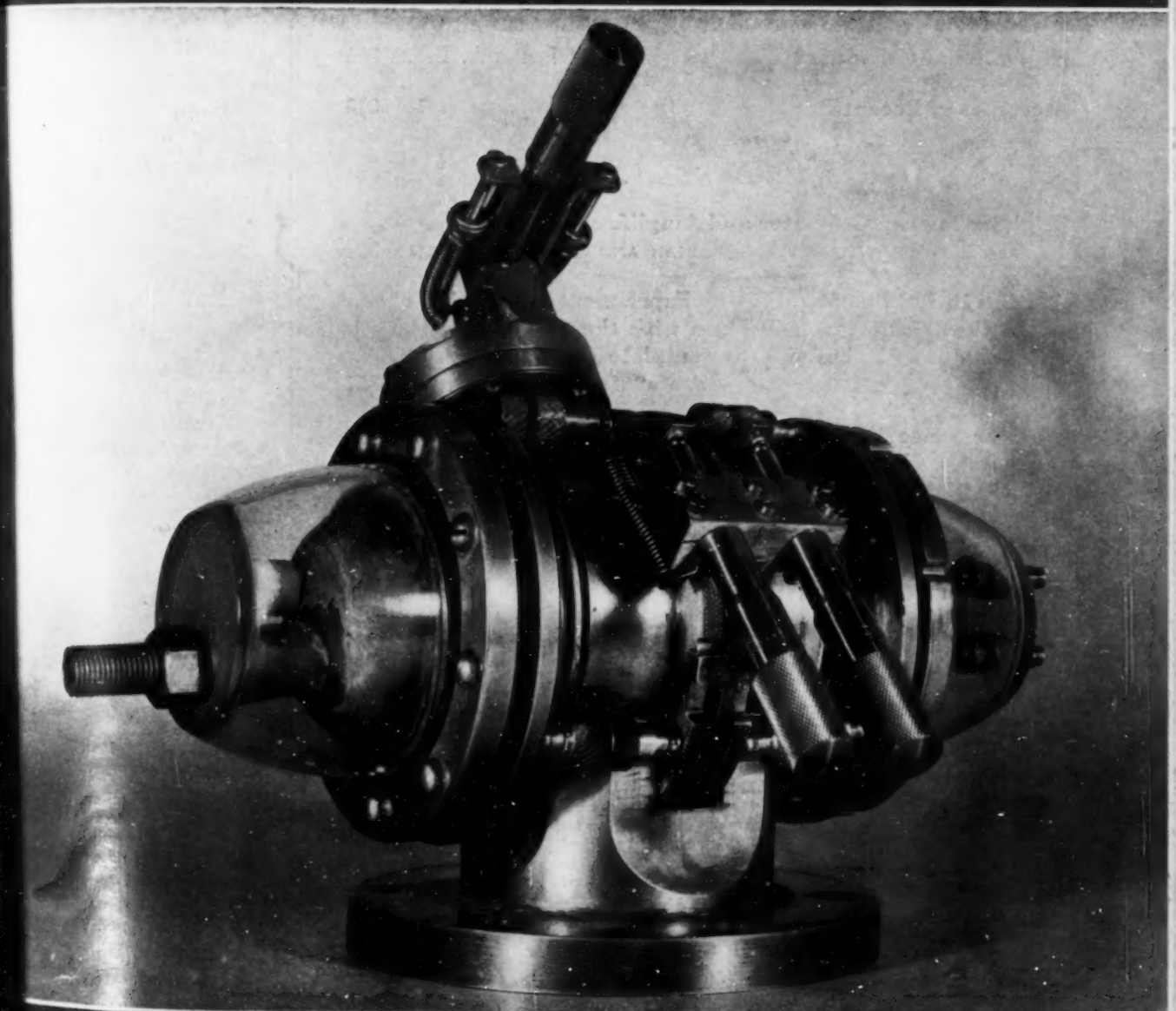

Recent Type High Frequency Oscillator

JOURNAL OF APPLIED
# PHYSICS

MAY, 1939 Vol. 10, No. 5

## *In This Issue*

*Page*

**New Frontiers for Industry** CARL BREER 271

**Review of the Photoelastic Method of Stress Analysis. II** RAYMOND D. MINDLIN 273

**Application of Hardening Resins in Three-Dimensional Photoelastic Studies** M. HETÉNYI 295

**Operational Calculus. III** LOUIS A. PIPES 301

**Resumés of Recent Research** 313

*Contributed Original Research*

**High Frequency Oscillator and Amplifier** RUSSELL H. VARIAN AND SIGURD F. VARIAN 321

**Studies in Lubrication. IV. The Experimental Variation of the Coefficient of Friction with the Strength of the Lubricant Source for a Complete Journal Bearing** F. MORGAN AND M. MUSKAT 327

**Luminescence During Intermittent Electron Bombardment** R. B. NELSON, R. P. JOHNSON AND W. B. NOTTINGHAM 335

*In Every Issue*

**New Books** 315

**Here and There** 317

**Contributors to this Issue** 320

**BOARD OF EDITORS**

ELMER HUTCHISSON, *Editor*

*Associate Editors*

F. BITTER
W. E. FORSYTHE
L. A. JONES
W. F. MEGGERS
B. E. WARREN
J. B. WHITEHEAD
V. K. ZWORYKIN

**Publication of the American Institute of Physics**

**ADMINISTRATIVE STAFF**

HENRY A. BARTON, *Director*

MADELINE M. MITCHELL, *Publications Manager*

WILLIAM C. COPP, *Advertising Manager*

**GOVERNING BOARD**

JOHN T. TATE, *Chairman*
KARL T. COMPTON
E. C. CRITTENDEN
WHEELER P. DAVEY
FLOYD A. FIRESTONE
HARVEY FLETCHER
ARTHUR C. HARDY
PAUL E. KLOPSTEG
MELVIN MOONEY
FREDERIC PALMER, JR.
R. L. PEEK, JR.
GEORGE B. PEGRAM
W. B. RAYTON
F. K. RICHTMYER
WALLACE WATERFALL

THE JOURNAL OF APPLIED PHYSICS, published monthly at Prince and Lemon Sts., Lancaster, Pa., is devoted to physics in its role as the science basic to other natural sciences and to the arts and industries. Previous to 1937 this publication was known as PHYSICS. It aims to be of service not only in physical laboratories, but also in the laboratories of industrial, chemical, geological, geophysical, meteorological, radio, and similar concerns. THE JOURNAL OF APPLIED PHYSICS publishes editorials, news of physicists and reviews, as well as technical papers of applied physics.

SUBSCRIPTION PRICE

| | U. S., POSS. AND CANADA | FOREIGN |
|---|---|---|
| To members of scientific societies | $5.00 | $5.70 |
| To all others | 7.00 | 7.70 |

**Manuscripts** should be submitted to Elmer Hutchisson, Editor, University of Pittsburgh, Pittsburgh, Pennsylvania.

**Changes of address,** proofs, and complaints of failure to receive the JOURNAL OF APPLIED PHYSICS should be addressed to the Publications Manager. New copies can be sent free only if notice of nondelivery is received within three months of date of issue.

**Subscriptions** and orders for back numbers should be addressed to Prince and Lemon Streets, Lancaster, Pa. or to the American Institute of Physics, 175 Fifth Avenue, New York, N. Y.

**Advertising rates** supplied on request. Orders, advertising copy and cuts should be sent to the American Institute of Physics.

Entered as second class matter at the Post Office at Lancaster, Pennsylvania, under the Act of March 3, 1897. Accepted for mailing at the special rate of postage provided for in the Act of February 28, 1925, authorized May 2, 1932.

Copyright 1939, by the American Institute of Physics.

Sample cup is quickly filled. Only a 5 ml sample of solution is necessary for accurate determinations.

Cup is easily placed in holder. Entire corner of the case swings out leaving holder and electrodes freely accessible.

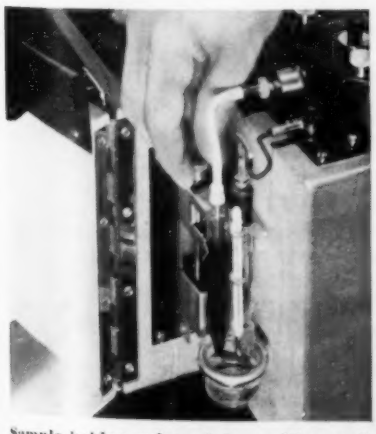

Sample holder swings into position and is raised to immerse electrode tips. Filling the cup, inserting it and immersing the electrodes takes but a few seconds.

# UNIVERSAL pH INDICATOR

## FAST—SIMPLE—EASY TO MANIPULATE

An assurance of accuracy which accompanies simple, straightforward operation comes to users of the Universal pH Indicator. The logical, well-marked sequence of manipulation is quickly learned. Knobs and switches are easily accessible. Measurements are made at maximum speed. Because operation is so easily understandable, the probability of errors arising from faulty manipulation is practically non-existent.

Standardizations and compensations are made individually . . . to a high degree of accuracy. They are quickly checked whenever desired.

Particularly convenient is the electrode compartment shown at the left. Sample cup and electrodes are freely accessible for cleaning and filling. Solution is easily agitated and equilibrium is quickly reached. Cup is positively positioned and cannot touch electrodes when they are properly installed.

Not only is the operator's time saved by speedy operation, but wastes arising from incorrect pH values are minimized.

*Write For Catalog E-96(1)*

Jrl Ad E-96(13)

LEEDS & NORTHRUP COMPANY, 4978 STENTON AVE., PHILA., PA.

LEEDS & NORTHRUP

**Measuring Instruments • Telemeters • Automatic Controls • Heat-Treating Furnaces**

*Have you received your copy?*

**CATALOG M138**

*describes our complete line of*

MEASURING MICROSCOPES
MICROMETER SLIDES
TELESCOPES
STANDARD SCALES
DIVIDING MACHINES
CATHETOMETERS
COMPARATORS, ETC.

*Sent on Request*

**THE GAERTNER SCIENTIFIC CORPORATION**

**1212 WRIGHTWOOD AVENUE, CHICAGO**

★ ★ ★ ★ ★ *A Record of Sustained Success* ★ ★ ★ ★ ★

**SMITH'S**

# ELEMENTS OF PHYSICS

By Alpheus W. Smith
Professor of Physics, Ohio State University

775 pages, 6 x 9, illustrated. $3.75

THE new fourth edition of this outstanding text shows a rapidly growing adoption record which again places it in the position of leadership it has held for so many years. Over sixty colleges and universities have adopted the text during the current school year. The following institutions are representative:

University of Cincinnati
Colorado State College
Connecticut State College
Dartmouth College
University of Kansas
Ohio State University
Purdue University
Rensselaer Polytechnic Institute
Tulane University
U. S. Military Academy
Virginia Polytechnic Institute
Yale University

*Send for copies on approval*

**McGRAW-HILL BOOK COMPANY, Inc.**

**330 West 42nd Street** **NEW YORK, N. Y.**

# EPPLEY THERMOPILES *for* RADIANT ENERGY MEASUREMENTS

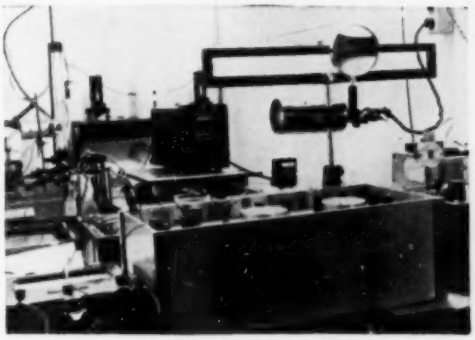

*A view of some of the apparatus used for calibrating thermopiles at the Eppley Laboratory, Inc.*

Adequate manufacturing, testing and calibrating equipment in the hands of our skilled and experienced technicians insures satisfaction to the users of Eppley Thermopiles.

We are prepared to furnish thermopiles of either bismuth-silver or copper-constantan, mounted in vacuum or air type cases. We also furnish thermopiles and mountings especially designed to meet individual needs. A card will bring you our Bulletin R–3 which contains illustrations, sample curves, complete descriptive matter, prices, references, etc., with regard to Eppley Thermopiles.

EPLAB

THE EPPLEY LABORATORY, INC.

SCIENTIFIC INSTRUMENTS

NEWPORT, R.I.

U.S.A.

# RCA 9-INCH *General Purpose* CATHODE-RAY OSCILLOGRAPH

TYPE 304-A

RCA has designed the type 304-A Cathode-Ray Oscillograph to meet the requirements of the experimental and research engineer for a high quality large screen oscillograph at a moderate price.

The trace is very sharp and permits fast photographic recordings of transients.

The deflection amplifiers are essentially flat over a frequency response range of from 4 cycles to 100,000 cycles and will faithfully reproduce square waves as low as 10 cycle frequency.

An additional amplifier is provided for modulation of the cathode beam from an external timing source, and provides a very convenient means for establishing a time constant of the trace.

# RCA HIGH GAIN *Low Frequency* PRE-AMPLIFIER

TYPE 9784

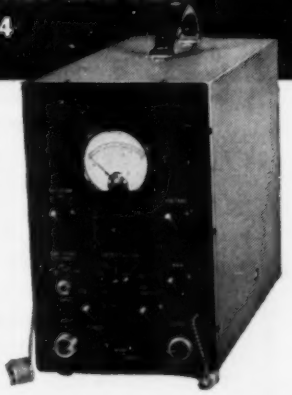

Here is an outstanding portable AC operated amplifier. It has a very high input resistance of 90 megohms, making it ideally suited for use with Piezo electric crystal generators and cathode-ray oscillographs.

**Use RCA Radio Tubes in test instruments for greatest precision.**

RCA

# PRECISION TEST EQUIPMENT

Engineering Products Division

RCA MANUFACTURING CO., INC., CAMDEN, N. J.

A Service of the Radio Corporation of America

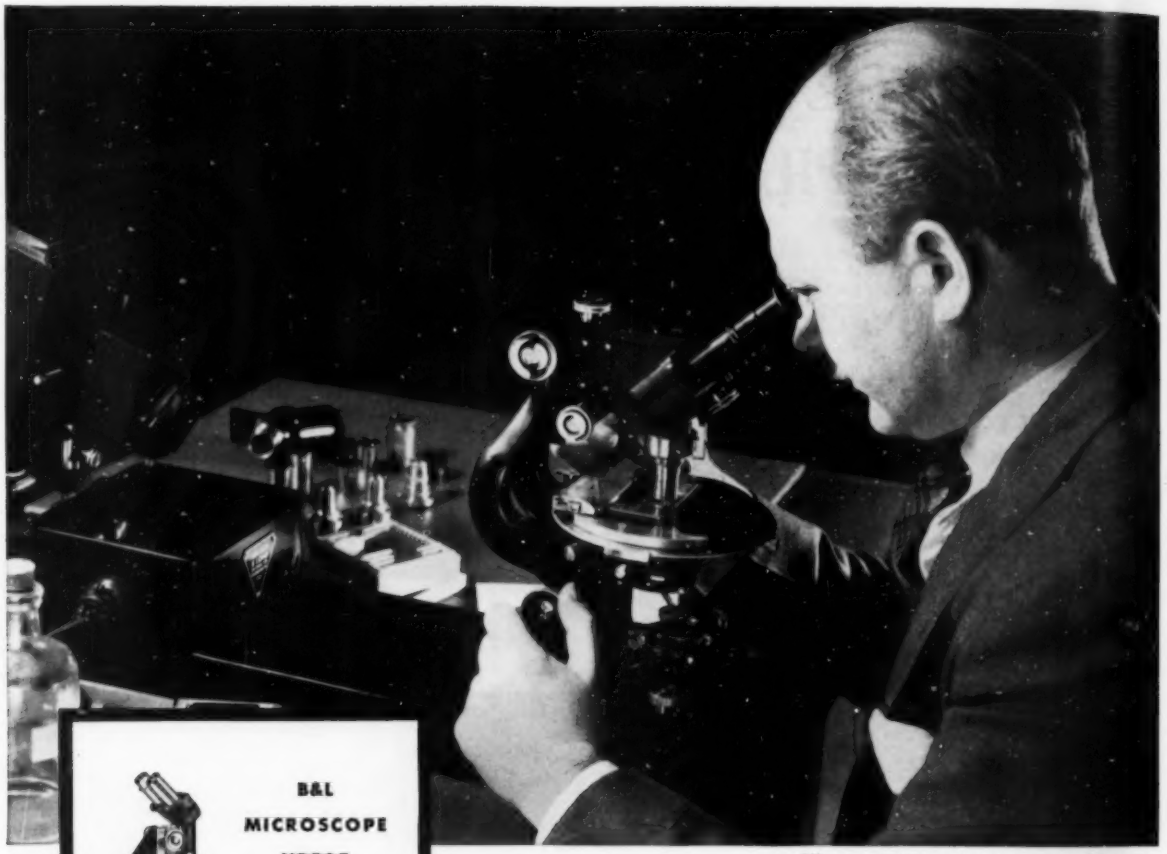

*Illustrated above—B&L Microscope DDE a complete research model for the most critical work.*

**B&L MICROSCOPE HREAT**

Stand—rigid, stable, and well balanced. Smooth and positive coarse adjustment. Ball-bearing fine adjustment ceases action upon touching cover glass. Dustproof nosepiece and objectives permanently centered and designed for maximum definition, resolution and color correction. Available with either Achromatic, Fluorite, or Apochromatic Objectives. Cone type eyepieces with high eyepoint, a feature valuable to wearers of glasses. Integral mechanical stage with long range. Rack and pinion substage, 1.25 Abbe condenser.

# *His Choice* WILL ALWAYS BE A B&L MICROSCOPE

He is dealing with an exact science, demanding the utmost in accuracy and precision. His instruments must meet these needs. That's why you will find B&L Microscopes in use in laboratories throughout the world.

Mechanically and optically, from stand to objectives, each B&L Microscope is designed and built to the highest standards. Whether the microscope is used visually or for photomicrography, the user is certain of the satisfaction that comes from work accurately done. As the demands of his work increase or as new methods of procedure are developed his B&L Microscope can always be adapted, through available accessories, to a broader field of usefulness.

Address inquiries to Bausch & Lomb Optical Co., 670 St. Paul St., Rochester, N. Y.

# BAUSCH & LOMB

FOR YOUR EYES, INSIST ON BAUSCH & LOMB EYEWEAR, MADE FROM BAUSCH & LOMB GLASS TO BAUSCH & LOMB HIGH STANDARDS OF PRECISION . . . . . .

HARVARD COLLEGE
MAY 2 1939
LIBRARY

Journal of Applied

Physics

Volume 10 May, 1939 Number 5

# New Frontiers for Industry*

BY CARL BREER

*Chrysler Corporation, Detroit, Michigan*

PROGRESS in any form of human endeavor depends largely on finding new things to do and the discovery of better ways of doing old things. The very word "research" implies not only a search for new things and new ways of doing them, but also a re-searching of old things and finding new uses and applications for them. This entails a constant re-examination of the old ways of doing the things we now do.

All progress—individual, corporate or national—is based upon the understanding of problems and, secondly, the solution of those problems. Among savage peoples and, indeed, in all simple societies, men have been content because their problems were few and elementary—and their progress was correspondingly slow. They used the old "hit or miss," "trial and error" methods of problem solution.

It has been the same in the business world. When business was simple there was not so much need of research, but today we see a society that has become complex—complex in its requirements, its mode of living, its needs and aspirations. So it is natural, and inescapable, that business, too, should have become complicated for it lives only by satisfying the multitudinous needs of today's complex society.

To meet the new demands made upon it, business must find new things to do and better ways of doing old things. It is senseless to continue doing old things in old ways in a world that demands new and better things. And to find the ways and means of doing these new things in the best possible manner is the essential function of research.

I have devoted my life to research. To me it is high adventure. All true research men find in their work the call, the lure and fascination to which, in other days, the pioneer responded. They must be dreamers, but their dreams must come true. To them the future and far-off horizons are still entrancing. Today many miss the thrill of the frontiersman because they mistake the frontiers. Geographical frontiers have almost vanished. You may regret that there are few new lands awaiting discovery, few shores unexplored, few hidden bays in which to drop anchor. But why worry! The early pioneer split rails. The modern pioneer splits molecules!

These new modern frontiers are not reached on foot, on horseback or in creaky old ships. They are sought by active, imaginative, inquiring minds, but, once found, they yield the same satisfying returns to our modern pioneer as the discovery of new and fertile lands gave to the geographical pioneer of former days.

No modern industry, or business, can survive or function efficiently—and certainly cannot hope to progress—without well organized and intelligently directed research. Examples by the score are all around you of the discovery of just one new law of physical science leading to the creation of a new industry or the revolutionizing of an old industry or product. And thousands or, perhaps, millions of others as yet unknown—

* Condensed from an address by Dr. Carl Breer at the National Association of Manufacturers' Congress of American Industry, December 8, 1938.

because they are beyond our present horizons—await our coming.

A common expression among executives is, "If we only had a financial endowment what a wonderful job we could do in the discovery and development of new things."

There was a time in our industry when we had that very viewpoint, but we soon found it was not money we needed primarily. In reality it was new ideas and men with ideas. An idea does not cost much to explore, and a valuable idea is not difficult to sell for development costs.

When bankers or investors look at industry, they are attracted by past and present performance, but in addition they want to know, and have a right to know, about futures. No progressive manufacturing industry can succeed unless it has futures in progress. The best investment in the future any enterprise can have is a good research organization.

In our yearly-cycle industry, success certainly depends upon futures. In your industry, in any industry, success depends upon futures. Why not stimulate futures? Open up the fields to men of imagination, guide them, become interested in what they have to offer, give them facilities to proceed and they will leave a wake behind them by which all mankind will benefit. By coordinated and organized effort new industries that we dare not even dream of today will be opened up. New industries cannot start without creating happiness, through the added employment and enjoyment they give to human beings.

With proper emphasis upon research the next century will be outstanding in its accomplishments. We know much about science, but what we now know compared to what remains to be learned is nothing. Research is not a complex thing. It is simply recognizing the fact that the universe itself is, so to speak, an engineered project and then attempting to understand and utilize as many of its fundamental laws as possible.

The laws are the same today as they were 10,000 years ago. We must simply try to learn more ways to use them. We must try to use some of the same ingenuity as the man who first made the wheel. All he did was to use existing materials and put them to use. We can still do that.

If you have a research program in your business, cooperate fully with the men who are carrying it on. If you do not have such a program, may I recommend that you move in that direction soon. Organize your research wisely, then stand back of it sympathetically, and if you are not in too much of a hurry for results, it will repay you handsomely in satisfaction, and in dollars and cents.

But lest I be misunderstood, let me add that there are two important, two essential factors necessary. These are interest and guidance on the part of management, and a reasonable investment. It will take some money, of course, yet more adventures in research have come to grief because of lack of interest on the part of management than because money was lacking.

But more important still it will take interest on the part of management to secure the right men. The genuine type of research mind is not common, but such minds do exist and *can* be found. It is management's responsibility.

In conclusion, research in industry is simply *search*, and then search some more, and, having done that, start searching all over again. In a changing world, a business cannot stand still. It either moves forward or backward. If we move by accident, by outside pressure, or by guess, our business is probably doomed to failure. But if by intelligent research we direct our products and our policies toward new horizons to meet the new services needed, our progress will be sure and sound.

# A Review of the Photoelastic Method of Stress Analysis. II*†

BY RAYMOND D. MINDLIN

*Department of Civil Engineering,*
*Columbia University, New York, New York*

## *Part IV. Independent Determination of the Principal Stresses*

### 20. METHODS FOR MEASURING PRINCIPAL STRESSES

THE techniques described in Section 15 make possible the determination of the directions of and the difference between the two principal stresses in the plane of the plate. As we have seen, at an unloaded boundary of the plate, the principal stresses normal to the boundary vanish, so that the information already obtained is sufficient to determine the principal stresses at the boundary *independently*. In many cases of engineering interest, the greatest stresses in the model and prototype occur at a free boundary and, since these stresses are the most important for a wide range of design problems, it is often unnecessary to proceed further with the investigation. However, there are also problems in which knowledge is required of the complete state of stress at points in the interior of the plate or at points along a loaded boundary. These requirements have led to the development or adaptation of the following methods for the independent determination of the principal stresses, which will be described in Sections 21 to 31.

1. Filon's graphical integration method.
2. Neuber's graphical method.
3. Lateral extensometer method.
4. Air-film interference method.
5. Stress concentration method.
6. Favre's interferometer method.
7. Fabry's interferometer method.
8. Hiltscher's converging light method.
9. Membrane method.
10. Electrical method.
11. Numerical method.

* Publication assisted by the Ernest Kempton Adams Fund for Physical Research of Columbia University.

† This is the last half of this paper. The first half appeared in the April issue.

### 21. FILON'S METHOD

A consideration of the equilibrium of a small curvilinear rectangle bounded by four nearby isostatics (Fig. 21.1) leads to the following two equations of equilibrium* which govern the variations of the principal stresses along the isostatics:

$$\left.\begin{aligned}\frac{\partial p}{\partial s_1} &= -\frac{p-q}{\rho_2}\\ \frac{\partial q}{\partial s_2} &= -\frac{p-q}{\rho_1}\end{aligned}\right\}, \tag{21.1}$$

in which $s_1$ and $s_2$ are orthogonal curvilinear coordinates measured along the $p$ and $q$ isostatics, respectively, while $\rho_1$ and $\rho_2$ are the respective radii of curvature of these isostatics (Fig. 21.1).

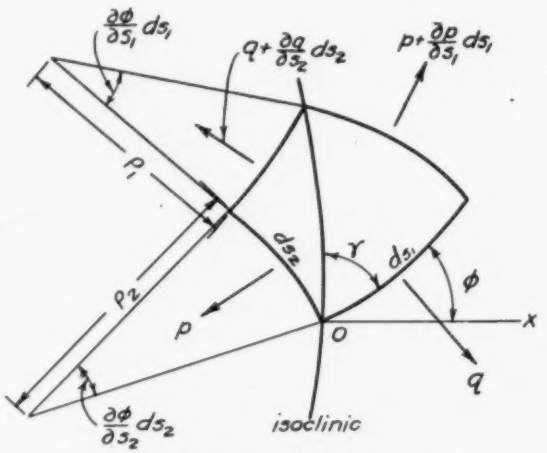


FIG. 21.1. Curvilinear rectangle bounded by four near isostatics.

Maxwell pointed out[104] that these equations, combined with a knowledge of the isochromatics and isostatics, are sufficient to determine the

* Coker and Filon, reference 5, p. 142.

values of $p$ and $q$ throughout the plate. The numerators of the right-hand sides of the equations are known from the measurement of relative phase retardation and the denominators can be measured from the isostatics. The equations can therefore be integrated graphically, starting from a point on the boundary where the stress is known. However, the form of Eqs. (21.1) is not conducive to accurate graphical manipulation on account of the difficulty of measuring $\rho_1$ and $\rho_2$ with any degree of precision.

Filon[55] has made the method practical by showing that the equations may be written in the form

$$\left.\begin{aligned} p &= p_0 + \int_{\phi_0}^{\phi} (p-q)\cot\gamma\, d\phi \\ q &= q_0 - \int_{\phi_0}^{\phi} (p-q)\cot\gamma\, d\phi \end{aligned}\right\}, \qquad (21.2)$$

in which $\gamma$ is the angle between the isoclinic and the isostatic $p$, as shown in Fig. 21.1; $\phi$ is, as before, the angle between the isostatic $p$ and an arbitrary $x$ direction; $p_0$ and $q_0$ are the known values of $p$ and $q$ at the starting point of the integration. The procedure is as follows: At a series of points $A_0, A_1, A_2, \cdots$ along an isostatic (say $p$, Fig. 21.2), the values of $(p-q)$, $\gamma$ and $\phi$ are determined by one of the methods described in Section 15. $(p-q)\cot\gamma$ is then plotted against $\phi$ as in Fig. 21.3. The area under the curve from $\phi_0$ to, say, $\phi_2$ is

$$\int_{\phi_0}^{\phi_2} (p-q)\cot\gamma\, d\phi$$

and this, added to the known value $p_0$ at $A_0$, is the stress $p$ at $A_2$. Since $p-q$ is known at $A_2$, $q$ is thus also determined. A similar procedure is followed for succeeding points and also for the isostatic $q$.

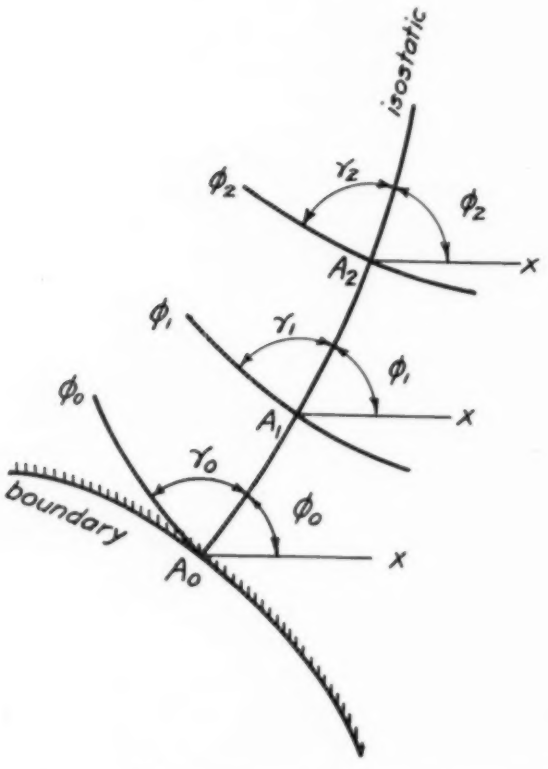


FIG. 21.2. Filon's integration method along an isostatic $p$.

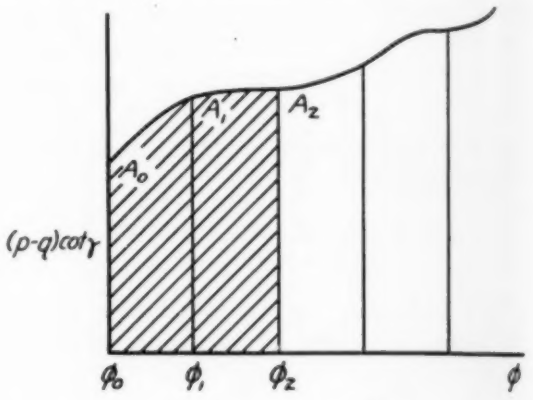


FIG. 21.3. Graphical integration of $\int_{\phi_0}^{\phi}(p-q)\cot\gamma d\phi$.

The inaccuracies of the method arise chiefly from the difficulty of precisely determining the angles $\phi$ and $\gamma$. These depend upon the isoclinic lines which are usually observed in the polariscope as broad, poorly defined bands.

Variations of the method suitable for special types of stress distributions have been devised by Filon,[5] Föppl,[61] Baud,[26] and Frocht.[69]

## 22. Neuber's Graphical Method

Still another variation of the form of Eqs. (21.1) has led Neuber[125] to a method for determining $p$ and $q$ by a graphical construction not involving integration. This method yields a family of curves, called isopachics, which

represent contours of constant $p+q$. The significance of the term isopachic will appear in the next section. Having $p+q$ and $p-q$ at any point, the values of $p$ and $q$ are obtained by addition and subtraction.

In Fig. 22.1, $O1$ and $O2$ represent the directions of the isostatics $p$ and $q$, respectively, through a point $O$. These are the same as the directions along which $ds_1$ and $ds_2$ are measured in Fig. 21.1. The direction of the isopachic line through $O$ is given by $O3$ and its normal by $O4$. The direction of the isochromatic through $O$ is $O5$ and its normal is $O6$. Finally, the direction $O7$ is that of the isoclinic through $O$ and $O8$ is its normal. As before, $\phi$ is the angle which the $p$ isostatic ($O1$) makes with the $x$ axis and $\gamma$ is the angle between the isoclinic and the isostatic $p$. In addition, $\xi$ and $\eta$ are the angles which the isopachic and the isochromatic, respectively, make with the isostatic $p$.

From Figs. 21.1 and 22.1 we find the following identities (letting $p+q=P$, and $p-q=Q$)

$$\frac{1}{\rho_1}=\frac{\partial\phi}{\partial s_1}=-\sin\gamma\frac{\partial\phi}{\partial s_8};\qquad \frac{\partial P}{\partial s_1}=-\sin\xi\frac{\partial P}{\partial s_4};$$

$$\frac{\partial Q}{\partial s_1}=-\sin\eta\frac{\partial Q}{\partial s_6}.$$

$$\frac{1}{\rho_2}=\frac{\partial\phi}{\partial s_2}=\cos\gamma\frac{\partial\phi}{\partial s_8};\qquad \frac{\partial P}{\partial s_2}=\cos\xi\frac{\partial P}{\partial s_4};$$

$$\frac{\partial Q}{\partial s_2}=\cos\eta\frac{\partial Q}{\partial s_6}.$$

Substituting these in Eqs. (21.1) there result

$$\left.\begin{aligned}\frac{\partial P}{\partial s_4}\sin\xi&=-\frac{\partial Q}{\partial s_6}\sin\eta+2Q\frac{\partial\phi}{\partial s_8}\cos\gamma\\ \frac{\partial P}{\partial s_4}\cos\xi&=\frac{\partial Q}{\partial s_6}\cos\eta+2Q\frac{\partial\phi}{\partial s_8}\sin\gamma\end{aligned}\right\},\qquad (22.1)$$

which are Neuber's forms of the equilibrium equations.

Let the stress increments of the successive orders of the isochromatics be $\Delta Q$ so that the parameters of the isochromatics are $Q=0$, $\Delta Q$, $2\Delta Q$, $\cdots$. The same stress increments will be taken for the successive orders of isopachics, so that $\Delta P=\Delta Q$. For the isoclinics, the successive parameters will be taken to differ by $\Delta\phi$. Let $a$ be the distance between two successive isopachics, $b$ that between two successive isochromatics, and $c$ that between two successive isoclinics, so that $a$, $b$ and $c$ are measured in the directions 4, 6 and 8, respectively. Then Eqs. (22.1) may be written in the approximate form

$$\left.\begin{aligned}\frac{\Delta P}{a}\sin\xi&=-\frac{\Delta Q}{b}\sin\eta+2Q\frac{\Delta\phi}{c}\cos\gamma\\ \frac{\Delta P}{a}\cos\xi&=\frac{\Delta Q}{b}\cos\eta+2Q\frac{\Delta\phi}{c}\sin\gamma\end{aligned}\right\}.\qquad (22.2)$$

All the quantities on the right of Eqs. (22.2) can be measured from the isoclinics, isochromatics and isostatics, and on the left $\Delta P$ is taken equal to $\Delta Q$. There are thus only two unknown quantities, $\xi$ and $a$, and two equations to determine

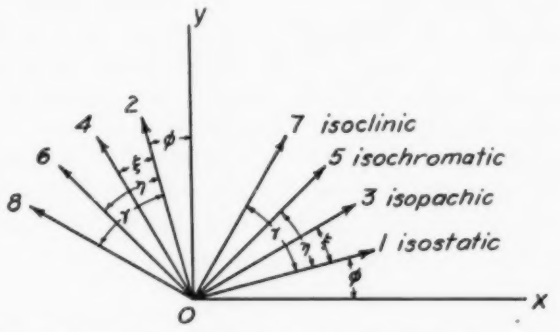


FIG. 22.1. Diagram used in explanation of Neuber's method.

them. The angle $\xi$ gives the direction of the isopachic at any point. Having these directions for many points throughout the plate, the isopachics may be constructed from them in the same manner as the isostatics are constructed from the isoclinics.

At a free boundary, $P=Q$, if the boundary is a line 1, and $P=-Q$ if the boundary is a line 2. Hence the *order* of an isopachic is determined by the order of the isochromatic which it meets at a free boundary. Neuber gives an alternative procedure when the isopachic does not intersect a boundary.

As in Filon's method, the accuracy of the construction depends upon the precision with which the angles $\phi$, $\gamma$ and $\eta$ can be measured.

## 23. Lateral Extensometer Method

Mesnager[106] observed that the strain in the direction of the normal to the plate is proportional to the sum of the principal stresses so that by measuring the change in thickness of the plate at any point, we may determine $p+q$ at that point. Since $p+q$ is constant along contours of constant thickness, the origin of Filon's term *isopachic*, meaning *same thickness*, is apparent.

If the plane of the plate is the $x,y$ plane, $\sigma_z$ vanishes and the strain in the direction of the plate normal becomes, from Eqs. (7.1), (10.7) and (10.8),

$$\epsilon_z = -(\nu/E)(p+q). \tag{23.1}$$

Taking $d$ as the thickness of the plate and $\Delta d$ as the change in thickness we have, therefore,

$$p+q = -\Delta d E/\nu d. \tag{23.2}$$

To obtain an idea of the magnitude of $\Delta d$, suppose the model is of Bakelite, for which we may take $E=600{,}000$ lb. per sq. in. and $\nu=0.24$. Further, let $p+q=1000$ lb. per sq. in. and $d=0.25$ in. Then $d=0.0001$ in. Hence we require an extensometer which will measure at least to a hundred-thousandth of an inch.

Mesnager designed an interferometer caliper for the measurement of $\Delta d$. It consists of a pair of bars, $AB$ and $CD$, Fig. 23.1, hinged together

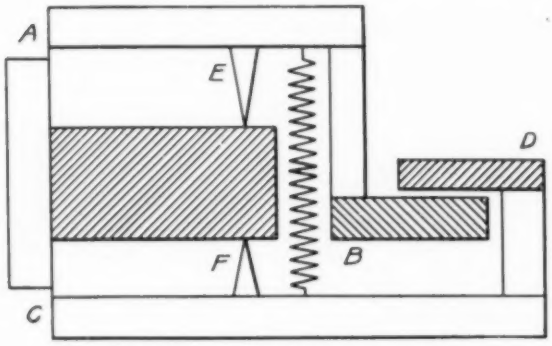


Fig. 23.1. Mesnager's interferometer caliper.

at the ends $A$ and $C$ with a flexible steel plate. A pair of contact points at the intermediate points $E$ and $F$ engage the model so that as the thickness of the model changes there is a somewhat magnified change in distance between the ends $B$ and $D$ of the bars. The relative motion is measured by observing the movement of interference fringes formed in the air film between a pair of optical flats fixed at $B$ and $D$. If the 5461A line of the mercury spectrum is used as a light source, a movement of one fringe corresponds to a displacement of 0.00001075 in.

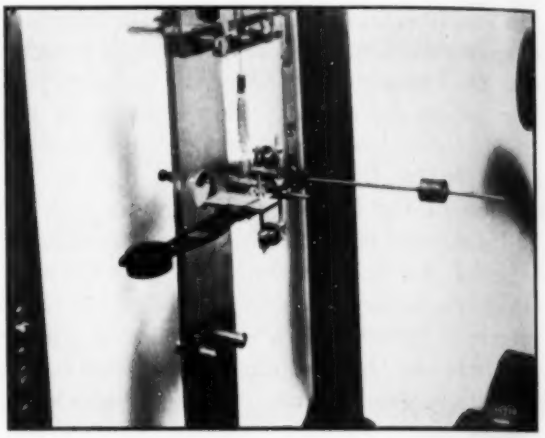

Fig. 23.2. Westinghouse lateral extensometer.

An instrument based on the same principle as Mesnager's but of improved design has been used by Vose.[175]

The Westinghouse Research Laboratory has adapted the Huggenberger tensometer to the measurement of $\Delta d$ as shown in Fig. 23.2.

In Coker's[45] lateral extensometer, Fig. 23.3, the gage points actuate a mechanical lever which, in turn, rotates a small concave mirror. The sweep of a beam of light reflected from the mirror is a measure of $\Delta d$. The instrument is mounted on a movable platform so that the changes in thickness all along a line in the plane of the model may be determined by traversing the line before and after loading. The three instruments previously mentioned have an advantage over Coker's extensometer in that their gage points move with the model as the latter deflects under load.

The $\Delta d$ method for determining $p+q$ is one of the best available in that (1) the measurements are independent of $p-q$ and $\phi$, (2) the measurement at one point of the model is made independently of the measurements at other points, (3) the apparatus is inexpensive.

## 24. Air-Film Interference Method

A procedure applied by Maris[101] involves the determination of $\Delta d$ by observing interference fringes in the thin air film formed between the

surface of the model itself and an auxiliary optical flat. The method has been further developed by Tesař[157] and Frocht[66, 70] so that the entire field of the isopachic contours may be viewed or photographed.

Since the interference fringes are loci of points of constant air film thickness, they will also be loci of points of constant model thickness if the auxiliary optical flat is properly oriented with

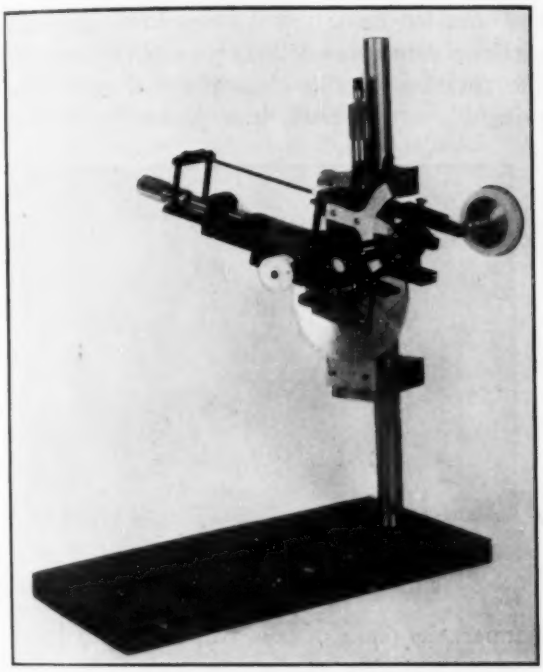

FIG. 23.3. Coker's lateral extensometer.

respect to the model. Successive fringe orders will then represent isopachic contours of equal increments of $p+q$.

Regarding the proper orientation of the auxiliary flat with respect to the model, Tesař[157] has described the following procedure. Three points, not on the same straight line, are chosen on free boundaries of the model. The values $(Q_1, Q_2, Q_3)$ of $p-q$ at these points are known from the isochromatics so that the values $(P_1, P_2, P_3)$ of $p+q$ are also known at the same points. The auxiliary flat is then adjusted so that the orders of the isopachics at the three points are in the ratio $P_1 : P_2 : P_3 = Q_1 : Q_2 : Q_3$, proper consideration being given to algebraic sign as explained in Section 15. This procedure can be used when the surface of the model is so well polished that, when the model is not loaded, the surface is flat to a degree commensurate with the least error desired in the $\Delta d$ measurement. For models not so well polished, a preliminary set of fringes may be observed on the unloaded model to determine surface irregularities so that appropriate corrections may be applied to the isopachic fringes. Tesař also suggests making observations on both faces of the model. For each face the fringes determine the ordinates to the model surface with respect to a plane determined by three points on the edge. The relative orientation of the two reference planes is then determined from the known thickness changes at the three pairs of points.

The method involves an elaborate and delicate technique but it has the advantage that it gives a complete set of isopachic curves rather than point by point information.

## 25. Stress Concentration Method

This method, attributed to Tesař[10] and Baud[1] makes use of the Kirsch solution* for the stress concentration at a small hole in a uniform tension field. Referring to Fig. 25.1(a), if $p$ is the uniform tension in a plate far from the hole, the stresses at $A$ and $A'$ are $3p$ and at $B$ and $B'$ are $-p$. If on this stress field there is superposed a stress $q$ at right angles (Fig. 25.1(b)) the stresses at $A$ and $A'$ will be $P_M = 3p-q$ and $P_m = -p+3q$. $P_M$ and $P_m$ will be, respectively, the maximum and minimum stresses around the hole. Then

$$\left.\begin{aligned} p &= \tfrac{1}{8}(P_m + 3P_M) \\ q &= \tfrac{1}{8}(P_M + 3P_m) \end{aligned}\right\}. \qquad (25.1)$$

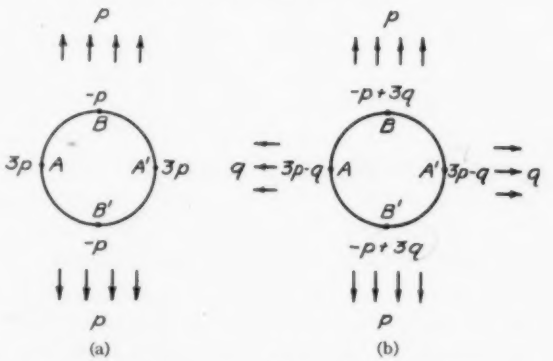


FIG. 25.1. Diagram used in explanation of stress concentration method.

* Coker and Filon, reference p. 5, p. 482.

To determine $p$ and $q$ at a point in a photoelastic plate it is proposed to drill a small hole at that point, determine $P_M$ and $P_m$ from the resulting isochromatics on the boundary of the hole (Fig. 16.1) and calculate $p$ and $q$ from Eqs. 25.1.

There are at least two difficulties involved in the method: (1) It does not seem likely that a small hole can be drilled without producing "edge effect;" (2) in the light of Vose's experiments (see Section 13) the values of $P_m$ and $P_M$ might not be reliable since the diameter of the hole would have to be of the same order of magnitude as the thickness of the plate.

## 26. Favre's Interferometer Method

As we have seen in Section 11, measurement of the absolute phase retardations of the waves polarized in the directions of $p$ and $q$ will give $p$ and $q$ directly. Favre[53, 54, 56] has designed an interferometer of the Mach-Zehnder type to effect the required measurements. In this instrument (Fig. 26.1) light from a source $S$ is polarized by a prism $P$ and is split into two rays, $T$ and $R$, by the half-silvered $M_1$. The transmitted ray ($T$) is reflected at the full-silvered mirror $M_2$, passes through the model $M$, and is reflected into a telescope by the half-silvered mirror, $M_3$. The other ray ($R$) is reflected at $M_4$, passes through $M_3$, and rejoins the first ray. A half-wave plate $H_1$ is used to rotate the plane of polarization so as to coincide with one or the other of the principal stress directions at a point in the model (which can be determined previously).

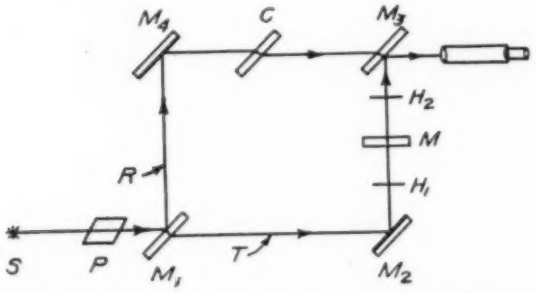


Fig. 26.1. Favre's interferometer-polariscope.

The second half-wave plate ($H_2$) rotates the plane of polarization back to its original position. A glass plate $C$ is rotated to bring the phases of the rays $T$ and $R$, traversing the separate paths, into coincidence when the model is not loaded. With the plane of polarization in the direction of, say, $p$, the model is loaded and the phase of the ray $T_p$ is altered with respect to that of the ray $R$ for two reasons. First, the index of refraction for a wave polarized in the direction of $p$ changes from $n_0$ to $n_1$ and, second, the thickness of the model changes by an amount $\Delta d$. The phase difference between $T_p$ and $R$ is then

$$\Delta_1=(2\pi/\lambda)[d(n_1-n_0)+(n_0-1)\Delta d], \quad (26.1)$$

the notation being the same as in the preceding sections. A measure of $\Delta_1$ is obtained by recording the rotation of the glass plate $C$ required to bring $T_p$ and $R$ back into phase. In the same

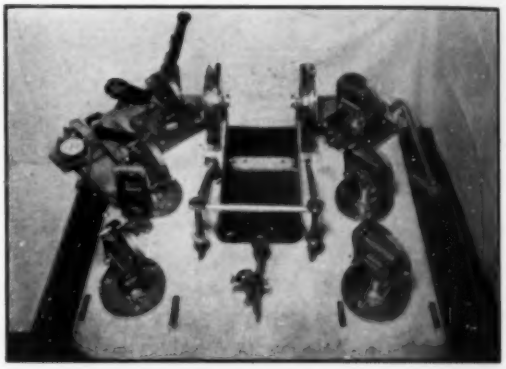

Fig. 26.2. Favre apparatus. (J. H. A. Brahtz, U. S. Bureau of Reclamation).

manner, the plane of polarization of $T$ is rotated so as to coincide with $q$ and we find another phase retardation, this time between $T_q$ and $R$ of magnitude

$$\Delta_2=(2\pi/\lambda)[d(n_2-n_0)+(n_0-1)\Delta d]. \quad (26.2)$$

Substituting into Eqs. (26.1) and (26.2) the values of $(n_1-n_0)$, $(n_2-n_0)$ and $\Delta d$ given in Eqs. (11.1) and (23.2), we find

$$\left.\begin{aligned}\Delta_1&=ad\,p+bd\,q\\ \Delta_2&=bd\,p+ad\,q\end{aligned}\right\}, \quad (26.3)$$

where

$$\left.\begin{aligned}a&=\frac{2\pi}{\lambda}\left[C_1-\frac{\nu}{E}(n_0'-1)\right]\\ b&=\frac{2\pi}{\lambda}\left[C_2-\frac{\nu}{E}(n_0-1)\right]\end{aligned}\right\}. \quad (26.4)$$

The constants $a$ and $b$ depend upon the model material and the wave-length of the light source,

and may be determined in terms of the angle of rotation of the glass plate $C$ by a simple tension experiment.

Hence, knowing $\Delta_1$, $\Delta_2$, $d$, $a$, $b$ in Eqs. (26.3), we may solve for $p$ and $q$. This procedure is carried out point by point over the entire plate. Very accurate measurements can be obtained by this method if (1) the model surfaces are accurately plane and parallel (glass is usually used), (2) the interferometer-polariscope and the loading device are well designed and constructed, proper precautions being taken especially to maintain constant temperature. A photograph of the Favre type instrument built at the photoelastic laboratory of the U. S. Bureau of Reclamation is shown in Fig. 26.2.

Tank[151] has suggested a procedure whereby Favre's interferometer may be used to measure $(p-q)$ and $(p+q)$ point by point.

## 27. Fabry's Interferometer Method

In this method,[52] the two faces of the model are half-silvered and are used as interferometer surfaces. Parallel light is passed through the model at normal incidence and the interference which takes place between rays transmitted directly through the plate and rays undergoing two reflections (Fig. 27.1) at the surfaces is observed through an analyzer. The light entering the loaded model is split into two waves, $p$ and $q$,

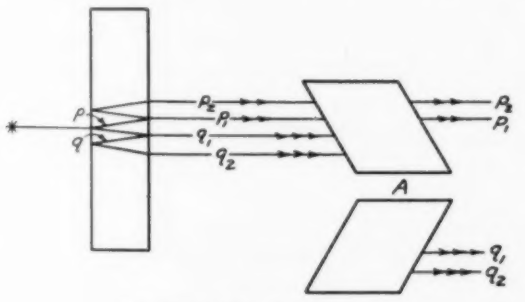


Fig. 27.1. Fabry's method.

plane polarized at right angles to each other. Each of these waves is partly transmitted ($p_1$ and $q_1$) and partly reflected ($p_2$ and $q_2$) at the second surface. The reflected waves ($p_2$ and $q_2$) undergo another reflection (at the first surface) and then pass out of the model in their original direction and through the analyzer with $p_1$ and $q_1$. By rotating the analyzer, one pair, say $q_1$ and

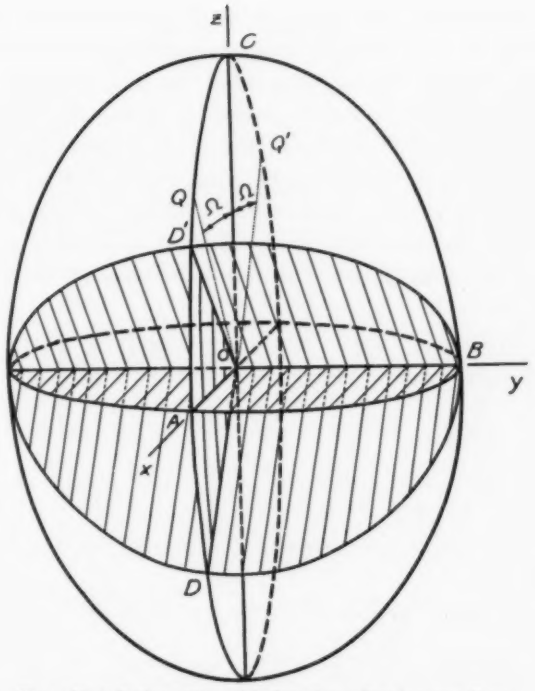


Fig. 28.1 Index ellipsoid showing circular sections.

$q_2$, may be extinguished, since they are both polarized at right angles to $p_1$ and $p_2$, and interference will be observed between $p_1$ and $p_2$ due to their path difference through the plate. By rotating the analyzer through 90°, interference will be observed between $q_1$ and $q_2$.

Again, this is necessarily a point by point method since the polarization directions of $p$ and $q$ vary over the model, and also the model surfaces must be accurately polished plane and parallel.

## 28. Hiltscher's Converging Light Method

Returning to our consideration of the index ellipsoid (Section 8 and Fig. 8.3), we observe that there are two planes $BOD$ and $BOD'$ in Fig. 28.1) containing the intermediate principal axis, $OB$, which intersect the ellipsoid in circles. The normals, $OQ$ and $OQ'$, to these planes are called the *optic axes* and the included angle, $2\Omega$, is the *optic axial angle*. When the differences between the principal refractive indices $n_a$, $n_b$, $n_c$ are small, as they are in photoelasticity, it may be shown, from the geometry of the ellipsoid that

$$\sin^2\Omega=\frac{n_a-n_b}{n_a-n_c},\quad \cos^2\Omega=\frac{n_b-n_c}{n_a-n_c}. \tag{28.1}$$

We also recall (Section 8) that any radius $ON$ (Fig. 8.3) represents a possible direction for the wave normal and that the plane through $O$ perpendicular to $ON$ intersects the ellipsoid in an ellipse $DE$ whose semi-axes $OD$ and $OE$ are proportional to the indices of refraction $n_1$ and $n_2$ of the two waves traveling through the doubly refracting medium. Now, if $\theta_1$ (Fig. 8.3) is the angle between the wave normal and the optic axis $OQ$, and if $\theta_2$ is the angle between the wave normal and the optic axis $OQ'$, it may be shown, from the geometry of the ellipsoid that

$$n_1-n_2=(n_a-n_c)\sin\theta_1\sin\theta_2 \qquad (28.2)$$

when the differences between the principal indices are small.

Now, from Eq. (9.1) we find

$$\left.\begin{aligned} n_c-n_a&=C(\sigma_3-\sigma_1)\\ n_a-n_b&=C(\sigma_1-\sigma_2)\\ n_b-n_c&=C(\sigma_2-\sigma_3)\end{aligned}\right\}, \qquad (28.3)$$

so that, combining Eqs. (28.1), (28.2), (28.3), and (8.2), there results

$$\left.\begin{aligned} \sigma_3-\sigma_1&=\frac{\lambda\Delta}{2\pi dC}\frac{1}{\sin\theta_1\sin\theta_2},\\ \sigma_2-\sigma_1&=\frac{\lambda\Delta}{2\pi dC}\frac{\sin^2\Omega}{\sin\theta_1\sin\theta_2},\\ \sigma_3-\sigma_1&=\frac{\lambda\Delta}{2\pi dC}\frac{\cos^2\Omega}{\sin\theta_1\sin\theta_2},\end{aligned}\right\} \qquad (28.4)$$

We have already seen how to measure all of the quantities on the right of Eqs. (28.4) excepting $\Omega$, $\theta_1$ and $\theta_2$. Hence, if we can measure these three angles, we can determine the three principal stress differences. Further, since at least one of the three principal stresses is zero at any point in a two-dimensional stress system, the other two can then be determined directly from Eqs. (28.4).

Hiltscher[81] has measured $\Omega$, $\theta_1$ and $\theta_2$ by means of converging polarized light, a technique widely used by petrologists* for determining the corresponding information for natural crystals.

Another technique which might also be adapted involves the use of the universal rotating stage.**

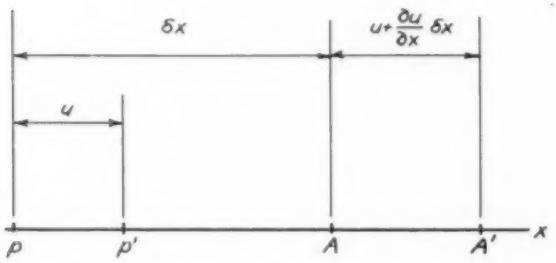


FIG. 29.1. Strain and displacement along the $x$ axis.

## 29. MEMBRANE METHOD

Consider a small strain $\epsilon_x$ in a line segment $PA$ (Fig. 29.1) of length $\delta x$ parallel to the $x$ axis. The displacement of $P$ to $P'$ is $u$ and the displacement of $A$ to $A'$ is $u+(\partial u/\partial x)\delta x$. Hence the strain of $PA$ is

$$\epsilon_x=\frac{P'A'-PA}{PA}$$

$$=\frac{[(\delta x-u)+(u+(\partial u/\partial x)\delta x)]-\delta x}{\delta x}=\frac{\partial u}{\partial x}. \qquad (29.1)$$

Similarly, the strain $\epsilon_y$ parallel to the $y$ axis is

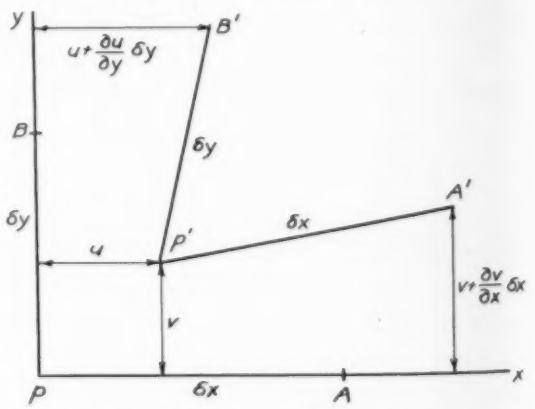


FIG. 29.2. Shearing strain in the $x,y$ plane.

expressed in terms of the displacement $v$ in the $y$ direction by

$$\epsilon_y=\partial v/\partial y. \qquad (29.2)$$

To determine the corresponding relations for

* A. Johannsen, *Manual of Petrographic Methods*, Chapters 24 to 34.

** A. Johannsen, *Manual of Petrographic Methods*, Chapters 35, 36.

the shearing strain $\gamma_{xy}$ in the $x,y$ plane, consider the change in angle between adjacent edges $PA$ and $PB$ of an element in this plane (Fig. 29.2). $P$ is displaced to $P'$, $A$ to $A'$, and $B$ to $B'$. If the perpendicular distance from $P'$ to $PA$ is $v$, then, to a first approximation, the perpendicular distance from $A'$ to $PA$ is $v+(\partial v/\partial x)\delta x$. Hence, the sine of the angle between $P'A'$ and $PA$ is

$$\frac{(v+(\partial v/\partial x)\delta x)-v}{\delta x}=\frac{\partial v}{\partial x}$$

and, since the angle is small, $\partial v/\partial x$ represents the angle between $P'A'$ and $PA$. Similarly, $\partial u/\partial y$ is the angle between $P'B'$ and $PB$. The small shearing strain $\gamma_{xy}$ is the total change in angle between the two edges. Hence

$$\gamma_{xy}=\partial v/\partial x+\partial u/\partial y. \qquad (29.3)$$

It is apparent that, when the strain varies throughout the $x,y$ plane, the three strain components $\epsilon_x$, $\epsilon_y$ and $\gamma_{xy}$ are not independent quantities but are related through the two components of displacement $u$ and $v$. To find the relation, differentiate Eq. (29.1) twice with respect to $x$, Eq. (29.2) twice with respect to $y$, Eq. (29.3) once with respect to $x$ and once with respect to $y$, and add the results; obtaining

$$\partial^2\epsilon_x/\partial y^2+\partial^2\epsilon_y/\partial x^2=\partial^2\gamma_{xy}/\partial x\partial y. \qquad (29.4)$$

This is known as a compatibility equation and expresses the law which governs the permissible variations of the strain components throughout the plate to the end that the material remains geometrically continuous.

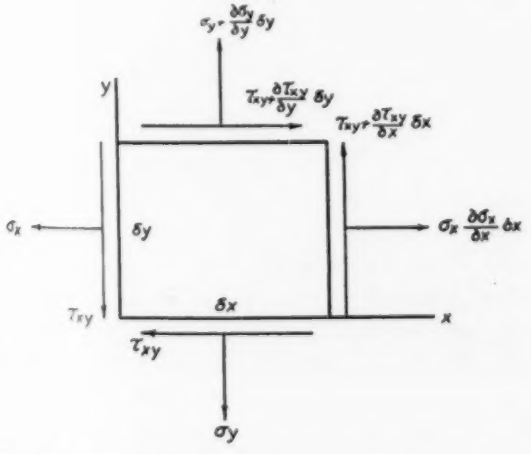


FIG. 29.3. Stresses acting on a rectangular element in the $x,y$ plane.

Consider, now, the laws which govern the variations of the stress components so that the forces on an element in the $x,y$ plane shall be in static equilibrium. Such an element, with the stresses acting on it, is shown in Fig. 29.3. Summing the forces in the $x$ and $y$ directions, we find the following equilibrium equations:

$$\left.\begin{aligned}\partial\sigma_x/\partial x+\partial\tau_{xy}/\partial y=0\\ \partial\sigma_y/\partial y+\partial\tau_{xy}/\partial x=0\end{aligned}\right\}. \qquad (29.5)$$

Differentiating the first of Eqs. (29.5) with respect to $x$ and the second with respect to $y$, and adding, we obtain

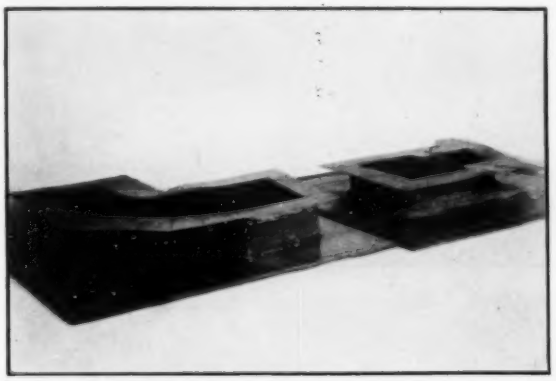

FIG. 29.4. Models used in membrane analogy (E. E. Weibel).

$$\partial^2\sigma_y/\partial y^2+\partial^2\sigma_x/\partial x^2+2\partial^2\tau_{xy}/\partial x\partial y=0. \qquad (29.6)$$

Now, the strains are related to the stresses through Hooke's law (Eq. 7.1). In the case of plane stress in the $x,y$ plane, we have

$$\left.\begin{aligned}E\epsilon_x=\sigma_x-\nu\sigma_y\\ E\epsilon_y=\sigma_y-\nu\sigma_x\\ E\gamma_{xy}=2(1+\nu)\tau_{xy}\end{aligned}\right\}. \qquad (29.7)$$

Substituting Eqs. (29.7) into (29.4) and using (29.6), we find

$$(\partial^2/\partial x^2+\partial^2/\partial y^2)(\sigma_x+\sigma_y)=0. \qquad (29.8)$$

Since, from Eqs. (10.7) and (10.8), $(\sigma_x+\sigma_y)=(p+q)$, we have, finally, Laplace's equation

$$(\partial^2/\partial x^2+\partial^2/\partial y^2)(p+q)=0 \qquad (29.9)$$

as the equation governing the variation of the sum of the principal stresses. Den Hartog,[50] Biot[31] and Biezeno and Koch[36] observed that Eq. (29.9) is the same as the equation governing the ordinates to the surface of a uniformly stretched membrane which is deflected a small amount by forces applied only at its boundaries. To make use of this analogy, a hole of the same shape as the boundary of the model is cut in a plate, and around the edge of the hole ordinates

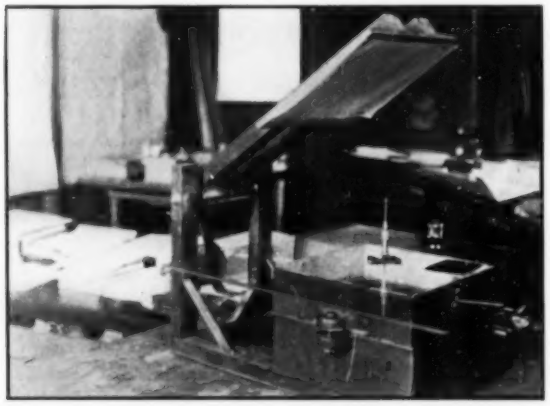

FIG. 29.5. Membrane analogy apparatus (University of Michigan).

are erected normal to the plate and proportional to $p+q$ at each point of the boundary. The membrane is stretched across the opening and is constrained to follow the boundary ordinates. The ordinate to any point of the membrane is then proportional to the magnitude of $p+q$ at that point.

The method is very easy to apply and is applicable to all regions in the neighborhood of boundaries along which $p+q$ can be previously determined. It has been applied with success by Weibel[177, 178] (see Figs. 29.4 and 29.5) using a soap film as the membrane, and by Biot and Smits,[35] and McGivern and Supper[121, 122] with a thin rubber sheet as the membrane. The method is necessarily limited to regions in the neighborhood of boundaries along which the stresses are completely known.

### 30. Electrical Method

If the boundary values of $p-q$ are known, Eq. (29.9) may be solved in other manners than the membrane method.

It is known, for example, that potential of a two-dimensional electric field is governed by the same equation. If, then, a metal plate is cut to the shape of the model and an electrical potential proportional to $p+q$ at each point is impressed along the boundary, the potential at any point in the interior of the plate will be proportional to $p+q$ at that point.

The method is described by Biezeno and Koch,[36] Biot,[31] Malavard,[100] and Meyer and Tank.[110]

### 31. Numerical Method

Liebmann[97] has shown that Laplace's equation may be solved for given boundary values by a process of successive numerical approximations. In this method, a network of rectangular lines is superposed on the region, and approximate values of $p+q$ are assigned to each point of intersection. Liebmann pointed out that the value of the function at any point should be equal to the average of the values at the four neighboring points. Hence, by repeatedly traversing the network, adjusting the value at each point with regard to the values at the four neighboring points, a set of values will be reached which fits the boundary values.

Shortley and Weller[142] have devised methods for greatly accelerating the convergence of the process.

## *Part V. Special Developments and Applications*

### 32. Goodier's Hydrodynamic Analogy

Goodier[73] has described a very complete analogy between the quantities observed in photoelasticity and those involved in the slow motion of a viscous fluid in two dimensions. The isopachic lines correspond to lines of constant fluid vorticity; the lines orthogonal to the isopachics correspond to lines of constant fluid pressure; the isochromatic lines correspond to lines of constant maximum rate of shearing strain (distortion) in the fluid; the isostatic network corresponds to lines showing the orientation of the elements having maximum distortion at points in the fluid. It seems possible that this analogy might form the basis of a method for solving fluid flow problems by the photoelastic method.

## 33. Biot's Gravitational and Thermal Analogies

Biot[32–34] has shown how the stresses due to gravitational loading or temperature variation can be analyzed photoelastically without actually reproducing the gravitational force or heating the model.

Stresses due to the weight of a large body may be calculated from the stresses produced in a small model of the same shape loaded on its boundaries by a normal pressure distribution varying linearly with the depth.

The stresses, due to a steady state of heat flow in a hollow cylinder, may be found from the stresses in a plate model by slitting the plate so as to connect the inner and outer boundaries and displacing or rotating the two edges of the slit (dislocation) by an amount which may be calculated. Weibel[179] has applied the method to various cross-sectional shapes (see Fig. 33.1).

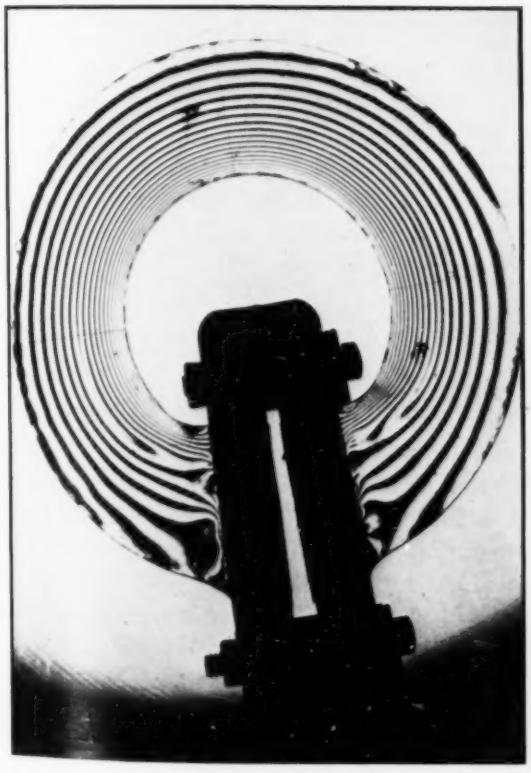

Fig. 33.1. Application of Biot's thermal stress analogy (E. E. Weibel).

Stresses in a solid cylinder due to a transient thermal state may be calculated from a plane model of the same shape as the cylinder cross section and loaded on the boundary. Biot and Smits[35] have applied this to the investigation of thermal and shrinkage stresses in a dam.

Stresses in a hollow cylinder due to a transient thermal state require a dislocation in addition to boundary loading.

## 34. Three-Dimensional Photoelasticity

In the preceding sections, photoelastic methods for analyzing two-dimensional stress systems have been described. The various techniques are not directly applicable to the analysis of three-dimensional distributions of stress because, in these, both the magnitudes and directions of the three principal stresses vary along the line of propagation of the light. Only integrated effects over the total path may be observed, whereas the optical properties of each element along the path are required. No analytical procedure for relating the integrated effects to the state of stress at an interior point has yet been evolved.

Favre[55] suggested observing the stress-optical effect on a small cube of photoelastic material embedded in a transparent model made of a material whose stress-optical coefficients are zero; but the experimental difficulties involved in the procedure seem insurmountable.

Mesnager[108] proposed a method applicable to a limited class of three-dimensional problems. The successful application of the method would lead to a determination of the "extreme fiber" stress produced in a plate by forces applied normal to the plane of the plate. The procedure begins with the coating of the polished surface of a metal plate with a thin layer of transparent material which becomes doubly refracting when strained. Bending of the plate out of its plane strains the coating so as to produce an essentially two-dimensional stress system, and the resulting double refraction is measured by analyzing light reflected from the polished metal surface. No successful application of the suggestion seems to have been made.

Timby and Hedrick[164] have proposed another technique for analyzing extreme fiber stresses. They suggest cementing to the surface of a transparent model a thin sheet of Polaroid. Over this is cemented a sheet of photoelastic material. Light emerging from the model passes through the Polaroid so that its ellipticity is annulled. Hence only plane polarized light passes through the outer layer of doubly refracting material. Observations on the emerging light then yield information on the two-dimensional state of stress in the outer layer.

In 1851 Maxwell[104] performed an experiment which has been developed, in the last few years, into a very promising three-dimensional method. Maxwell took a hollow cylinder of hot isinglass and rotated the inner surface of the cylinder, with respect to the outer surface, through a small angle about the axis of the cylinder. He allowed the isinglass to cool with the twisting couple still applied and observed that the resulting double refraction in the isinglass represented an *elastic* stress distribution. He was unable to explain the phenomenon and the matter was apparently ignored until 1935 when Solakian[145] heated a solid cylindrical bar of Marblette, applied a twisting couple about the axis of the bar, and allowed the material to cool with the couple still applied. He then cut out a slice perpendicular to the axis of the bar and examined the plate in a polariscope. However, the resulting fringe pattern did not correspond with the state of stress which is predicted by the St. Venant torsion theory, as was later pointed out by Hetényi.[77]

Oppel[128] made a similar experiment with a block of Trolon. He heated the block, pressed a metal sphere against it, and cooled the block under load. He observed that slices cut from the cooled block exhibited a fringe pattern corresponding to an elastic state of stress.

The recent experiments of Hetényi (see Section 12), and a discussion by Kuske[93] furnish an explanation of the phenomenon. At the elevated temperature, the elastic, infusible skeleton alone resists the applied forces. When the material is cooled under load, the fusible part freezes around the deformed skeleton and essentially maintains the deformation when the load is removed. The resulting material is thus in a state of deformation corresponding to the elastic state of stress at the elevated temperature. This state of stress is not seriously disturbed by careful slicing of the model because the equilibrium between the fusible and infusible parts exists over regions of molecular proportions. A difficulty in the procedure is that, while Young's modulus is diminished in the ratio of about 640 : 1 at the elevated temperature, the relative stress optical coefficient is increased only in the ratio of 26 : 1. Hence, the strain which must be applied to obtain high double refraction is so large as to change seriously the shape of the model.

The interpretation of the double refraction in the slice is rather more complicated than for two-dimensional stress systems. In general, a principal plane of optical symmetry does not coincide with the plane of the slice, so that the relative retardation is not a measure of a difference between principal indices of refraction, and is accordingly not proportional to a difference between principal stresses. The three principal stress differences may, however, be determined, as Hiltscher has shown,[81] by the additional measurement, at each point of the slice, of the optic axial angle $2\Omega$ and the angles $\theta_1$ and $\theta_2$ between the normal to the slice and the optic axes (see Sections 8 and 28).

### 35. Special Cases of Three-Dimensional Systems

There are certain special cases[114] for which it is not necessary to measure all of the three angles $\Omega$, $\theta_1$, and $\theta_2$.

Most important is the case where the stress distribution has a plane of symmetry. This will occur when both the model and the loading system are geometrically symmetrical about a plane. The plane of symmetry is a principal plane of stress so that a slice which contains this plane will have a relative retardation proportional to one of the three principal stress differences. The plane which contains the optic axes will be either parallel or perpendicular to the plane of symmetry. In the latter case, the bisector of the optic axial angle is either parallel

or perpendicular to the plane of the slice. Hence we have $\theta_1=\theta_2=\pi/2$ or $\theta_1=\theta_2=\pi/2-\Omega$ or $\theta_1=\theta_2=\Omega$ depending on which principal plane of optical symmetry coincides with the plane of the slice. Hence, if we measure $\theta_1$ and $\Omega$ in addition to $\Delta$, we may calculate the three principal stress differences from Eqs. (28.4).

In a prismatic or cylindrical bar subjected to St. Venant torsion,* one of the three principal stresses at any point in the bar is zero and the other two are equal in magnitude and opposite in sign. The zero principal stress direction is perpendicular to a generator of the cylinder and the other two principal stress directions make angles of 45° with the generator. This state of stress corresponds to a biaxial crystal with an optic axial angle of $\pi/2$, the optic axes being parallel and perpendicular to the generator. A slice of the bar normal to a generator therefore gives zero phase difference for light at normal incidence; but a slice at any other angle to a generator will give a phase difference from which we may calculate the principal stresses. To effect this calculation, it is necessary to know the angles $\theta_1$ and $\theta_2$ which the wave normal makes with the optic axes. One of these will be constant and equal to the angle between the axis of the bar and the normal to the slice, but the other will vary over the section. For each point in the slice we need therefore measure only the latter angle ($\theta_2$) and the phase difference $\Delta$. Then Eqs. (28.4) give the principal stresses directly, provided the wave-length $\lambda$, the slice thickness $d$, and the stress optical coefficient $C$, are known. It was observed by Hetényi[78] that a 45° slice exhibits the maximum number of fringes, but it should be noted that the fringes do not represent loci of constant principal stress difference. It is necessary to know the angle $\theta_2$ for each point in the 45° slice. This angle may be determined in the following manner: Let $O$ be a point in the 45° slice, at which $\theta_2$ is to be found. The normal to the slice at $O$ and the line through $O$ parallel to a generator of the bar determine a plane which intersects the plane of the slice in a line $OA$. Let $OB$ be a polarizing axis of the slice at $O$ (determined from the isoclinics in the usual manner) and let angle $AOB=\alpha$. Then it may be shown[114] that

$$\sin\theta_2=(1+\cos^2 2\alpha)^{\frac{1}{2}}.$$

Similar formulas hold for slices cut at other angles or viewed obliquely.

## 36. Determination of $\sigma_3$, $\sigma_2$ and $\sigma_1$ in Three-Dimensional Systems

As Hiltscher[81] pointed out, measurement of $\Delta$, $\Omega$, $\theta_1$ and $\theta_2$ in any number of slices will yield only the directions of the three principal stresses and their differences except on a free boundary. To determine the principal stresses independently in the general case, it is necessary to measure $n_a$, $n_b$ and $n_c$ or to resort to other than optical measurements.

There are three standard methods for measuring the principal refractive indices, but none of them appears to be suitable for the current development in three-dimensional photoelasticity.

In Stokes' method* the slice would be placed over a rectangular grid of ruled lines and the latter observed through a microscope. On account of the double refraction in the plate, each family of parallel lines will appear in focus at two positions of the microscope objective. The three indices can be calculated from the relative focus positions. However, the photoelastic double refraction is so weak that this method does not appear feasible.

The prism method** would require the cutting of a small prism from the model for each point at which the stress is desired.

The total reflection methods† are very accurate but they measure the optical properties of a surface layer of the specimen. In a photoelastic slice, the surface properties are not a reliable indication of the internal optical characteristics.

Kuske[93] has suggested that by heating the slice and measuring changes in thickness accompanying the resulting relief of stress, there will be sufficient data, combined with that previously determined, to calculate $\sigma_3$, $\sigma_2$ and $\sigma_1$.

---

* S. Timoshenko, *Theory of Elasticity* (McGraw-Hill Book Company, New York, 1934), p. 228.

* J. Walker, *Analytical Theory of Light* (Cambridge University Press, 1904), p. 225.

** J. Walker, preceding reference, p. 230.

† J. Walker, preceding reference, p. 242.

## 37. Dynamic Problems

There are three classes of problems involving motion to which the photoelastic method has been applied: (1) Steady state of stress, (2) cyclic variation of stress, (3) transient state of stress.

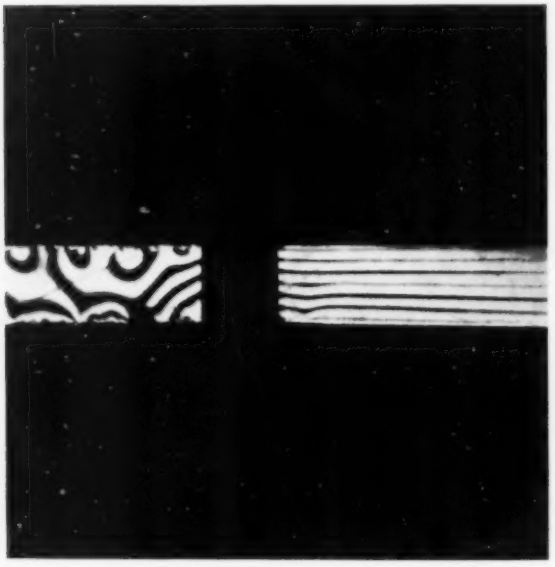

Fig. 37.1. Fringe photograph of a cantilever beam vibrating at 60 cycles per second (W. M. Murray).

Frost and Whitcomb[71] have investigated the stresses in a disk rotating with constant angular speed. This is a case in which the stresses do not vary with time.

Investigations of the cyclical stress in the teeth of rotating gears were made by Himes and Baud.[82] Stresses in vibrating beams have been studied by Ravilly[136] and Murray.[119] Fig. 37.1 is a photograph made by Murray of a cantilever beam vibrating at sixty cycles per second.

Transient stresses due to impact have been examined by Tuzi,[169] Tuzi and Nisida,[170, 171] Frocht,[65] and Thouvenin.[163] Murray[119] has given a critical review of the difficulties involved in transient stress analysis.

## 38. Miscellaneous Applications

The photoelastic method has been applied to the analysis of a wide variety of problems in the fields of machine design, steel and concrete

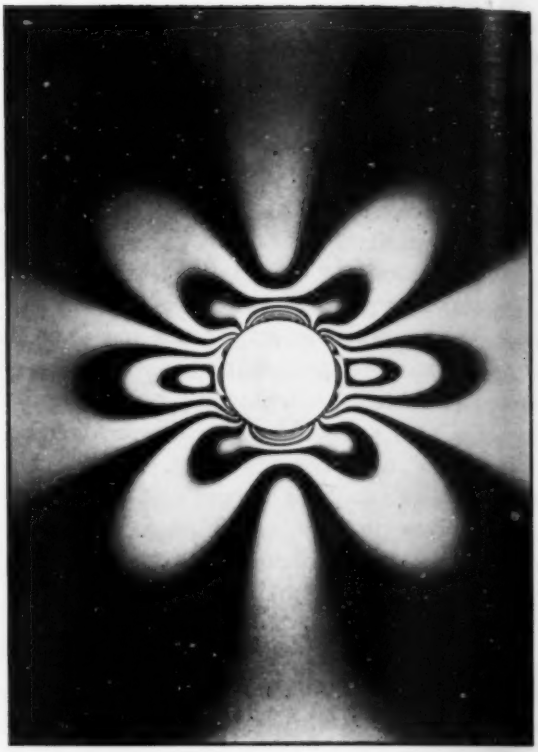

Fig. 38.1. Stress concentration around a hole in a tension bar (M. M. Frocht).

structures, mining engineering, naval architecture, aeroplane structures, materials testing, physical research, glass working, machine shop practice, soil mechanics and foundations, railway engineering, and many other related branches of engineering and applied physics. Some of the applications which have been made in the last few years are given in the following table. The numbers following each item refer to the bibli-

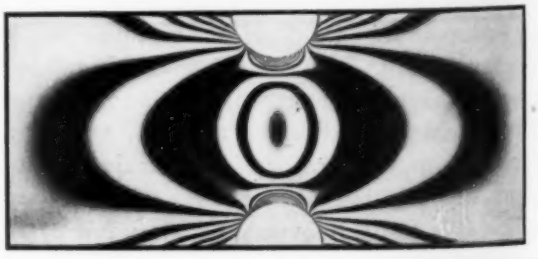

Fig. 38.2. Stress concentration due to semi-circular notches in a tension bar (M. M. Frocht).

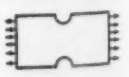

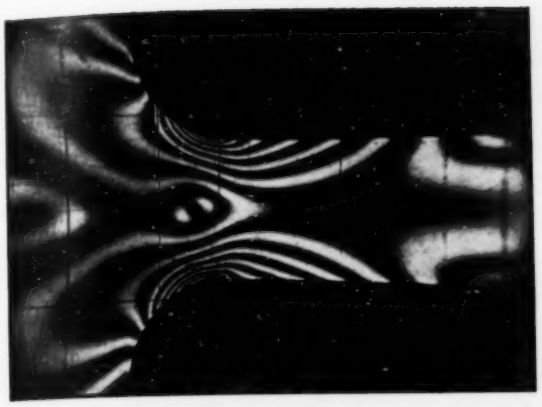

FIG. 38.3. Stress concentration at the fillets of a cantilever bar (E. E. Weibel).

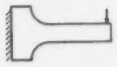

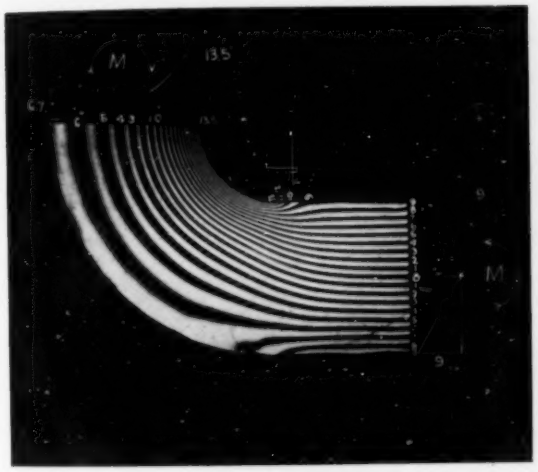

FIG. 38.4. Curved beam in pure bending (E. E. Weibel).

ography in the next section, and the papers given there should be consulted for details of the different investigations.

Arch bridges[23, 107, 127]
Bridge trusses[22]
Car wheels[47, 141]
Concrete stresses[98, 148]
Dams[33, 41, 160]
Fatigue testing[131, 132]
Flat slabs[164]
Fluid flow[73, 138, 139]
Gears[37, 82]
Glass working[85, 154, 155]
Indeterminate structures[87]
Keys and keyways[147]
Materials testing[99, 101, 120, 156]
Reinforced concrete[30, 102]
Retaining walls[42]
Ribbed slabs[149]
Rotating disks[71]
Rubber manufacture[161, 162]
Screw threads[74, 86]
Shrinkage stresses[35]
Soil mechanics[84]
Stress concentration[67, 68, 137, 175, 176, 177]
Structural elements[38, 42, 158, 159, 168]
Thermal stresses[31, 32, 133, 179]
Torsion[77, 78]
Tunnel linings[143]
Welded joints[46, 48, 144]

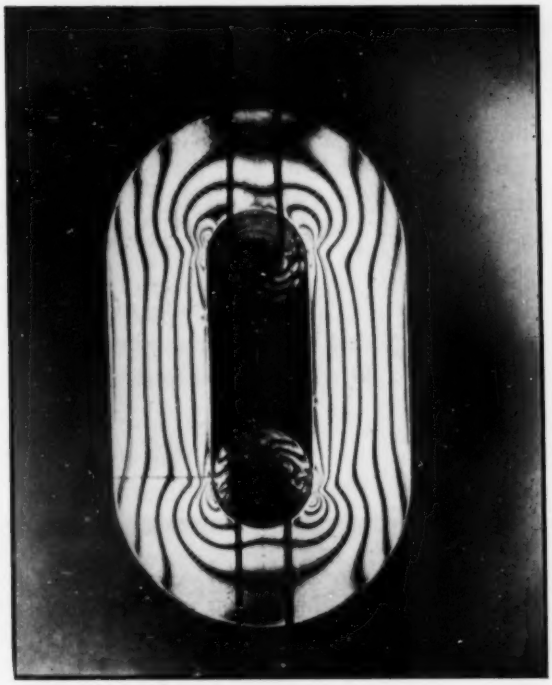

FIG. 38.5. Chain link (W. M. Murray).

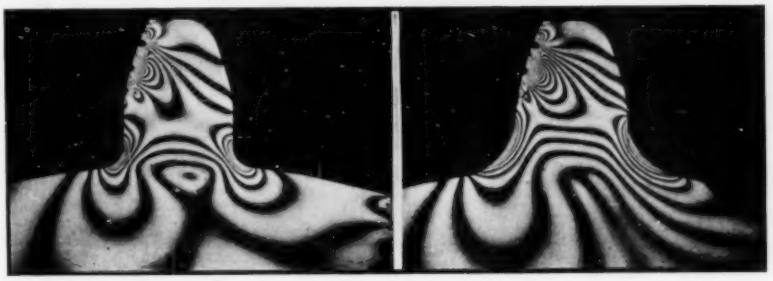

(a) (b)

FIG. 38.6. Stresses in gear teeth (T. J. Dolan).

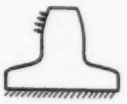

FIG. 38.7. Stresses in the main plate of a riveted joint (W. M. Murray).

Space limitation prohibits a detailed description of so great a number of special studies but a few applications for which striking fringe photographs have been obtained are noted briefly in this section. Figs. 38.1, 38.2 and 38.3 are typical of a great many investigations of stress concentrations resulting from holes, notches and fillets. Fig. 38.4 shows a curved beam in pure bending. The fringe photograph for a loaded chain link is shown in Fig. 38.5. Photographs from a study of the effect of tooth contour on the stresses in gear teeth are shown in Figs. 38.6(a) and (b).

The stresses in the main plate of a riveted joint are illustrated by the fringe photograph in Fig. 38.7. Figs. 38.8(a), (b) and (c) were made in

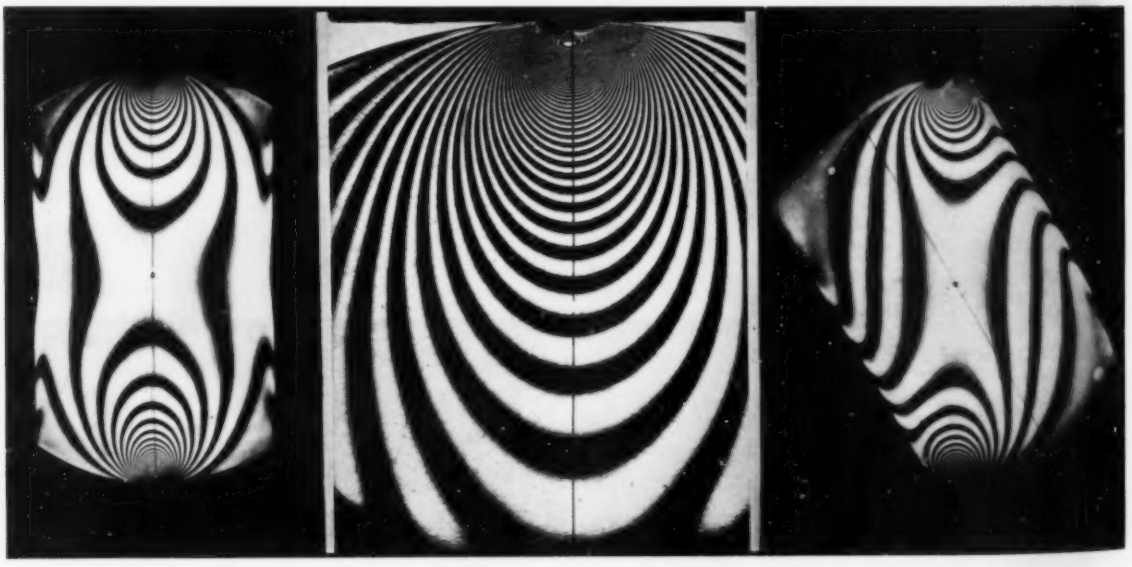

(a) (b) (c)

FIG. 38.8. Study of stresses in a bridge rocker (J. H. A. Brahtz): (a) Rocker centrally loaded. (b) Enlarged view of region immediately under the concentrated load. (c) Rocker loaded near its edge.

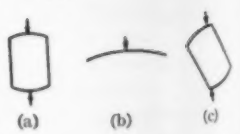

(a) (b) (c)

FIG. 38.9. Stresses in a railway car wheel (T. J. Dolan).

a study of the stresses in a bridge rocker. Fig. 38.8(a) shows the rocker centrally loaded and Fig. 38.8(b) is an enlarged view of the region immediately under the concentrated load. Fig. 38.8(c) shows the rocker loaded near its edge.

A photograph from an investigation of the stresses in a railway car wheel under different loading conditions is shown in Fig. 38.9.

An interesting device for the photoelastic analysis of stresses resulting from gravitational loading has been developed by Bucky, Solakian and Baldin.[42] The model is rotated in a centrifuge to simulate gravitational acceleration and the fringe pattern is observed with a stroboscopic polariscope (see Fig. 38.10).

***Acknowledgments***

I wish to thank Dr. M. Salvadori for his kindness in reading the manuscript and for his many criticisms and suggestions.

Mr. D. C. Drucker was of great assistance in the preparation of Part III.

Many of the leading investigators in photoelasticity in this country were asked to contribute photographs of apparatus and fringe patterns for use as illustrations. For their courtesy in responding to this invitation I am pleased to acknowledge my indebtedness to Dr. J. H. A. Brahtz, U. S. Bureau of Reclamation; Professor T. J. Dolan, University of Illinois; Professor M. M. Frocht, Carnegie Institute of Technology; Dr. M. Hetényi, Westinghouse Research Laboratories; Dr. O. J. Horger, Timken Roller Bearing Company; Dr. W. M. Murray, Massachusetts Institute of Technology; Professor E. E. Sechler, California Institute of Technology; Professor F. G. Switzer, Cornell University; Professor E. K. Timby, Princeton University; Dr. E. E. Weibel, University of California.

***Bibliography***

An extensive bibliography, which covers the field of Photoelasticity up to about 1930, appears in Coker and Filon's *Treatise*. The following list includes papers which have appeared in the interval, 1930–1938, and also a few earlier papers mentioned in the body of this review. The first nineteen references are to textbooks and reviews, while the remainder are recent research papers dealing with theory, technique, apparatus, and applications.

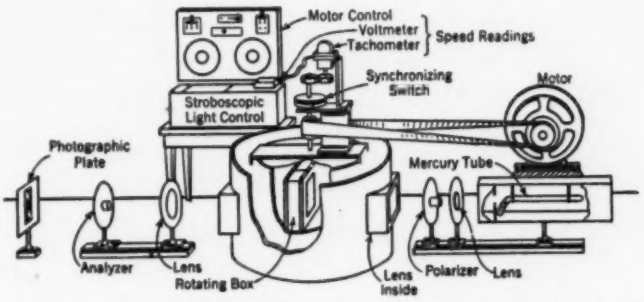


FIG. 38.10. Centrifuge-polariscope apparatus (P. B. Bucky, A. G. Solakian and L. S. Baldin, reference 42).

## Bibliography


1. R. V. Baud, "Entwicklung und heutiger Stand der Photoelastizität und der Photoplastizität im Rahman der Gesamt-Experimentalelastizität," Schweizer Archiv für angewandte Wissenschaft und Technik **4**, 1–15, 48–53 (1938).
2. R. V. Baud, "Technische Methoden Photoelastischer Forschung," Schweizerische Bauzeitung, **100** (1932).
3. E. G. Coker, "Photo-elasticity for Engineers," Gen. Elec. Rev. **23**, 870–877 (1920); **23**, 966–973 (1920); **24**, 82–88 (1921); **24**, 222–226 (1921); **24**, 455–466 (1921).
4. E. G. Coker, "Photo-elasticity," J. Frank. Inst. **199**, 289–331 (1925).
5. E. G. Coker and L. N. G. Filon, *A Treatise on Photoelasticity* (Cambridge University Press, Cambridge, 1931).
6. L. N. G. Filon, *Manual of Photo-Elasticity for Engineers* (Cambridge University Press, Cambridge, 1936).
7. L. Föppl, "Spannungsmessung mit Hilfe der optischen Doppelbrechung," Zeits. f. tech. Physik **15**, 430–436 (1934).
8. L. Föppl, "Die Spannungsoptik im Dienste des Bauingenieurs," Der Bauingenieur **19**, 341–5 (1938).
9. L. Föppl and H. Neuber, *Festigkeitslehre mittels Spannungsoptik* (R. Oldenbourg, München and Berlin, 1935).
10. P. Laurent and A. Popoff, "La photoélasticité," Rev. de Metallurgie **35**, 363–78, 407–24, 448–74 (1938).
11. G. Mesmer, "Das Spannungsoptische Verfahren," die Messtechnik, **11**, 217–221, 238–241 (1935).
12. A. Mesnager, *Détermination expérimentale des efforts intérieurs dans les solides*, Fascicule X du Mémorial des Sciences Physiques (Gauthier-Villars, Paris, 1929).
13. G. Oberti, "Fotoelasticita," Rendiconti del Seminario di matematico e fisica d. R. Univ. Milano **6**, 217–251 (1932).
14. G. Oberti, "Indagini sperimentali sulle costruzioni con l'uso dei modelli," Atti, Ricerche e Studi, R. Politecnico di Milano, Hoepli, Milano (1935).
15. G. Oberti, "L'uso dei modelli per lo studio dello stato di sollecitazione in strutture: concetti basiliari e recenti applicazioni," Energia Elettrica **13**, 16–23 (1936).
16. Photoelastic Journal, 55 West 42 Street, New York, New York. A. G. Solakian, Editor.
17. M. Salvadori, "Recenti progressi della tecnica fotoelastica," Annali dei Lavori Pubblici **75**, 90–110 (1937).
18. V. Tesař, "Les progrès récents et les applications de la photo-élasticimétrie," La Technique Moderne **30**, 259–265 (1938).
19. E. E. Weibel, "Developments in Photoelasticity," S. Timoshenko, 60th Anniversary Volume (Macmillan Company, New York, N. Y., 1938), pp. 257–267.

* * * * *

20. I. Arakawa, "On the determination of stress-optical coefficient of Bakelite with initial stress," Proc. Phys.-Math. Soc. Japan **5**, 117–136 (1923).
21. I. Arakawa, "Some advantages obtained from Bakelite in photo-elastic observation," Proc. Phys.-Math. Soc. Japan **7**, 160–180 (1925).
22. L. Baes, "La Poutre Vierendeel," L'Ossature Métallique **5**, 457 (1936), and **6**, 432 (1937).
23. L. Baes, "L'arc élastique parfaitement encastré à ses deux extremités," La Technique des Travaux **13**, 442 (1937).
24. R. V. Baud, "Further development in photoelasticity," J. Opt. Soc. Am. and Rev. Sci. Inst. **18**, 422–437 (1929).
25. R. V. Baud, "Effect of elliptical polarization on energy transmission," J. Opt. Soc. Am. **21**, 119–122 (1931).
26. R. V. Baud, "On the determination of principal stress from crossed Nicol observations," J. Frank. Inst. **211**, 457–474 (1931).
27. R. V. Baud and W. D. Wright, "Analysis of colours observed in photoelastic experiments," J. Opt. Soc. Am. **20**, 381–395 (1930).
28. R. V. Baud and F. Tank, "Ermittlung von zweidimensionalen Potentialfeldern bei beliebigen Randbedingungen," Schweizerische Bauzeitung **III**, 176–177 (1938).
29. L. Bergmann, "Messung elastischer Konstanten mit Ultraschall," V. D. I. Zeits. **81**, 878–82 (1937).
30. A. H. Beyer and A. G. Solakian, "Photoelastic analysis of stresses in composite materials," Proc. Am. Soc. Civil Eng. **59**, 1121–1132 (1933).
31. M. A. Biot, "Contribution à la technique photo-élastique," Annales Soc. scientifique Bruxelles **B53**, 13–15 (1933).
32. M. A. Biot, "Propriété générale des tensions thermiques en régime stationnaire dans les corps cylindriques. Application à la mésure photo-élastique de ces tensions," Annales Soc. scientifique Bruxelles **B54**, 14–18 (1934).
33. M. A. Biot, "Distributed gravity and temperature loading in two-dimensional elasticity replaced by boundary pressures and dislocations," J. App. Mech. **2**, 41–45 (1935).
34. M. A. Biot, "A general property of two-dimensional thermal stress distribution," Phil. Mag. **19**, 540–549 (1935).
35. M. A. Biot and H. Smits, "Étude photo-élastique des tensions de contraction dans un barrage," Bull. Tech. No. 4, p. 10, Bulletin technique de l'Union des Ingénieurs sortis des Écoles spéciales de Louvain (1933).
36. C. B. Biezeno and J. J. Koch, "Über einige Beispiele zur elektrischen Spannungsbestimmung," Ingenieur Archiv **4**, 384–393 (1933).
37. P. H. Black, "An investigation of relative stresses in solid spur gears by the photoelastic method," University of Illinois Engineering Experiment Station, Bulletin 288, 1–29 (1936).

38. L. Blanjean and F. Temmermann, "Étude de la région voisine du point d'inflexion d'une pièce droite prismatique en flexion plane composée avec effort tranchant," Soc. Roy. Belge des Ingénieurs et des Industriels, No. 9, 823–863 (1937).
39. A. V. Blom, "Der Spannungs-optische Koeffizient als Materialkonstante," Kolloid Zeits. **80**, 212–215 (1937).
40. J. H. A. Brahtz, "Photoelastic apparatus at the California Institute of Technology," Rev. Sci. Inst. 5, 80–83 (1934).
41. J. H. A. Brahtz, "Stress function and photoelasticity applied to dams," Proc. Am. Soc. Civil Eng. **61**, 983–1020 (1935).
42. P. B. Bucky, A. G. Solakian and L. S. Baldin, "Centrifugal method of testing models," Civil Eng. 5, 287–290 (1935).
43. R. B. Carleton, "Suitability of materials for photoelastic investigations," Rev. Sci. Inst. **5**, 30–32 (1934).
44. E. G. Coker, "Photoelasticity," Engineering (London) 90, 1–4 (1911).
45. E. G. Coker, "Lateral extensometers," Engineering (London) **129**, 465–467 (1930).
46. E. G. Coker and R. Russell, "Stress distributions in fusion joints of plates connected at right angles," Institution of Naval Architects **5**, 1–8 (1933).
47. E. G. Coker and M. Salvadori, "Stress waves in the tyres of locomotives," Proc. Inst. Mech. Eng. **131**, 493–512 (1935).
48. E. G. Coker and B. P. Haigh, "An experimental investigation of cracking in mild steel plates and welded seams," Trans. Roy. Inst. Naval Architects, **77**, 193–207 (1935).
49. J. W. Cookson and H. Osterberg, "A formula for the birefringence of vibrating media," Physics **7**, 166 (1936).
50. J. P. Den Hartog, "Experimentelle Lösung des ebenen Spannungsproblems," Zeits. f. angewandte Math. und Mech. **11**, 156 (1931).
51. R. G. Edmonds and B. T. McMinn, "Celluloid as a medium for photoelastic investigation," Trans. Am. Soc. Mech. Eng. **54**, 77–82 (1932).
52. C. Fabry, "Sur une nouvelle méthode pour l'étude expérimentale des tensions élastiques," Comptes rendus, Paris **190**, 457–460 (1930).
53. H. Favre, "Méthode purement optique de détermination des tensions intérieures se produisant dans les constructions," Schweizerische Bauzeitung 90 (1927).
54. H. Favre, "Sur une nouvelle méthode optique de détermination des tensions intérieures," Rev. d'Optique **8**, 193–213, 241–261, 289–307 (1929).
55. H. Favre, "Sur une méthode optique de détermination des tensions intérieures dans les solides à trois dimensions," Comptes rendus, Paris **190**, 1182–1184 (1930).
56. H. Favre, "La detérmination optique des tensions intérieures," Rev. d'Optique **11**, 1–21 (1932).
57. B. Ferretti, "Optical method for the determination of variable elastic stresses," Nuovo Cimento **15**, 77–87 (1938).
58. L. N. G. Filon, "On the graphical determination of stress from photo-elastic observations," Engineering (London) **116**, 511–512 (1923).
59. L. N. G. Filon, "Exploration of stress near an isotropic point in an elastic plate," Phil. Mag. **22**, 187–206 (1936).
60. L. N. G. Filon and H. T. Jessop, "On the stress-optical effect in transparent solids strained beyond the elastic limit," Trans. Roy. Soc. London **A223**, 89–125 (1923).
61. L. Föppl, "Untersuchung der ebener Spannungszustände mit Hilfe der Doppelbrechnung," Sitz. d. math. naturwiss. Abt. d. Bayerischen Akad. München, 247–265 (1928).
62. L. Föppl, "Neue Erfolge in der Spannungsoptik," Zeits. V. D. I. **81**, 137–141 (1937).
63. P. Frenkel, "Photoélasticimétrie et ses applications aux constructions civiles," Travaux Architecture-Construction, **19**, 33–38, 149–155, 182–187 (1935).
64. M. M. Frocht, "Recent advances in photoelasticity," Trans. Am. Soc. Mech. Eng. **53**, 135–153 (1931).
65. M. M. Frocht, "Kinematography in photoelasticity," Trans. Am. Soc. Mech. Eng. **54**, 54–59 (1932).
66. M. M. Frocht, "On the application of interference fringes to stress analysis," J. Frank. Inst. **216**, 73–89 (1933).
67. M. M. Frocht, "Factors of stress concentration photoelastically determined," J. App. Mech. **2**, A67, A68 (1935).
68. M. M. Frocht, "Photoelastic studies in stress concentration," Mech. Eng. **58**, 485–9 (1936).
69. M. M. Frocht, "A rapid method for the determination of principal stresses across sections of symmetry from photoelastic data," J. App. Mech. **5**, 24–28 (1938).
70. M. M. Frocht, "On the optical determination of isopachic stress patterns," Proceedings of the 5th International Congress for Applied Mechanics, Cambridge, Massachusetts (1938).
71. T. H. Frost and K. F. Whitcomb, "The stresses in rotating disks," Trans. Am. Soc. Mech. Eng. **53**, 1–11 (1931).
72. A. Goetz, "A modified optical arrangement for photoelastic measurements," Rev. Sci. Inst. **5**, 84 (1934).
73. J. N. Goodier, "An analogy between the slow motions of a viscous fluid in two dimensions and systems of plane stress," Phil. Mag. **17**, 554 (1934).
74. S. G. Hall, "Determination of stress concentration in screw threads by the photo-elastic method," University of Illinois Engineering Experiment Station Bulletin No. 245 (1932).
75. F. C. Harris, "The photo-elastic constants of glass as affected by high temperatures and by lapse of time," Proc. Roy. Soc. London **106**, 718–23 (1924).

76. F. C. Harris and B. R. Seth, "The variation of double refraction in celluloid with the amount of permanent stretch at constant temperature and at different temperatures," Proc. Phys. Soc., London **48**, 477–487 (1936).
77. M. Hetényi, "Photoelastic studies of three-dimensional stress problems," Proceedings of the 5th International Congress for Applied Mechanics, Cambridge, Massachusetts (1938).
78. M. Hetényi, "The fundamentals of three-dimensional photoelasticity," J. App. Mech. **5**, A149–A155 (1938).
79. M. Hetényi, "Photoelastic stress analyses made in three dimensions," Machine Design **10**, 40–1 (1938).
80. W. Herzog and G. Szivessy, "Über die Messung von Phasendifferenzen mit einer empfindlichen Methode von uneingeschränktem Messbereich," Physik. Zeits. **38**, 129–133 (1937).
81. R. Hiltscher, "Polarisationsoptische Untersuchung des raumlichen Spannungszustandes im konvergenten Licht," Forschung auf dem Gebiete des Ingenieurwesens **9**, 91–103 (1938).
82. W. H. Himes and R. V. Baud, "The use of motion pictures to illustrate the generation of involute gearing and the use of motion pictures and polarized light as a method of studying gear stresses," Iron and Steel Engineer **6**, 372–380 (1929).
83. O. J. Horger, "Photoelastic analysis practically applied to design problems," J. App. Phys. **9**, 457–464 (1938).
84. B. K. Hough, Jr., "Stability of embankment foundations," Proc. Am. Soc. Civil Eng. **63**, 1340–1357 (1937).
85. A. W. Hull and E. E. Burger, "Strain analyser for glass seals," Rev. Sci. Inst. **7**, 98–100 (1936).
86. H. Jehle, "Polarisationsoptische Spannungsuntersuchungen an einer Schrauben-verbindung und an einzelnen Gewinde Zähnen," Forschung auf dem Gebiete des Ingenieurwesens **7**, 19–30 (1936).
87. A. Jona, "La foto-elasticità e sua applicazione allo studio delle strutture iperstatiche," Aerotecnica **15**, 180–193 (1935).
88. J. Kuno, "Law of photoelastic extinction," Phil. Mag. **12**, 503–511 (1931).
89. J. Kuno, "Law of photoelastic extinction," Phil. Mag. **13**, 810–824 (1932).
90. J. Kuno, "Relation between strain and photoelastic effect in phenolite," Phil. Mag. **16**, 353–362 (1933).
91. J. Kuno, "Practical methods of determining the coefficient of photoelastic extinction," Phil. Mag. **19**, 457–466 (1935).
92. J. Kuno, "Effect of age of phenolite on the coefficient of photoelastic extinction," Phil. Mag. **23**, 63–64 (1937).
93. A. Kuske, "Das Kunstharz Phenolformaldehyd in der Spannungsoptik," Forschung auf dem Gebiete des Ingenieurwesens **9**, 139–149 (1938).
94. A. Kuske, "Berechnung von Fehlern Infolge von Vorspannungen in der Spannungsoptik," V. D. I. Zeits. **82**, 1455–8 (1938).
95. M. v. Laue, "Einsatz über Eigenspannungen," Sitz. der preussischen Akad. der Wissenschaften Berlin **21**, 377–382 (1931).
96. G. H. Lee and C. W. Armstrong, "Effect of temperature on physical and optical properties of photoelastic materials," J. App. Mech. **5**, 11–12 (1938).
97. H. Liebmann, "Die angenäherte Ermittlung harmonischer Funktionen. . . . " Sitz. der math.-phys. Klasse der Bayer. Akad. München, p. 385 (1918).
98. G. Mabboux, "Applications de la photoélasticimétrie à l'étude des ouvrages en béton," Rev. d'Optique **11**, 501–507 (1932).
99. C. W. MacGregor, "Concerning the distribution of stress in a laterally compressed strip," Physics **5**, 140–145 (1934).
100. L. Malavard, "L'analogie electrique comme méthode auxiliaire de la photo-élasticité," Comptes rendus, Paris **206**, 38–39 (1938).
101. H. B. Maris, "Photoelastic investigations of the tensile test specimen, the notched bar, the ship propeller strut, and the roller path ring," J. Opt. Soc. Am. **15**, 194–200 (1927).
102. H. E. L. Martin, "Some experiments with reinforced materials examined by aid of plane polarized light," Trans. Liverpool Eng. Soc. **36**, 59–98 (1915).
103. T. V. Matthew, "Stress distribution in irregular sections using photo-elastic models," J. Roy. Tech. College Glasgow **4**, 121–134 (1937).
104. J. C. Maxwell, "On the equilibrium of elastic solids," Trans. Roy. Soc. Edinburgh **20**, 87 (1850).
105. G. Mesmer, "Vergleichende spannungsoptische Untersuchung und fliess Versuche unter konzentriertem Druck," Zeits. f. Tech. Mech. Thermodynamik, V. D. I. **1** (1930).
106. A. Mesnager, "Contribution à l'étude de la déformation élastique," Ann. des Ponts et Chaussées **4**, 128–190 (1901).
107. A. Mesnager, "Détermination complète sur un modèle réduit des tensions qui se produiront dans un ouvrage," Ann. des Ponts et Chaussées **16**, 133–186 (1913).
108. A. Mesnager, "Sur la détermination optique des tensions intérieures des solides à trois dimensions," Comptes rendus, Paris **190**, 1249 (1930).
109. H. Meyer, "Spannungsoptische Untersuchung ebener Schwingungsvorgänge," Ingenieur-Archiv **7**, 273–293 (1936).
110. H. Meyer and F. Tank, "Uber ein verbessertes elektrisches Verfahren zur Auswertung der Gleichung $\Delta\phi=0$ und seine Anwendung bei photoelastischen Untersuchung," Helv. Phys. Acta **8**, 315–317 (1935).
111. R. D. Mindlin, "A reflection polariscope for photoelastic analysis," Rev. Sci. Inst. **5**, 224–228 (1934).
112. R. D. Mindlin, "Analysis of doubly refracting materials with circularly and elliptically polarized light," J. Opt. Soc. Am. **27**, 288–291 (1937).
113. R. D. Mindlin, "Distortion of the photoelastic fringe pattern in an optically unbalanced polariscope," J. App. Mech. **4**, A170–172 (1937).

114. R. D. Mindlin, "Optical aspects of three-dimensional photoelasticity," Eighth Semi-Annual Meeting, Eastern Photoelasticity Conference, N. Y. (1938).
115. H. Mueller, "Theory of photoelasticity in amorphous solids," Physics **6**, 179–184 (1935).
116. H. Mueller, "Theory of the photoelastic effect of cubic crystals," Phys. Rev. **47**, 947–957 (1935).
117. H. Mueller, "Light diffracted by supersonic waves in solids," Phys. Rev. **52**, 223–229 (1937).
118. H. Mueller, "Determination of elasto-optical constants with supersonic waves," Zeits. f. Krist. **99**, 122–141 (1938).
119. W. M. Murray, "Some aspects of dynamic problems in photoelasticity," Eighth Semi-Annual Meeting, Eastern Photoelasticity Conference, N. Y. (1938).
120. H. Mussmann, "Die elastische Nachwirkung und ihre Zusammenhang mit dem optischen Nachwirkung," Ann. d. Physik **31**, 121–144 (1938).
121. J. G. McGivern and H. L. Supper, "Membrane analogy supplementing photoelasticity," J. Frank. Inst. **217**, 491–504 (1934).
122. J. G. McGivern and H. L. Supper, "A membrane analogy supplementing photoelasticity," Trans. Am. Soc. Mech. Eng. **56**, 601–604 (1934).
123. J. G. McNally and S. E. Sheppard, "Rate of deformation of cellulose nitrate-camphor films under static stresses," J. Phys. Chem. **35**, 2498–2507 (1931).
124. Masataka Nisida, "On the physical properties of photoelastic material 'Phenolite,'" Sci. Pap. Inst. Phys. Chem. Research **22**, 269–283 (1933).
125. H. Neuber, "New method of deriving stresses graphically from photoelastic observations," Proc. Roy. Soc., London **141**, 314–24 (1933).
126. H. Neuber, "Exact construction of $(\sigma_1+\sigma_2)$ network from photoelastic observations," Trans. Am. Soc. Mech. Eng. **56**, 733–737 (1934).
127. G. Oberti, "Studi sul comportamento statico di archi circolari considerati come elementi di dighe a volta," Energia Ellettrica **13**, 578–584 (1936).
128. G. Oppel, "Polarisationsoptische Untersuchung raumlicher spannungs- und dehnungszustände," Forschung auf dem Gebiete des Ingenieurwesens **7**, 240–8 (1936).
129. G. Oppel, "Photoelastic investigation of three-dimensional stress and strain conditions," Nat. Advisory Com. for Aeronautics—Technical Memo. No. 824 (1937).
130. G. Oppel, "Das polarisationsoptische Schichtverfahren zur Messung der Oberflächenspannung am beanspruchten Bauteil ohne Modell," V. D. I. Zeits. **81**, 803–4 (1937).
131. R. E. Peterson and A. M. Wahl, "Fatigue of Shafts at Fitted Members with a Related Photoelastic Analysis," J. App. Mech., Trans. Am. Soc. Mech. Eng. 57, A1–A11 (1935).
132. R. E. Peterson and A. M. Wahl, "Two- and three-dimensional cases of stress concentration and comparison with fatigue tests," J. App. Mech. **3**, A15–A22 (1936).
133. H. Poritsky, "Analysis of thermal stresses in sealed cylinders and the effect of viscous flow during anneal," Physics **5**, 406–411 (1934).
134. G. M. Pugno, "Studio sperimentale sugli stati piani di tensione," Atti della Accad. della Science di Torino, **71**, 55–71 (1935).
135. G. M. Pugno, "Sulla rappresentazione degli stati piani di tensione dedotta mediante l'esperimento," Atti della Acad. della Science di Torino, **71**, 110–115 (1935).
136. Ravilly, Publications Scientifiques du Ministere d l'Air, Paris, No. 120 (1938).
137. J. J. Ryan and L. J. Fischer, "Photoelastic analysis of stress concentration for beams in pure bending with central hole," J. Frank. Inst. **225**, 513–526 (1938).
138. Ch. Sadron, "Sur une nouvelle méthode optique d'exploration d'un champ de vitesses bidimensional," Comptes rendus, Paris **197**, 1293–1296 (1933).
139. Ch. Sadron and E. D. Alcock, "An optical method for measuring the distribution of velocity," Guggenheim Aeronautical Laboratory, California Institute of Technology, Publication No. 44 (1934).
140. M. Salvadori, "Alcune richerche fotoelastiche nel Laboratorio dello University College di Londra," Annali dei Lavori Pubblici **7**, 865–879, 1050–1091 (1934).
141. M. Salvadori, "Sulle tensioni interne nelle ruote motrici delle locomotive," Ricerchi d'Igegneria, **3**, 113–118 (1935).
142. G. H. Shortley and R. Weller, "The numerical solution of Laplace's equation," J. App. Phys. **9**, 334–348 (1938).
143. J. E. Soehrens, R. T. Cass and J. E. Sower, "Eliminating local stress concentrations in photoelastic model," Civil Eng. **6**, 594–5 (1936).
144. A. G. Solakian, "Stresses in transverse fillet welds by photoelastic methods," J. Am. Welding Soc. **13**, 22–29 (1934).
145. A. G. Solakian, "A new photoelastic material," Mech. Eng. **57**, 767–771 (1935).
146. A. G. Solakian, "Photoelastic models with cemented elements," Photoelastic J. **1**, 14–17 (1938).
147. A. G. Solakian and G. B. Karelitz, "Photoelastic study of shearing stresses in keys and keyways," Trans. Am. Soc. Mech. Eng. **54**, 97–123 (1931).
148. H. Souillot, "La photo-élasticimétrie méthode G. Mabboux dans l'étude des déformations des ouvrages en béton armé," Tech. des Travaux **19**, 157–9 (1935).
149. M. Suquet, "Recherches photoélasticimétriques sur les dalles nervurées poursuivies au laboratoire de l'École National des Ponts et Chaussées," Ann. des Ponts et Chaussées," **104**, 34–39 (1934).
150. F. Tank, "Die Tätigkeit des photo-elastischen Laboratoriums der Eidg. Technischen Hochschule 1927 bis 1933," Schweizerische Bauzeitung **104**, 45–48 (1935).
151. F. Tank, "Eine neue Methode der interferometrischen Spannungsmessung," Helv. Phys. Acta **9**, 611–616 (1936).

152. F. Tank, R. V. Baud and E. Schiltknecht, "Die neuen Einrichtungen des photoelastischen Laboratoriums an der Eidg. Techn. Hochschule und an der Eidg. Materialprufungsanstalt," Schweizerische Bauzeitung **109**, 249–52 (1937).
153. F. Tank, R. V. Baud and E. Schiltknecht, "Les nouvelles installations du laboratoire de photoélasticimétrie de l'École Polytechnique de Zurich," Genie Civil **111**, 482–3 (1937).
154. P. Tarbés, "Méthode pour l'étude de la soudure et de la dilatation des verres. Compensature de biréfringence," Comptes rendus, Paris **195**, 222–224 (1932).
155. M. H. L. Tardy, "Méthode pratique d'examen de mésure de la biréfringence des verres d'optique," Rev. d'Optique **8**, 59–69 (1929).
156. F. Temmermann and L. Blanjean, "Un problème de résistance des matériaux et de photoélasticité," Ossature Metallique **7**, 132–7 (1938).
157. V. Tesař, "Photoélasticité méthode purement optique pour déterminer les déformations d'épaisseurs des modèles, etc.," Rev. d'Optique **11**, 97–104 (1932).
158. V. Tesař, "Détermination expérimentale des tensions dans les extrémités des pièces prismatiques munies d'une semiarticulation," Assoc. Int. des Ponts et Charpentes **1**, 497–505 (1932).
159. V. Tesař, "Étude expérimentale des contraintes produites dans une poutre par des charges concentrées," Int. Verein. der Brucken-und-Hochbau **4**, 543–570 (1936).
160. V. Tesař, "Les procédés photoélasticimétriques et leur application aux barrages-voutes," Ann. des Ponts et Chaussées **107**, 627–662 (1937).
161. W. E. Thibodeau and A. T. McPherson, "Photoelastic properties of soft vulcanized rubber," Nat. Bur. Stand. J. Research **13**, 887–896 (1934).
162. W. E. Thibodeau and L. A. Wood, "Photoelastic determination of stresses around a circular inclusion in rubber," Nat. Bur. Stand. J. Research **20**, 393–409 (1938).
163. J. Thouvenin, "Application de la photoélasticité à l'étude des percussions," Comptes rendus, Paris **201**, 769–771 (1935).
164. E. K. Timby and I. G. Hedrick, Jr., "Photoelastic analysis broadened," Eng. News-Record **121**, 179–81 (1938).
165. Z. Tuzi, "A new material for the study of photoelasticity," Inst. Phys. Chem. Research Japan **7**, 79–96 (1927).
166. Z. Tuzi, "Photoelastic study on a specimen of three-dimensional form," Sci. Pap. Inst. Phys. Chem. Research Japan **7**, 97–103 (1927).
167. Z. Tuzi, "On the development of experimental methods in photoelasticity," Sci. Pap. Inst. Phys. Chem. Research Japan **12**, 21–69 (1929).
168. Z. Tuzi, "Stress distribution in an angle plate," Sci. Pap. Inst. Phys. Chem. Research Japan **16**, 140–146 (1931).
169. Z. Tuzi, "Photographic and kinematographic study of photoelasticity," Sci. Pap. Inst. Phys. Chem. Research Japan **8**, 247–267 (1928).
170. Z. Tuzi and M. Nisida, "Photoelastic study of stress due to impact," Sci. Pap. Inst. Phys. Chem. Research Japan **26**, 277–309 (1935).
171. Z. Tuzi and M. Nisida, "Photoelastic study of stresses due to impact," Phil. Mag. **21**, 448–473 (1936).
172. Z. Tuzi and M. Nisida, "On a new apparatus for photo-elasticity-stress-type quarter-wave-plate of a large field," Sci. Pap. Inst. Phys. Chem. Research Japan **31**, 99–107 (1937).
173. R. von Mises, "Das Verhalten der Hauptspannungen in der Umgebung einer Verzweigungstelle," Zeits. f. angewandte Math. Mech. **18**, 74–76 (1938).
174. R. von Mises, "Über den singulären Punkt zweiter Ordnung im ebenen Spannungsfeld," S. Timoshenko, 60th Anniversary Volume (Macmillan Company, New York), pp. 147–154.
175. R. W. Vose, "An application of the interferometer strain gage in photoelasticity," J. App. Mech. **2**, A99–A102 (1935).
176. A. M. Wahl and R. Beeuwkes, "Stress concentration produced by holes and notches," Trans. Am. Soc. Mech. Eng. **56**, 617–625 (1934).
177. E. E. Weibel, "Studies in photoelastic stress determination," Trans. Am. Soc. Mech. Eng. **56**, 637–658 (1934).
178. E. E. Weibel, "Application of soap-film-studies to photoelastic stress determination," Assoc. Int. des Ponts et Charpentes—Mémoires **3**, 421–38 (1935).
179. E. E. Weibel, "Thermal stresses in cylinders by the photoelastic method," Proc. 5th Int. Cong. for App. Mech., Cambridge, Massachusetts, 1938.
180. G. Wertheim, "Mémoire sur la double refraction temporairement produite dans les corps isotropes. . . . " Ann. de Chimie et de Phys. **60**, 156 (1854).
181. H. E. Wessman, "New universal straining frame aids photoelastic research," Civil Engineering **8**, 614 (1938).

# The Application of Hardening Resins in Three-Dimensional Photoelastic Studies

By M. Hetényi

*Westinghouse Research Laboratories, East Pittsburgh, Pennsylvania*

Recent photoelastic tests made with hardening resins at elevated temperatures furnish a striking demonstration of the current theory for the molecular structure of these resins while the results of such tests lay the foundation for a new line of photoelasticity dealing with three-dimensional states of stress distribution.

The fundamentals of the new method can be easily demonstrated by subjecting a bar of such hardening resin, phenol-formaldehyde resin for instance, to some simple loading at a temperature of about 110°C. We can observe that while the material becomes very flexible at this temperature it remains perfectly elastic, that is it assumes its final deformation in a few seconds upon application of the load, while upon unloading the piece the original shape is also recovered almost instantaneously. If we leave the loading on the test piece at the elevated temperature and by slow cooling return to room temperature, after the removal of the loading we obtain a permanently deformed sample which, however, exhibits in polarized light an isochromatic fringe pattern corresponding to an elastic state of stress. This observation, that a permanently deformed body can exhibit an elastic stress distribution, is quite unusual in itself, though we find that the obtained test piece has also some other curious properties. We will observe that careful sawing or machining of the sample will not disturb its isochromatic pattern and the original fringes will be preserved in every small portion cut out of the test piece. Thus we can conclude that the annealing procedure has furnished us a solidified, "frozen" form of elastic deformation, which is completely preserved through the whole bulk of the test piece. Supposing that the isochromatic lines are due to strains in the material, their preservation will be due probably to the same particular properties of the structure of hardening resins which produced the obtained frozen form of the elastic strains. Accepting the validity of the above observations they will evidently provide means of investigating photoelastically three-dimensional states of stress distribution. Subjecting any three-dimensional model to the above-mentioned annealing procedure we obtain a sample where the elastic strains produced by the loading at the elevated temperature are preserved in a frozen form. Since cutting of the test piece does not disturb this solidified state, we will be able to cut out thin slices of the sample and each of the slices will show in polarized light the stress pattern existing in the original three-dimensional piece in the corresponding plane.

All the above-mentioned experimental observations can be well explained on the basis of the current molecular theory of heat-hardening resins. We will discuss therefore briefly this molecular theory[1] taking the phenol-formaldehyde resin as a prototype for our material.

The phenol-formaldehyde resin is a result of interaction between phenol and formaldehyde. Reacting these two chemicals at suitable temperature, we obtain a clear resin-like material which is in a solid state at room temperature, can be fused, however, and will dissolve in solvents such as alcohol and acetone. The assumed chemical reaction scheme of phenol-formaldehyde resins is shown in Fig. 1. In the first (*A*) stage the material is fusible and soluble and its molecules adhere only by the secondary bonds of the van der Waals forces. The benzene nuclei, however, are assumed to possess three active spots (shown by crosses in Fig. 1) which gives a possibility for a three-dimensional molecular growth. Upon heating this *A* stage material, the assumed chemically active spots will react with one another, creating thus a strong primary bond among them. As this reaction proceeds a strong molecular network will be built up throughout

the whole bulk of the resin. The molecules of this network will be then in primary bond with one another, being thus in an infusible and insoluble state. Because of some particular features of the

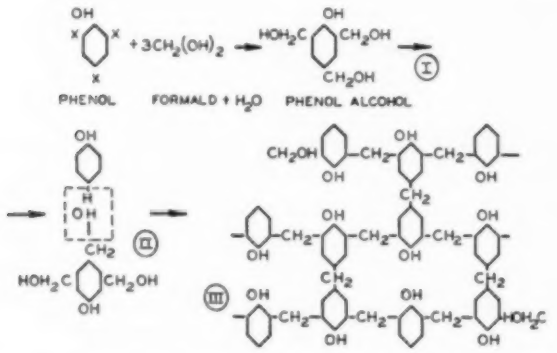


FIG. 1. A reaction scheme of the phenol-formaldehyde resins (hardening type).

structure, however, not all the possible chemically active spots will be able to react and within the globular micelles of the three-dimensional network in the resin there will be material which is still in the fusible and soluble state. This process, as the *A* stage material arrives through the *B* (partly fusible and soluble) stage to the *C* (infusible and insoluble) stage is termed as polymerization. The synthetic resins of the hardening type used in photoelastic tests are largely in this latter stage, where their molecular structure can be depicted as shown in Fig. 2. This state is termed isogel, because there is no difference in the chemical composition between the fusible and infusible part of the material.

When a piece of such resin is heated, the *A* stage material within the cells will be gradually fused, becoming liquid at a certain temperature. At that point the only load-carrying element of the material will be its skeleton given by the strong primary network throughout the resin. The strength and elasticity of this network will, however, not be affected by the temperature which was able to melt the *A* stage filling material. When we load such a piece at the elevated temperature, the load will be carried completely by the primary network and consequently the deformation in all its characteristics will be purely elastic. If we have now the load on the sample and lower the temperature, the fusible *A* stage material will return gradually to a solid state again, and surrounding with its large mass the elastically deformed skeleton of the material will keep the piece in its deformed position even when the load is removed. In this state there is an equilibrium between the elastically deformed network and the restraining mass of the filling material. Since the equilibrium is of molecular dimensions, we have the explanation of why the deformation together with the accompanying birefringence can be preserved in any arbitrarily small piece cut out of the original sample.

In order to obtain quantitative results of the properties of some hardening resins at elevated temperature the writer has conducted simple bending and tension tests with Bakelite and Marblette, both of the heat-hardening type. Fig. 3 shows the results of some bending tests with BT-61-893 Bakelite bars.[2] This material is glycerine phthalic anhydride, but being also

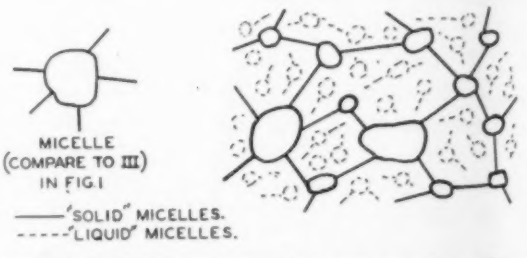


FIG. 2. A hardening resin in the isogel state (according to R. Houwink in the *British Plastics*, 1935).

three-dimensional polymer its molecular structure has the same characteristics as the ones described above for phenol-formaldehyde resins.[3]

The dimensions of the test bars and the loading were the same in each case, only the applied temperature was different as is shown in Fig. 3. It is seen that while the speed of deformation depended on the applied temperature the final amount of deformation was the same in each case. Above 110°C the bar assumed its final deformation in a few seconds after the application of the load; the deformation then remained the same and no creep phenomena could be observed. At 90°C it took about 8 hours for the sample to arrive to the same amount of deformation which it assumed almost instantaneously at 120°C.

On the basis of the above-described theory the structure of hardening resins can be symbolically represented by a parallel coupling of an elastic

spring (the primary network) and a dashpot (the fusible filling material) as shown in Fig. 4. By assigning various viscosity coefficients depending on temperature to the viscous material in the dashpot, the curves of Fig. 3 could be reproduced by such a model. At the moment when an external force $P$ is applied to this model, the load will be carried first mainly by the viscous component, on whose gradual yielding then the elastic spring will come in action, asymptotically approaching the limit where all the load will be carried by the elastic part. The transition will depend on the viscosity coefficient $\eta$ of the material in the dashpot. For phenol-formaldehyde resin in the fusible stage the viscosity coefficient decreases approximately to 1/10 of its value by each 10°C rise in temperature.[4] This means that even if the final deformation takes place at 120°C in 1 to 2 seconds, at room temperature the time required for the sample to arrive to the same amount of deformation under the same loading would be of the order of ten thousand years.

At the annealing temperature, where the resistance of the large fusible part is practically eliminated, great elastic deformation of the samples can be observed. Bakelite material having at room temperature a modulus of

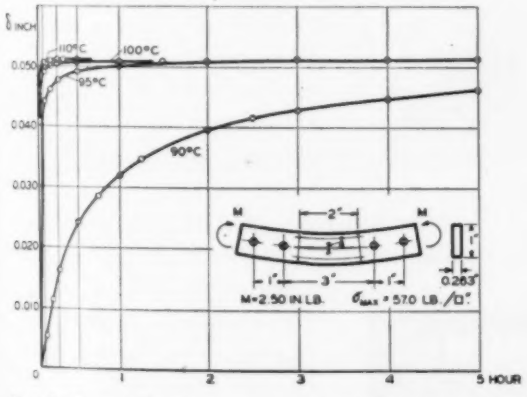


FIG. 3. Time deflection curves for Bakelite at elevated temperature.

elasticity $E=710{,}000$ lb./sq. in. and an optical sensitivity such that 1 isochromatic fringe = 85 lb./sq. in. per inch will give at the annealing temperature $E=1080$ lb./sq. in. and 1 fringe = 3.34 lb./sq. in. per inch which means a reduction of the modulus of elasticity by 640 times while in the optical sensitivity of the

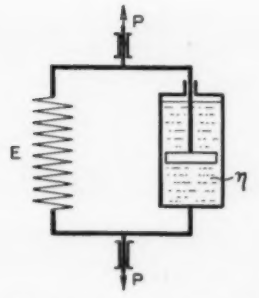


FIG. 4. Mechanical analogy to the structure of hardening resins.

material a 26-fold increase was observable. This means that after the sample has been annealed under the load, upon removal of the loading 1/640 of the deformation and 1/26 of the number of isochromatic bands will be recovered from their respective values produced at the elevated temperature.

The experimental fact that a "frozen" sample preserves its fringe pattern even if it is cut in places is illustrated in Fig. 5. The upper picture shows the fringe pattern in a Bakelite bar after it has been annealed under a concentrated load applied at the center of the span. The lower picture shows the same bar after it has been cut in at two places. During the cutting process some precautions should be taken not to warm up the sample by frictional heat produced by such action. An ordinary, not too fine, mechanically driven jig saw with use of abundant lubricating oil assures good results.

The application of the method to the solution of three-dimensional stress problems is illustrated in Fig. 6. The upper picture shows the Bakelite model, a shaft with a keyway which has been subjected at 115°C to simple bending. After the annealing process thin slices were cut out of the test piece which were then examined in polarized light as is done in the usual photoelastic method. The fringe pictures show the amount of stress concentration (that is the ratio of the peak stress to a properly chosen nominal stress) at two ends of the keyway. At the sled-runner end the maximum stress was observed in the vertical central slice taken through the keyway which gave a stress concentration factor $k=1.38$ while the peak stress at the profiled end was observed in the horizontal surface slice giving $k=1.79$. Both of these concentration factors are

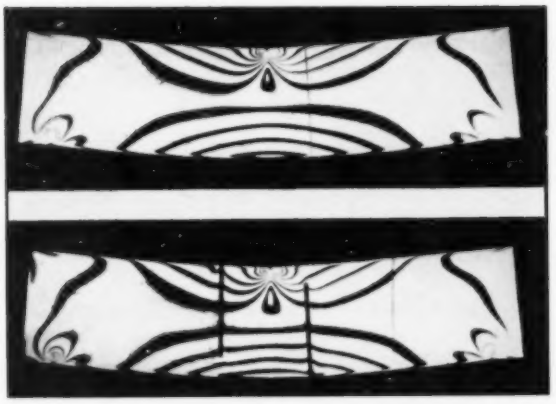

FIG. 5. Illustration showing that careful sawing does not disturb appreciably the frozen fringe pattern.

in good agreement with the results derived from fatigue tests by R. E. Peterson.[5]

This new photoelastic method can be applied in all cases where the test piece is subjected to constant loads. This is the case with rotating disks when the centrifugal loading is constant as long as the speed of rotation of the disk is maintained the same. On the basis of this consideration the method has been used by the writer to determine the distribution of centrifugal stresses in rotating disks. The procedure consisted in rotating the test piece in an oven at elevated temperature (115°C) for about one hour and then slowly cooling it down while maintaining the same speed of rotation. This way a sample was obtained which exhibited a solidified form of the deformations and birefringence produced by the centrifugal stresses at the annealing temperature.

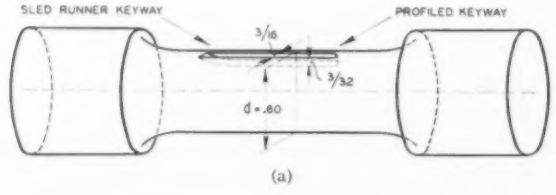


(a)

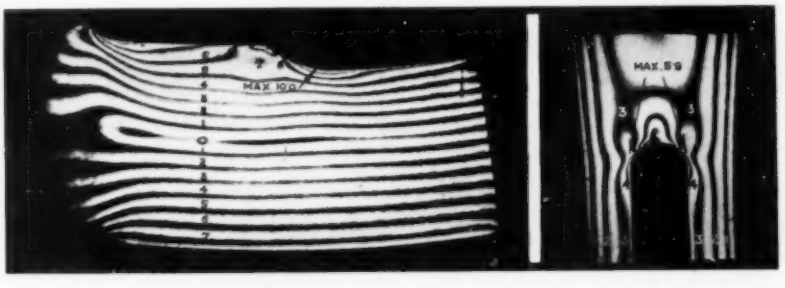


(b) (c)

FIG. 6. Problem of shaft with keyway. (a) View of Bakelite test piece. (b) Vertical slice through sled-runner keyway stress concentration factor $k=10.00/7.25=1.38$. (c) Horizontal slice through profiled keyway $k=5.9/3.3=1.79$.

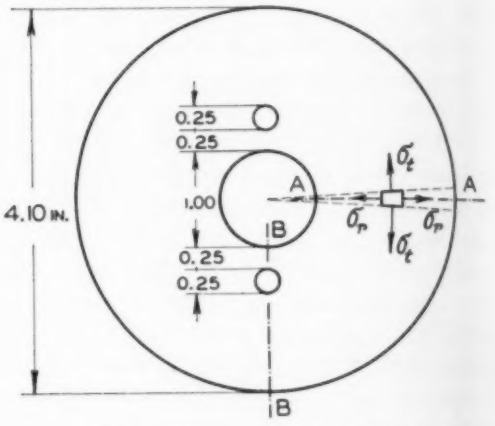


FIG. 7. Dimensions of test piece.

The dimensions of one of the test pieces, a disk with two holes, are shown in Fig. 7. The disk was rotated at a speed of 3100 r.p.m. during the annealing process, and the resulting frozen sample gave then in polarized light an isochromatic fringe pattern as shown in Fig. 8. By calibrating the 0.40-inch thick material (Bakelite 61-893) of the sample it was found that one isochromatic line corresponds to 8.27 lb./sq. in. difference in principal stresses $(\sigma_1-\sigma_2)$.[6] Knowing this from Fig. 8, the difference of principal stresses could be determined at every point of the test piece. In order to derive values for each of the principal stresses, lateral extension measurements were made on the sample determining the change of thickness produced by the centrifugal forces. It is known that the change of thickness $\Delta t=-(\mu t/E)(\sigma_1+\sigma_2)$ is proportional to the sum of principal stresses where $\mu$ is Poisson's ratio and $E$ is the modulus of elasticity. Measuring the thickness of the test piece before test and after the annealing process, these $\Delta t$

values were determined along section $A$–$A$ and $B$–$B$ at several points. Since at the annealing temperature $E=1080$ lb./sq. in. and $\mu=1/2$ due to one fringe value (8.27 lb./sq. in.) a $\Delta t=(0.50\times0.400''/(1080$ lb./sq. in.))8.27 lb./sq. in. $=0.00165''$ lateral extension of the 0.400-inch thick sample will be produced. With a ball pointed micrometer[7] reading 0.0001 inch, this $\Delta t$ value can be measured with about 6 percent accuracy, but for higher stress values the accuracy will be proportionally increased. This way, for both of the symmetry sections $A$–$A$ and $B$–$B$, the values for each of the principal stresses could be determined. The final results are shown in Figs. 9 and 10, respectively.

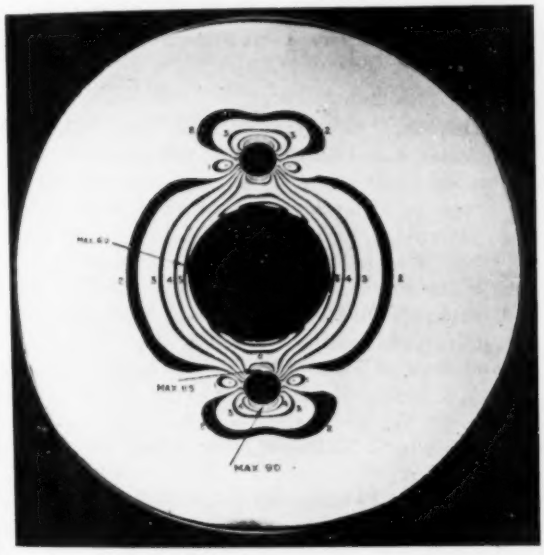

FIG. 8. Isochromatic lines due to centrifugal stresses in a disk with two holes.

For the solid $A$–$A$ section the stresses were computed also analytically.[8] The good agreement found between the theoretical and experimental solution for section $A$–$A$ is shown in Fig. 9. For section $B$–$B$ no theoretical solution is available at present. Considering as concentration factor $k$ for the present case the ratio of the maximum stress at the hole in section $B$–$B$, to the maximum stress which would be produced in a solid section ($A$–$A$) without the hole, a value of $k=95.1/49.6=1.92$ can be derived.

An enlarged picture of the isochromatic pattern around the hole is shown in Fig. 11.

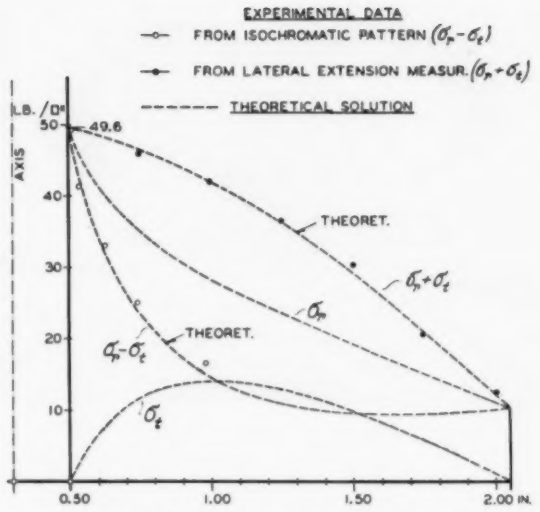


FIG. 9. Principal stresses in section $A$-$A$ (Fig. 7).

Using plane polarized light, the isoclinic lines can be determined at any part of the frozen sample, from which data then the directions of the principal stresses can be derived. This has been carried out on a portion of the sample around the hole and the results are shown in Fig. 12. The results of this test show that from the frozen sample a complete knowledge of the

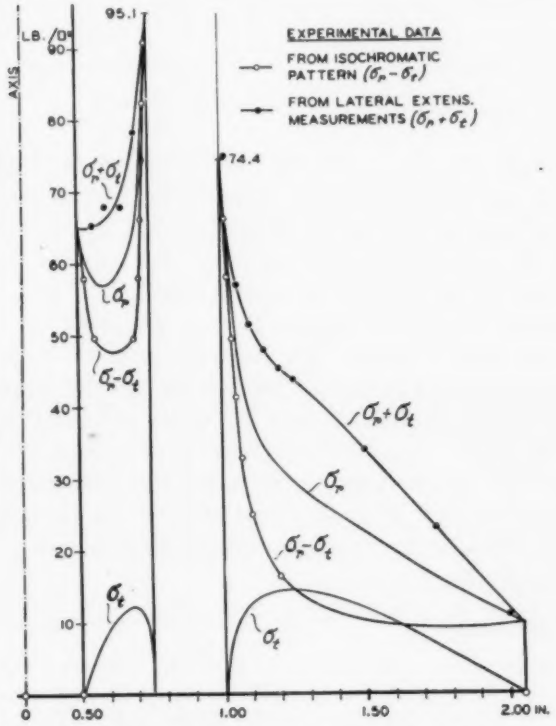


FIG. 10. Principal stresses in section $B$-$B$ (Fig. 7).

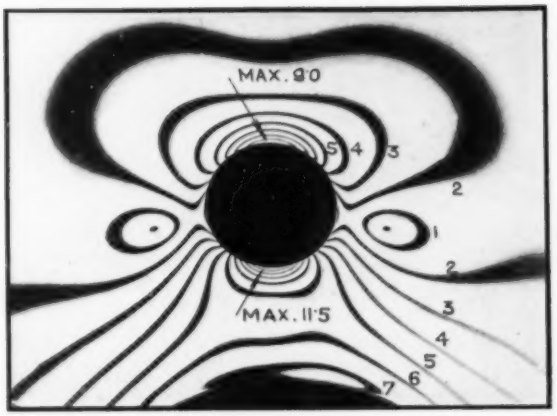


FIG. 11. Isochromatic lines. Detail of Fig. 8.

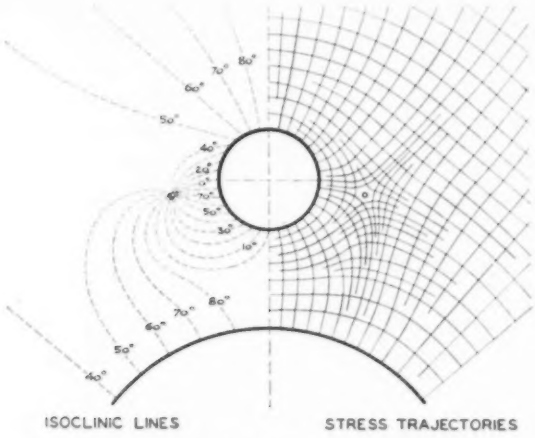


FIG. 12. Direction of principal stresses.

stress system, including the values of both of the principal stresses and their direction at any required point, can be derived.

The annealing process was also applied to rotating disks of various other designs. Fig. 13 shows the frozen fringe pattern obtained in a disk with 8 holes. The samples used in these tests were of constant thicknesses but the same method can be applied to disks of variable thickness. Since with some approximations gravity forces can be replaced by centrifugal loading, the above-described method can be also applied to determining stress distribution due to gravitational forces.

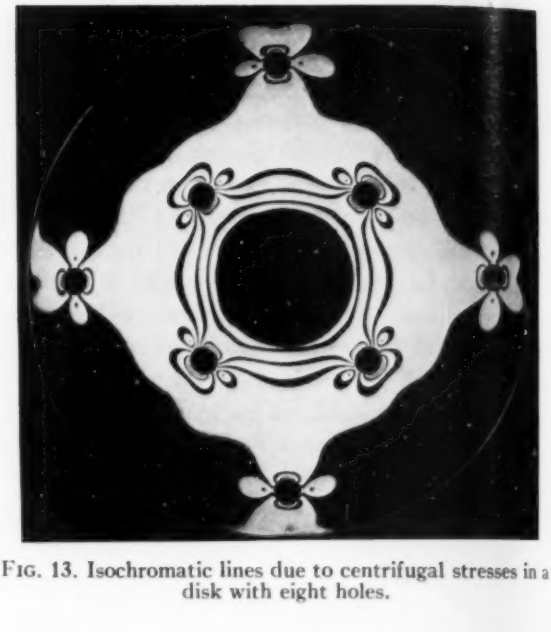

FIG. 13. Isochromatic lines due to centrifugal stresses in a disk with eight holes.

### *References*

1. For further reference see: (a) *The Phenomena of Polymerization and Condensation. A General Discussion Held by the Faraday Society. Sept., 1935*, 412 pages (Gurney and Jackson, London). (b) R. Houwink, *Elasticity, Plasticity and Structure of Matter* (Cambridge University Press, 1937).
2. More detailed results of bending and tension tests, together with other applications of the method can be found in the following publications of the writer: (a) "Photoelastic Studies of Three Dimensional Stress Problems," Proceedings of the Fifth International Congress for Applied Mechanics, Cambridge, Massachusetts, 1938. (b) "The Fundamentals of Three-Dimensional Photoelasticity," J. App. Mechanics, December (1938). Trans. A. S. M. E. **60**, A–149–155.
3. See article by R. Houwink, J. Soc. Chem. Ind. **55**, 247T (1926).
4. R. Houwink: *Physikalische Eigenschaften und Feinbau von Natur- und kunstharzen* (Akademische Verlagsgesellschaft, Leipzig, Germany, 1934), p. 62.
5. R. E. Peterson, "Fatigue of Shafts Having Keyways," presented at the Annual Meeting of the A. S. T. M., 1932.
6. In lines of symmetry, like in sections *A–A* and *B–B*, the direction of the principal stresses will be radial ($\sigma_r$) and tangential ($\sigma_t$), respectively, but at other places their direction will be different from these.
7. This method was suggested first by A. Kuske (*Das Kunstharz Phenolformaldehyd in der Spannungsoptik, Forschung auf d. Gebiete d. Ing. Wesens* (1938), Vol. 9, No. 3) who applied this method to measuring the thickness recovery of slices cut out of three-dimensional samples, after a load-free reannealing of the pieces. In those cases however, on account of the thinness of the slices, errors of not less than 10 percent could be expected.
8. S. Timoshenko, *Theory of Elasticity* (McGraw-Hill Book Company, New York, 1934), p. 68. (The specific gravity of the Bakelite used was 1.365.)

# The Operational Calculus. III*

By Louis A. Pipes**

*Electrical Engineering Department, The University of Wisconsin, Madison, Wisconsin*

## *V. Solution of Linear Partial Differential Equations with Constant Coefficients*

### A. The Vibrating String

As a simple example of the use of the operational method of solving partial differential equations with constant coefficients subject to one-point boundary conditions in one of the independent variables, let us consider the homogeneous wave equation in one dimension

$$\partial^2 u/\partial t^2 = a^2 \partial^2 u/\partial x^2. \tag{132}$$

To take a concrete example, let us consider the case of a vibrating string. In such a case $u$ is the lateral displacement of the string and $a^2 = T/m$, where $T$ is the tension of the string and $m$ is the mass per unit length. Let us consider the string fixed at the extremities $x=0$ and $x=L$, and let the disturbance be initiated with a displacement $u=F(x)$ at $t=0$. We have then, the following boundary conditions

$$u=0 \text{ at } x=0 \quad \text{and} \quad x=L. \tag{133}$$

Let us place

$$U(x, p) \doteqdot u(x, t) \tag{134}$$

and make use of the transforms of the second derivative by Eq. (6).

We then obtain the transform of Eq. (132) in the form

$$d^2U/dx^2 - p^2U/a^2 = -p^2F(x)/a^2, \tag{135}$$

where we have made use of the boundary conditions (133) which depend upon the time. We may consider the transformed equation as an ordinary differential equation in $x$ since $p$ enters only as a parameter. The method of variation of parameters may be used to solve this ordinary differential equation with constant coefficients by assuming a solution of the form

$$U = A(x)\cosh(px/a) + B(x)\sinh(px/a), \tag{136}$$

where we may impose the restriction

$$A'(x)\cosh(px/a) + B'(x)\sinh(px/a) = 0 \tag{137}$$

on the derivatives of the functions $A(x)$ and $B(x)$. Substituting (136) into (135) we obtain

$$A'(x)\sinh(px/a) + B'(x)\cosh(px/a) = -pF(x)/a. \tag{138}$$

Solving (138) and (136) for $A'(x)$ and $B'(x)$ and making use of the boundary conditions (133) on $x$, we obtain

$$A(x) = \int_0^x (p/a)F(v)\sinh(pv/a)dv \tag{139}$$

and

$$B(x) = -\coth(pL/a)\int_0^L (p/a)F(v)\sinh(pv/a)dv + \int_x^L (p/a)F(v)\cosh(pv/a)dv. \tag{140}$$

These values of $A$ and $B$ are substituted into Eq. (125), and we obtain, after some reductions,

$$U(x, p) = \int_0^x \frac{(p/a)F(v)\sinh(pv/a)\sinh p(L-x)/a\,dv}{\sinh(pL/a)} + \int_x^L \frac{(p/a)F(v)\sinh(px/a)\sinh p(L-v)/a\,dv}{\sinh(pL/a)}. \tag{141}$$

* This is the last of a series of three papers. The first and second parts appeared in the March and April issues, respectively.

** Now at Harvard University, Graduate School of Engineering, Pierce Hall, Cambridge, Massachusetts.

Before carrying out the integration with respect to $v$, we may first obtain the function $u(x, t)$ by means of the basic integral

$$u(x, t)=\frac{1}{2\pi i}\int_{c-i\infty}^{c+i\infty} e^{pt}U(x, p)dp/p. \quad (142)$$

For this purpose, we must compute the residues of the expression

$$\frac{F(v)}{a}\frac{e^{pt}\sinh (pv/a)\sinh p(L-x)/a}{\sinh (pL/a)}. \quad (143)$$

The zeros of the denominator, and hence the possible poles are at the values of $p$ for which

$$\sinh (pL/a)=0. \quad (144)$$

Now a product series expansion for $\sinh (z)$ is

$$\sinh (z)=z\prod_{S=1}^{\infty}\left(1+\frac{Z^2}{S^2\pi^2}\right). \quad (145)$$

Hence, $\sinh (z)=0$ at $z=ri\pi$ where $r=0, \pm 1, \pm 2$, etc.

Therefore the integrand has simple poles at $pL/a=ri\pi$ where $r$ has the above values. We may, therefore, write

$$\frac{(p/a)\sinh (pv/a)\sinh p(L-x)/a}{\sinh (pL/a)}\doteq\sum_{r=-\infty}^{r=+\infty}\frac{(ri\pi/L)\sinh (ri\pi v/L)\sinh ri\pi((L-x)/L)e^{ri\pi at/L}}{(ari\pi/L)\cosh (ri\pi)L/a}$$

$$=(2/L)\sum_{r=1}^{\infty}\sin (r\pi v/L)\sin (r\pi x/L)\cos (r\pi at/L). \quad (146)$$

By symmetry, the second term of (141) has the same transform and we may, accordingly, combine the two integrals and write

$$u(x, t)=\sum_{r=1}^{\infty}(2/L)\int_0^L F(v)\sin (r\pi v/L)dv$$

$$\times\sin (r\pi x/L)\cos (r\pi at/L). \quad (147)$$

This is the solution obtained by the classical method of normal coordinates. We note that if we place $t=0$ and hence $u(x, t)=F(x)$ we have

$$F(x)=\sum_{r=1}^{\infty}(2/L)\int_0^L F(v)\sin (r\pi v/L)$$

$$\times\sin (r\pi x/L)dv, \quad (148)$$

the usual Fourier sine series expansion for an arbitrary function $F(x)$ valid in the interval $(0-L)$.

The procedure followed in this example is typical of the way in which partial differential equations are solved by using the Laplacian transform theory. We note that the boundary conditions on the independent variable, $t$, are given at the single point $t=0$. This makes the transformation of the derivatives formally possible.

## B. The General Transmission Line

As a more complicated example of the method, let us consider the problem of determining the voltage and current distribution of a finite transmission line with terminal impedances and constant distributed parameters. If $i(x, t)$ denotes the current and $v(x, t)$ the voltage distribution at a point $x$ on the line, the differential equations giving the voltage and current along the line are:

$$L\frac{\partial i}{\partial t}+Ri=-\frac{\partial v}{\partial x}, \quad C\frac{\partial v}{\partial t}+Gv=-\frac{\partial i}{\partial x}, \quad (149)$$

where $R$ and $L$ are the resistance and inductance coefficients per unit length (including both sides of the line) and $G$ and $C$, are the leakage conductance and capacitance coefficients between the conductors per unit length. Let us now place

$$v(x, t)\doteq V(x, p) \quad \text{and} \quad i(x, t)\doteq I(x, p). \quad (150)$$

Then on the assumption that the initial current and voltage distribution of the line at $t=0$ is zero, we have the transformed equations

$$-dV/dx=(R+Lp)I,$$
$$-dI/dx=(G+Cp)V. \quad (151)$$

Eliminating $I$ between these two equations,

we obtain $$d^2V/dx^2=a^2V, \tag{152}$$

where $a$ is the operational propagation constant and is defined by

$$a^2=(Lp+R)(G+Cp). \tag{153}$$

Integrating the two differential equations, we obtain

$$\begin{aligned} V(x,p)&=A_1e^{-ax}+A_2e^{ax},\\ I(x,p)&=A_3e^{-ax}+A_4e^{ax}. \end{aligned} \tag{154}$$

If we use the Eq. (151), we may eliminate the constants $A_3$ and $A_4$ and obtain

$$V(x,p)=A_1e^{-ax}+A_2e^{ax} \tag{155}$$

and $$I(x,p)=A_1e^{-a}x/Z_0+A_2e^{a}x/Z_0,$$

where $Z_0$ is the characteristic operational impedance of the line and is defined by

$$Z_0=((R+Lp)/(G+Cp))^{\frac{1}{2}}. \tag{156}$$

To determine the constants $A_1$ and $A_2$, we assume an arrangement as shown in Fig. 5.

We assume an e.m.f. $e(t)$ impressed on the line at $x=0$ through a terminal impedance $Z_1$ and the line closed at $x=S$ through a second terminal impedance $Z_2$. We have, therefore, the boundary condition

$$\text{at } x=0 \quad v(0,t)=e(t)-Z_1i(t) \tag{157}$$

and $$\text{at } x=S \quad v(S,t)=Z_2i(S,t).$$

If we assume the impedances $Z_1$ and $Z_2$ to be initially without charges or currents at $t=0$, and let $E(p)\doteqdot e(t)$, we have the boundary conditions to be satisfied by the transforms

$$Z_2I(S,p)=V(S,p) \qquad \text{at } x=S \tag{158}$$

and $$V(0,p)=E(p)-Z_1I(0,p) \quad \text{at } x=0.$$

Substituting the expressions (154) for $V$ and $I$ into the boundary conditions (158), we obtain two equations in the unknown constants $A_1$ and $A_2$. These may be solved and we obtain the following expressions for $A_1$ and $A_2$:

$$\begin{aligned} A_1&=\frac{(1+w)E(p)}{(1+q)(1+w)-(1-q)(1-w)\exp(-2aS)},\\ A_2&=\frac{-(1-w)E(p)\exp(-2aS)}{(1+q)(1+w)-(1-q)(1-w)\exp(-2aS)}, \end{aligned} \tag{159}$$

where

$$q=Z_1/Z_0 \quad \text{and} \quad w=Z_2/Z_0. \tag{160}$$

If these constants are substituted into the Eq. (154) for $I(x,p)$ we find, after some reductions

$$I(x,p)=\frac{E(p)}{(Z_0+Z_1)} \times\frac{\{[\exp(-ax)+b_1\exp(-a[2S-x])]\}}{(1-b_1b_2\exp(-2aS))}, \tag{161}$$

where

$$b_1=(Z_0-Z_1)/(Z_0+Z_1) \tag{162}$$

and $$b_2=(Z_0-Z_2)/(Z_0+Z_2).$$

We then have directly

$$i(x,t)=\frac{1}{2\pi i}\int_{c-i\infty}^{c+i\infty}e^{pt}I(x,p)dp/p. \tag{163}$$

Many interesting special cases may be worked out directly. We note that if $e(t)=A\sin(\omega t)$, then $E(p)=A\omega p/(p^2+\omega^2)$. Evaluation of the integral at the poles $p=\pm i\omega$, gives the steady-state solution of the problem due to an impressed sinusoidal electromotive force. In general, the evaluation of the residues of the integrand to obtain the transient terms is a formidable task. Considerable simplification is effected in case $Z_0=Z_1=Z_2$ or in case the terminal apparatus

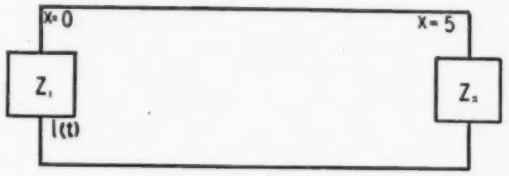


FIG. 5.

has an impedance that is equal to the characteristic impedance of the line. Then $b_1=b_2=0$, and we have

$$I(x,p)=E(p)e^{-ax}/2Z_0. \tag{164}$$

In case we have the further condition that the line parameters satisfy the equation

$$RC=GL, \tag{165}$$

then:

$$I(x,p)=\frac{E(p)\exp\{-Rx(C/L)^{\frac{1}{2}}\}\exp\{-xp(LC)^{\frac{1}{2}}\}}{Z_0}. \tag{166}$$

Now since $e(t) \doteqdot E(p)$, we may use our Theorem V, Eq. (10), which states that

$$\text{if} \qquad g(p) \doteqdot h(t), \tag{10}$$

$$\text{then} \qquad e^{-kp}g(p) \doteqdot \begin{matrix} h(t-k) & t>k, \\ 0 & t<k. \end{matrix}$$

Therefore,

$$i(x, t)=0 \quad \text{for} \quad t<x(LC)^{\frac{1}{2}},$$

$$i(x, t)=\frac{e(t-x(LC)^{\frac{1}{2}})\exp\{-Rx(C/L)^{\frac{1}{2}}\}}{2Z_0} \tag{167}$$

$$\text{for} \quad t>x(LC)^{\frac{1}{2}}.$$

In this case there is no current at the point $x$ until $t=x(LC)^{\frac{1}{2}}$ so the disturbance is propagated with a velocity of $1/(LC)^{\frac{1}{2}}$ and the current has the same form as the voltage impressed at the sending terminal but is attenuated by the exponential term. Such a line is called a distortionless line. Many other interesting special cases may be worked out such as open-ended line, lines short-circuited at the terminals, etc.

We shall now turn to a procedure which will give the solution in the general case. Let us return to our general equation for the transform of the current distribution along the line.

$$I(x, p)=\frac{E(p)}{(Z_0+Z_1)} \cdot \frac{\exp(-ax)+b_2\exp[-a(2S-x)]}{[1-b_1b_2\exp(-2aS)]}. \tag{161}$$

Let us place

$$M=Z_0/(Z_0+Z_1). \tag{168}$$

We may then write

$$I(x, p)=E(p)A(p), \tag{169}$$

where

$$A(p)=\frac{M}{Z_0}\frac{\exp(-ax)+b_2\exp[-a(2S-x)]}{1-b_1b_2\exp(-2aS)}. \tag{170}$$

Expanding $A(p)$ we obtain

$$A(p)=\frac{M}{Z_0}\{\epsilon^{-ax}+b_2\epsilon^{-a(2S-x)}+b_1b_2\epsilon^{-a(2S+x)} +b_1b_2^2\epsilon^{-a(4S-x)}+b_1^2b_2^2\epsilon^{-a(4S+x)}+\cdots+\}. \tag{177}$$

In obtaining the inverse transform of this expression by our basic formula we must have the real part of $p$ positive along the path of integration. Hence the series is absolutely convergent and term by term integration is justified. Therefore the expansion is legitimate.

The quantity $A(p)$ is the operational equivalent of the current distribution along the line due to the application of a constant unit electromotive force at the terminal. Such a quantity is known as the operational indicial admittance of the circuit. The various terms in the series have interesting physical interpretation.

The term $\exp(-ax)/Z_0$ is the operational formula for the current at a distance $x$ of an infinitely long line with unit e.m.f. impressed directly on the line at $x=0$. Let

$$\exp[-a(2S-x)]/Z_0 \doteqdot a_{2S-x}(t). \tag{172}$$

Then $\exp[-a(2S-x)]/Z_0$ is the operational formula for the current flowing at a point $(2S-x)$ of an infinitely long line with a unit electromotive force impressed directly on the line at the terminal. Let

$$\exp(-ax)/Z_0 \doteqdot a_x(t). \tag{173}$$

We now introduce a series of functions, $v_0$, $v_1$, $v_2$, etc. that satisfy the operational equations

$$\begin{matrix} v_0 \doteqdot M(p), & v_2 \doteqdot Mb_1b_2, \\ v_1 \doteqdot Mb_2, & v_3 \doteqdot Mb_1b_2^2, \quad \text{etc.} \end{matrix} \tag{174}$$

Then we may use our basic Theorem III (8b) that if

$$g_1(p) \doteqdot h_1(t) \quad \text{and} \quad g_2(p) \doteqdot h_2(t), \tag{8b}$$

then

$$g_1(p)g_2(p) \doteqdot \frac{d}{dt}\int_0^t h_1(t-u)h_2(u)du.$$

Hence if we let

$$B(x, t) \doteqdot A(x, p), \tag{175}$$

we have

$$B(x, t)=\frac{d}{dt}\int_0^t [v_0(t-u)a_x(u)+v_1(t-u)a_{2S-x} +v_2(t-u)a_{2S+x}+\cdots+]du. \tag{176}$$

Now the first term in the above expression represents the current at a point $x$ of an infinitely long line in response to a unit e.m.f. impressed at $x=0$ through an impedance $Z_1$. The second

term is a reflected wave from the other terminal produced by the irregularity which exists there. The third term is a reflected wave from the sending end terminal, etc.

The current distribution $i(x, t)$ due to the arbitrary e.m.f. $e(x, t)$ is obtained by our basic theorem in the form

$$i(x, t)=\frac{d}{dt}\int_0^t e(t-u)B(u)du. \qquad (177)$$

This so-called wave method of solution is most laborious but entirely possible and may be carried out if the importance of the problem justifies the labor involved.

### C. Application to Heat Conduction

The well-known equation which determines the distribution of temperature in a homogeneous substance of density $D$(g/cm³) specific conductivity $K$(cal./cm sec. °C) and specific heat, $C$(cal./g °C) is

$$\partial U/\partial t=h^2\nabla^2 U, \qquad (178)$$

where $U(x, y, z, t)$ is the temperature distribution in degrees centigrade and $h^2=K/CD$. $h^2$(cm²/sec.) is the thermometric conductivity and we have assumed that there are no sources of heat in the substance. As an application of the operational method of solving this equation, let us consider the problem of the cooling of a uniform rod whose sides are thermally insulated. To fix the problem, let us consider the boundary conditions as follows:

$$U=0 \text{ at } x=0,\ U=S \text{ at } x=L,\ U=S \text{ at } t=0. \qquad (179)$$

That is, the initial temperature of the rod is $U=S$. Then at time $t=0$, the end $x=0$ is cooled to temperature zero and maintained at that temperature. The end $x=L$ is kept at temperature $S$. The problem is to find the variation of temperature at other points of the rod.

In this one-dimensional case, the equation for the temperature distribution reduces to

$$\partial U/\partial t-h^2\partial^2 U/\partial x^2=0. \qquad (180)$$

Let $V\doteq U$ and we obtain the transformed equation

$$pV-h^2d^2V/dx^2=pS, \qquad (181)$$

where we have made use of the boundary condition $U=S$ at $t=0$. If we let

$$q^2=p^2/h^2, \qquad (182)$$

we must solve the inhomogeneous equation

$$d^2V/dx^2-q^2V=-q^2S \qquad (183)$$

subject to the boundary conditions (179) in $x$.

The solution of this equation subject to these boundary conditions is easily obtained by the method of variation of parameters and may be written in the form

$$V=S[1-\sinh q(L-x)/\sinh (qL)] \qquad (184)$$

and we have from our basic integral

$$U(x, t)=\sum_{\text{residues}} (Se^{pt})/p[1-\sinh q(L-x)/\sinh (qL)]. \qquad (185)$$

The residue at $p=0$ is

$$S[1-(L-x)/L]=Sx/L. \qquad (186)$$

If we now recall the product series expansion of the function sinh $(z)$ as in Eq. (145), we see that the other zeros of the denominator are at

$$q^2=-\pi^2r^2/L^2,\quad r=1, 2, 3, \cdots \qquad (187)$$

or

$$p=-\pi^2r^2h^2/L^2.$$

Summing the residues, the solution may be written in the form

$$U(x, t)=S[x/L+\sum_{n=1}^{\infty}(2/n\pi)\sin (n\pi x/L) \times\exp (-n^2\pi^2h^2t/L^2)]. \qquad (188)$$

This is a rapidly converging series. We see that as $t\to\infty$ the temperature tends to the steady distribution, $U=Sx/L$.

### D. General Considerations

From the above examples illustrating the use of the Laplacian transformation in the solution of some of the partial differential equations of mathematical physics, we see that the method is applicable where we deal with linear equations with constant coefficients having one-point boundary conditions in one independent variable, which in physical problems, is usually the time.

The application of the Laplacian transformation reduces the partial differential equation in two independent variables to an ordinary differential equation in one independent variable which may then be solved and then the calculation of the inverse transform gives the solution of the problem. In the case of more than two independent variables, the method of procedure is similar except that in this case the transform satisfies a partial differential equation rather than an ordinary one and hence the solution is somewhat more complicated.

### *VI. Evaluation of Integrals*

Operational processes may be employed to advantage in the evaluation of certain definite integrals. Many integrals may be evaluated by means of the following theorem:

If
$$g(p) \doteqdot h(t), \tag{189}$$

then
$$\int_0^\infty g(p)dp/p = \int_0^\infty h(t)dt/t.$$

The proof of this theorem is as follows:
By hypothesis

$$g(p)/p = \int_0^\infty e^{-pt}h(t)dt.$$

Hence,

$$\int_0^\infty g(p)dp/p = \int_0^\infty \left[\int_0^\infty e^{-pt}h(t)dt\right]dp.$$

But

$$\int_0^\infty e^{-pt}dp = 1/t$$

and, therefore, we obtain

$$\int_0^\infty g(p)dp/p = \int_0^\infty h(t)dt/t.$$

As an example, let it be required to evaluate the integral

$$\int_0^\infty \sin(t)dt/t. \tag{190}$$

Now by (38), $p/(p^2+1) \doteqdot \sin(t)$ therefore,

$$\int_0^\infty \sin(t)dt/t = \int_0^\infty dp/(p^2+1) = \left[\tan^{-1} p\right]_0^\infty = \pi/2. \tag{191}$$

As a second example, consider the integral

$$\int_0^\infty \frac{[e^{-at}-e^{-bt}]dt}{t}. \tag{192}$$

Now by (23), $p/(p+a) \doteqdot e^{-at}$, therefore,

$$\int_0^\infty \frac{[e^{-at}-e^{-bt}]dt}{t} = \int_0^\infty [1/(p+a)-1/(p-b)]dp = \log(b/a). \tag{193}$$

Another method depends on the use of a parameter that may be operationally represented. As an example, consider the integral

$$\int_0^\infty e^{-x^2}dx. \tag{194}$$

This is usually evaluated by a trick. Let $t \doteqdot 1/p$ and consider

$$\int_0^\infty e^{-tx^2}dx. \tag{195}$$

Now by (23) $p/(p+x^2) \doteqdot e^{-tx^2}$, hence

$$\int_0^\infty e^{-tx^2}dx \doteqdot \int_0^\infty pdx/(p^2+x^2) = \sqrt{p}\tan^{-1} x/\sqrt{p}\Big]_0^\infty = \frac{\pi}{2}\sqrt{p}. \tag{196}$$

But by (19), $\sqrt{p} \doteqdot 1(\pi t)^{\frac{1}{2}}$ and, therefore

$$\int_0^\infty e^{-tx^2}dx = (1/2)(\pi/t)^{\frac{1}{2}}. \tag{197}$$

If we place $t=1$, we obtain

$$\int_0^\infty e^{-x^2}dx = \sqrt{\pi}/2. \tag{198}$$

As a further example, consider

$$\int_0^\infty \cos(tx)dx/(1+x^2). \tag{199}$$

As before, let $t \doteqdot 1/p$. Now by (39) $\cos(tx) \doteqdot p^2/(p^2+x^2)$ and, therefore,

$$\int_0^\infty \cos(tx)dx/(1+x^2)$$

$$\doteqdot \int_0^\infty p^2 dx/(p^2+x^2)(1+x^2) = (\pi/2)p/(p+1). \quad (200)$$

But by (23) $p/(p+1) \doteqdot e^{-t}$, hence,

$$\int_0^\infty \cos(tx)dx/(1+x^2) = (\pi/2)e^{-t}, \quad (201)$$

or, placing $t=1$,

$$\int_0^\infty \cos(x)dx/(1+x^2) = (\pi/2)1/e. \quad (202)$$

The above illustrative examples show the general procedure.

## *VII. Solution of Integral Equations*

### A. Application to Electric Circuit Theory

Consider a series circuit containing linear, lumped, constant parameters of resistance $R$, inductance, $L$ and capacitance $C$, in series with an arbitrary electromotive force $e(t)$. The integro-differential equation of such a circuit is

$$Ldi/dt + Ri + (1/C)\int_{-\infty}^{t} idt = e(t). \quad (65a)$$

If we let: $I(p) \doteqdot i(t)$ and $e(t) \doteqdot E(p)$, and assume the circuit to be initially without charge or current, then (65) transforms into

$$Z(p)I(p) = E(p), \quad (203)$$

where

$$Z(p) = Lp + R + (1/Cp). \quad (204)$$

Now using our basic theorem (8), we see that if we let

$$A(t) \doteqdot 1/Z(p), \quad (205)$$

where $A(t)$ is the indicial admittance of the circuit, or the current response to a unit electromotive force impressed at $t=0$, then we have

$$i(t) = \frac{d}{dt}\int_0^t A(t-u)e(u)du$$

$$= \frac{d}{dt}\int_0^t A(u)e(t-u)du. \quad (206)$$

*Variable circuits.*—To illustrate the use of integral equations, let us consider the case of a variable circuit, that is, a circuit that has one or more elements varying with the time. To be specific, let us consider a series circuit containing the invariable elements $L$, $R$, $C$, in series with the variable elements, $L_v(t)$, $R_v(t)$, and $C_v(t)$ which are functions of the time, and connected to a source of e.m.f. $e(t)$.

This circuit may be treated as an invariable circuit by eliminating the variable elements $R_v$, $L_v$, $C_v$, and inserting an electromotive force $e_r(t) = i(t)R_v$ across the variable resistance, $e_L = (d/dt)[L_v(t)i(t)]$ across the variable inductance and

$$e_c = [1/C_v(t)]\int_0^t i(t)dt$$

across the variable capacitance. If we let $e_v = e_L + e_R + e_c$, then $-e_v$ represents the potential drop across these variable elements. We may, therefore, regard the total electromotive force impressed on the circuit to be:

$$[e(t) - e_v(t)], \quad (207)$$

and obtain

$$i(t) = \frac{d}{dt}\int_0^t [e(u) - e_v(u)]A(t-u)du. \quad (208)$$

In the case of a variable resistance element alone, we have

$$i(t) = \frac{d}{dt}\int_0^t e(u)A(t-u)du$$

$$- \frac{d}{dt}\int_0^t r_v(u)i(u)A(t-u)du. \quad (209)$$

In the absence of the element $r_v$, the current would be given by the first term on the right of this equation. This, then, represents the current that would flow in an invariable circuit of indicial admittance $A(t)$. We may, therefore, write

$$i(t)=i_0(t)-\frac{d}{dt}\int_0^t r_v(u)i(u)A(t-u)du. \quad (210)$$

Since the unknown occurs under the sign of integration, this is an integral equation. An effective method of solution is the following one. Let

$$i(t)=i_0(t)-i_1(t)+i_2(t)-i_3(t)+\cdots. \quad (211)$$

Now if we define the terms in the series so that

$$\begin{aligned} i_0(t)&=\frac{d}{dt}\int_0^t e(u)A(t-u)du,\\ i_1(t)&=\frac{d}{dt}\int_0^t r_v(u)i_0(u)A(t-u)du, \quad (212)\\ &\cdots\cdots\cdots\cdots\\ i_{(n+1)}(t)&=\frac{d}{dt}\int_0^t r_v(u)i_n(u)A(t-u)du. \end{aligned}$$

We find by direct substitution into the integral equation that this series formally satisfies the integral equation. An operational method of computing the terms in the series may be carried out as follows: Since $i_0(t)$ is the current flowing in the invariable network, its computation presents no difficulty. We have $A(t)\doteqdot 1/Z$, $r_v(t)$ is a known time function and hence the transform

$$b_1(p)\doteqdot r_v(t)i_0(t) \quad (213)$$

may be computed. Then we have directly

$$I_1(p)=b_1(p)/Z(p)\doteqdot i_1(t) \quad (214)$$

and hence $i_1(t)$ may be computed. Now if we let

$$b_2(p)\doteqdot r_v(t)i_1(t), \quad (215)$$

therefore

$$I_2(p)=b_2(p)/Z(p)\doteqdot i_2(t) \quad (216)$$

and $i_2(t)$ can be found. In general if

$$b_{n+1}(p)\doteqdot r_v(t)i_n(t), \quad (217)$$

then $$I_{n+1}(p)=b_{n+1}(p)/Z(p)\doteqdot i_{n+1}(t). \quad (218)$$

In general the operational manner of handling the set of integrals is simpler than direct computation. In case the magnitude of the variable element is small in comparison to the invariable elements, the series converges rapidly.

## B. Solution of Volterra's Integral Equations of the Second Kind

Let us consider the equation

$$F(t)=CG(t)+\int_0^t G(u)K(t-u)du, \quad (219)$$

where $F(t)$ is a known given function, $C$, is a constant parameter, and $K(t)$ is a known function called the nucleus. $G(t)$ is the unknown function to be determined. Eq. (219) is a Volterra's integral equation of the second kind with the special nucleus $K(t-u)$. If $C=0$, we have Volterra's integral equation of the first kind. Let us introduce the transforms

$$G(t)\doteqdot g(p), \quad F(t)\doteqdot f(p), \quad K(t)\doteqdot k(p). \quad (220)$$

Then, in view of the fact that by one of our fundamental theorems

$$\int_0^t G(u)K(t-u)du\doteqdot g(p)k(p)/p \quad (8a)$$

the integral equation (219) may be transformed into

$$f(p)=Cg(p)+g(p)k(p)/p \quad (221)$$

or

$$g(p)=f(p)/[C+k(p)/p] \quad (222)$$

and we have explicitly by our fundamental integral

$$G(t)=\frac{1}{2\pi i}\int_{c-i\infty}^{c+i\infty}\frac{e^{pt}f(p)dp}{Cp+k(p)}. \quad (223)$$

As an example, let us consider Abel's integral equation:

$$F(t)=\int_0^t\frac{G(u)du}{(t-u)^n} \quad \text{for } 0<n<1. \quad (224)$$

This is a special case in which $C=0$ and $K(t)=t^{-n}$. Now by (19) we have $t^{-n}\doteqdot\Gamma(1-n)/p^{-n}$ in the range $0<n<1$. Accordingly

$$g(p)=\frac{f(p)}{p^{n-1}\Gamma(1-n)} \quad (225)$$

is the transformed equation. Now from our basic transform (19) we have: $1/p^s\doteqdot t^s/\Gamma(s+1)$, hence, we obtain

$$\frac{1}{p^{n-1}\Gamma(1-n)} \doteqdot \frac{1}{\Gamma(1-n)\Gamma(n)t^{1-n}}. \quad (226)$$

Now, by a theorem on $\Gamma$ functions, we have

$$\Gamma(1-n)\Gamma n = \pi/\sin(n\pi), \quad 0<n<1 \quad (227)$$

therefore,

$$1/p^{n-1}\Gamma(1-n) \doteqdot \sin(n\pi)/\pi t^{1-n} \quad (228)$$

and since $f(p) \doteqdot F(t)$, we have the explicit solution of Abel's integral equation in the form

$$f(p)/p^{n-1}\Gamma(1-n)$$

$$\doteqdot \frac{\sin(n\pi)}{\pi}\frac{d}{dt}\int_0^t \frac{F(u)du}{(t-u)^{1-n}} = G(t). \quad (229)$$

As a second example, let us consider

$$\cosh(x) = \int_0^x G(u)\cos(x-u)du. \quad (230)$$

Now from our list of transforms we have

$$\cosh(x) \doteqdot p^2/(p^2-1), \quad (41a)$$

$$\cos(x) \doteqdot p^2/(p^2+1). \quad (39a)$$

Hence the transformed equation is

$$g(p) = p(p^2+1)/(p^2-1) \quad (231)$$

and calculating the inverse transform we obtain the explicit solution

$$G(x) = 2\sinh(x). \quad (232)$$

### *VIII. Differential Equations with Variable Coefficients*

By considering the direct operational solution of certain differential equations with variable coefficients, the operational equivalents of the functions which satisfy the differential equations may be obtained and the properties of these functions studied in an operational manner.

As an example, let the equation satisfied by the Bessel functions be considered. This equation may be written in the form

$$\frac{d^2z}{du^2} + \frac{1}{u}\frac{dz}{du} + [1-n^2/u]z = 0. \quad (233)$$

If the change in variables $z = u^{-n}y$ and $u^2 = 4x$ is made, the equation transforms into

$$xd^2y/dx^2 + (1-n)dy/dx + y = 0. \quad (234)$$

As in the case of equations with constant coefficients, we let

$$X(p) = \int_0^\infty e^{-px}y(x)dx \quad (235)$$

or

$$pX(p) \doteqdot y(x).$$

By integration by parts, we may construct the following list of formulas:

$$y \rightarrow X, \quad (236)$$

$$xy \rightarrow -dX/dp, \quad (237)$$

$$x^2y \rightarrow d^2X/dp^2, \quad (238)$$

$$dy/dx \rightarrow -y(0) + pX, \quad (239)$$

$$xdy/dx \rightarrow \frac{-d}{dp}(pX), \quad (240)$$

$$x^2dy/dx \rightarrow \frac{d^2}{dp^2}(pX), \quad (241)$$

$$\frac{d^2y}{dx^2} \rightarrow -y'(0) - py(0) + p^2X, \quad (242)$$

$$\frac{xd^2y}{dx^2} \rightarrow y(0) - \frac{d}{dp}(p^2X), \quad (243)$$

$$x^2d^2y/dx^2 \rightarrow \frac{d^2}{dp^2}(p^2X), \quad (244)$$

where we have used the notation that if

$$X(p) = \int_0^\infty e^{-px}y(x)dx$$

then

$$y \rightarrow X(p).$$

If we apply these transformations to (234) and take $y(0) = 0$, we obtain

$$\frac{pd(pX)}{dp} + (n-1/p)pX = 0. \quad (245)$$

Integrating this differential equation in $(pX)$ we obtain

$$pX = Cp^{-n}e^{-1/p}. \quad (246)$$

If we adjust the constant $C$ to the ordinary normalization of the Bessel functions, we obtain the transform

$$p^{-n}e^{-1/p} \doteqdot x^{n/2}J_n(2\sqrt{x}) \quad \text{valid for } n > -1. \quad (247)$$

We may now use our fundamental theorems to obtain some fundamental properties of the function $J_n$. By Theorem I, (6) we have that if:

$$g(p) \doteqdot h(x)$$

then

$$pg(p) \doteqdot \frac{d}{dx}h(x)$$

if $h(0)=0$. Hence applying this to (247) we obtain

$$p^{-n+1}e^{-1/p} \doteqdot \frac{d}{dx}[x^{n/2}J_n(2\sqrt{x})] = x^{(n-1)/2}J_{n-1}(2\sqrt{x}) \quad (248)$$

or

$$(n/x)J_n(x)+J_n'(x)=J_{n-1}(x). \quad (249)$$

If we multiply by $p^n$ and make use of repeated applications of Theorem I, (6), we obtain

$$\frac{d^n}{dx^n}[x^{n/2}J_n(2\sqrt{x})] \doteqdot p^n p^{-n}e^{-1/p} = e^{-1/p} \doteqdot J_0(2\sqrt{x}) \quad (250)$$

or

$$(d/xdx)^n[x^nJ_n(x)]=J_0(x). \quad (251)$$

From the above result we have

$$e^{-1/p} \doteqdot J_0(2\sqrt{x}) \quad (252)$$

and if we now make use of a theorem that if

$$g(p) \doteqdot h(x) \quad (253)$$

then

$$g(p/s) \doteqdot h(sx)$$

where $s$ is a constant whose absolute value is greater than zero. If we apply this to (252), we obtain:

$$e^{i/p} \doteqdot J_0(2(-ix)^{\frac{1}{2}}) = Ber(2\sqrt{x})+iBei(2\sqrt{x}) \quad (254)$$

and

$$e^{-i/p} \doteqdot J_0(2(ix)^{\frac{1}{2}}) = Ber(2\sqrt{x})-iBei(2\sqrt{x}). \quad (255)$$

Hence, separating reals and imaginaries, we have

$$\cos(1/p) \doteqdot Ber(2\sqrt{x}), \quad (256)$$

$$\sin(1/p) \doteqdot Bei(2\sqrt{x}). \quad (257)$$

These two formulas may be used to compute many interesting properties of these functions. The plan followed in this example on Bessel's equation may be carried out in the case of several other linear differential equations with variable coefficients and the properties of their solutions thus studied.

### *IX. Discontinuous Functions*

In many cases of physical interest, the electromotive forces acting on an electrical system or the forces acting on a mechanical system are discontinuous in nature. Usually these functions are periodic in nature and their effect may be computed by expanding them in a Fourier series and computing the effect of the harmonic terms separately. In case the problem is attacked operationally, however, the transforms of the discontinuous functions may be computed and then the computation of the inverse transform of the equation gives the desired solution.

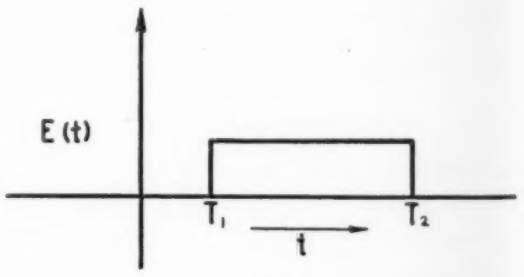


FIG. 6.

In order to give a simple illustration of the general procedure that may be followed in a typical physical problem of this type let us consider the case of a pulse of voltage applied to a simple circuit consisting of a resistance and inductance in series.

The equation satisfied by the current in such a circuit is

$$di/dt+(R/L)i=E(t)/L. \quad (258)$$

We will consider $E(t)$ to be a pulse of voltage as shown in Fig. 6. It has a constant magnitude $E$ and is formed at $t=T_1$ and ceases at $t=T_2$. Let us further assume that at $t=0$ there is an initial current flowing in the circuit $i=i_0$. Proceeding in the usual manner, we let

$$I(p) \doteqdot i(t). \quad (259)$$

By Theorem V, (10), the transform of the voltage pulse is

$$E[e^{-T_1 p}-e^{-T_2 p}] \tag{260}$$

and the transform of Eq. (258) is

$$I(p)=\frac{1}{(p+R/L)}\left(pi_0+\frac{E}{L}[e^{-T_1 p}-e^{-T_2 p}]\right). \tag{261}$$

By the use of transforms (23) and (10), we have

$$\begin{aligned} i(t)&=i_0e^{-Rt/L}, && 0<t<T_1,\\ i(t)&=i_0e^{-Rt/L}+E/R-(E/R)e^{-R(t-T_1)/L}, && T_1<t<T_2,\\ i(t)&=i_0e^{-Rt/L}-(E/R)e^{-R(t-T_1)/L} && \\ &\quad +(E/R)e^{-R(t-T_2)/L}, && t>T_2. \end{aligned} \tag{262}$$

More complicated cases may be handled in the same manner. The method is particularly valuable in case the function is not periodic and hence does not admit a Fourier series expansion. If the function does admit a Fourier series expansion, the application of this method yields a solution in closed form for any desired value of the time.

## *X. Conclusion*

The many fields in which the operational method is a valuable tool should be apparent from the above account. It has been the purpose of this discussion to present typical problems in a varied group of problems and to show how such problems may be attacked operationally. The reader who desires a more detailed account of the various fields of application here discussed so briefly will find the following bibliography to standard treatises and fundamental papers of value. It may be pointed out that some of the standard treatises do not base their discussion on the more general Laplacian transform point of view but follow the heuristic treatment of Heaviside. However, all results and theorems of these accounts may be translated without difficulty into Laplacian transform language, and proofs that are rather vague are seen to be clear-cut applications of the notion of contour integration. It is hoped that this account will help the reader bridge the gap between the two methods of presentation, and give him a sense of the utility of these methods.

## *Bibliography*


*A. Introduction and Historical Background*

1. H. T. Davis, *The Theory of Linear Operators* (Principia Press, 1936). An extensive account of linear operators in general. A discussion of the Laplacian transform is included. This treatise includes a very comprehensive bibliography.

2. E. Stephens, *The Elementary Theory of Operational Mathematics* (McGraw-Hill, 1937). An extensive account of differential operators. This book contains an excellent historical account and a bibliography.

3. J. L. Lagrange, *Mecanique Analytique* (1788), Vol. 7, p. 390.

*B. The Laplacian Transformation*

1. R. Courant und D. Hilbert, *Methoden der Mathematischen Physik* (Springer, 1924), Vol. 1, pp. 87–89. The development of the Laplacian transformation is carried out from the Fourier-Integral.

2. E. T. Whittaker and G. N. Watson, *Modern Analysis* (Cambridge, 1927), p. 115–116.

3. H. Bateman, *Report to the British Association* (1910). A comprehensive account of researches on integral equations.

4. G. Giorgi, "On the Functional Dependence of Physical Variables," Proc. International Math. Congress, Toronto 2, 31–56 (1924).

5. D. P. Dalzell, "Heaviside's Operational Method," Proc. Phys. Soc. London **42**, 41–2 (1928–30).

6. V. Bush, *Operational Circuit Analysis* (Wiley, 1929). Introduces the Fourier transform point of view.

*C. Development of Heaviside's Rules*

1. H. W. March, "The Heaviside Operational Calculus" Bull. Am. Math. Soc. **33**, 311–318 (1927).

2. H. Jeffreys, *Operational Methods in Mathematical Physics* (Cambridge, 1931).

3. M. S. Vallarta, "Heaviside's Proof of his Expansion Theorem," J. Am. Inst. Elec. Eng. **45**, 383–387 (1926).

*D. Solution of Linear Integro-Differential Equations with Constant Coefficients*

1. B. van der Pol, "A Simple Proof and an Extension of Heaviside's Operational Calculus for Invariable Systems," Phil. Mag. **7**, 1153–1162 (1929).

2. L. A. Pipes, "Laplacian Transform Circuit Analysis," Phil. Mag. **24**, 502–511 (1937).

3. L. A. Pipes, "Matrix-Operational Methods in Mechanical Vibrations," J. Frank. Inst. **225**, 343–49 (1938).

4. T. J. Bromwich, "Normal Coordinates in Dynamical Systems," Proc. London Math. Soc. **23** (2), 355–58 (1924).

5. E. J. Berg, *Heaviside's Operational Calculus* (McGraw-Hill, 1929). Extensive application to circuit theory.

6. Louis Cohen, *Heaviside's Electrical Circuit Theory* (McGraw-Hill, 1927).

*E. Solution of Linear Partial Differential Equations with Constant Coefficients*

1. H. Jeffreys, *Operational Methods in Mathematical Physics* (Cambridge University Press, 1931). This treatise contains an excellent exposition of the methods of Bromwich and applications to various physical problems. A bibliography to original papers is included.

2. E. J. Berg, *Heaviside's Operational Calculus* (McGraw-Hill, 1929).

3. J. R. Carson, *Electric Circuit Theory and the Operational Calculus* (McGraw Hill, 1926). An excellent discussion based upon the Laplace integral equation. The theory is extensively developed and applied to problems of circuit theory.

4. A. Lowan, "On the Operational Treatment of Certain Electrical and Mechanical Problems," Phil. Mag. **17**, 1134–1144 (1934); Phys. Rev. **44**, 769 (1933).

5. R. V. Churchill, "The Inversion of the Laplace transformation by a Direct Expansion in Series and its Application to Boundary-Value Problems," Mathematische Zeits. **42**, 567–579 (1937).

6. R. V. Churchill, "The Solution of Linear Boundary-Value Problems in Physics by Means of the Laplace Transformation," Mathematische Annalen **114**, 591–613 (1937).

*F. Evaluation of Integrals*

1. B. van der Pol, "On the Operational Solution of Linear Differential Equations and an Investigation of the Properties of these Solutions," Phil. Mag. **8**, 861–898 (1929).

2. G. Boole, "On the Inverse Calculus of Definite Integrals," Cambridge Math. J. **4**, 82–87 (1845).

3. Oliver Heaviside, *Electromagnetic Theory* (Benn Brothers, 1912), Vol. 3, p. 234.

*G. Solution of Integral Equations*

1. S. Koizumi, "Solution of Integral Equations," Phil. Mag. **11**, 7th series, 432 (1931).

2. J. R. Carson, "Theory and Calculation of Variable Electrical Systems," Phys. Rev. **17**, 116–134 (1921).

3. L. A. Pipes, "Operational and Matrix Methods in Linear Variable Networks," Phil. Mag. **25**, 585–600 (1938).

*H. Differential Equations with Variable Coefficients*

1. B. van der Pol, "On the Operational Solution of Linear Differential Equations and an Investigation of the Properties of these Solutions," Phil. Mag. **8**, 861–898 (1929).

2. B. van der Pol, "Symbolic Calculus," Phil. Mag. **13**, 537–577 (1932).

3. H. V. Lowry, "On the Operational Calculus," Phil. Mag. **13**, 1144–1163 (1932).

*I. Discontinuous Functions*

1. O. Heaviside, *Electromagnetic Theory* (Benn Brothers, 1912), Vol. 2.

2. B. van der Pol, "On the Operational Solution of Linear Differential Equations and an Investigation of the Properties of these Solutions," Phil. Mag. **8**, 861–898 (1929).

3. L. A. Pipes, "Operational Representation of Discontinuous Functions," J. Frank. Inst. **225**, 53–61 (1938).

For a fuller bibliography, the reader is referred to the treatises by Davis and Stephens.

# Resumés of Recent Research

**Recent advances in experimental and theoretical physics are described in these columns in nontechnical language. It is intended that sufficient background be given to introduce the reader to the subject.**

**The Further Concentration of $N^{15}$**

The early methods of separating isotopes depended on differences in physical properties related directly to mass. Several of these methods have been developed in recent years to produce substantial changes in isotopic ratios but yield only small quantities of product. Because relatively large amounts of the isotopes are needed for biological tracer work, as well as for many investigations of physical properties of the isotopes and their compounds, other methods of separation had to be developed. The electrolytic method proved to be most successful for concentrating large amounts of deuterium but it is not practical for concentrating isotopes of the other light elements.

Small differences in the chemical properties of the isotopes of the light elements which were first predicted by theoretical considerations of the isotopic molecules and later confirmed by experiment, made it possible for Professor Urey and his co-workers to develop chemical methods of separation.[1] Recently H. G. Thode and H. C. Urey[2] reported the successful concentration of nitrogen (15) in relatively large quantities. Their method depends on the isotopic exchange between ammonia gas and an ammonium salt solution according to the equation

$$N^{15}H_3\,\text{gas} + N^{14}H_4^+\,\text{solution} \rightleftarrows N^{14}H_3\,\text{gas} + N^{15}H_4^+\,\text{solution},$$

for which the equilibrium constant is about 1.023. This means that if we shake ammonia gas with an ammonium salt in water there will be 2.3 percent more $N^{15}$ in the salt solution than in the ammonia gas. This effect has been multiplied many times by using a counter current flow of ammonium salt in water and ammonia gas in apparatus of the distillation column type. The process consists of a flow of the liquid phase down through a fractionating column, liberation of the ammonia by the addition of sodium hydroxide and subsequent boiling and the return of the ammonia up through the column. Nitrogen (15) is transported down the column since it concentrates in the liquid phase.

A six-and-a-half-fold change in the concentration of $N^{15}$ was obtained by this method, using

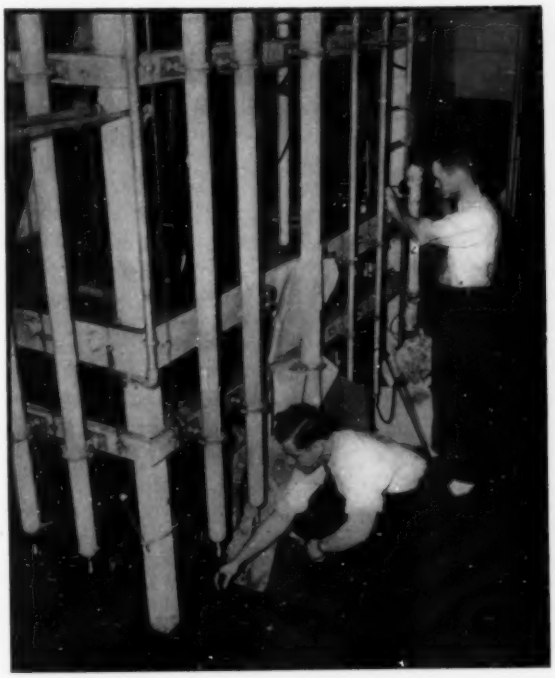

FIG. 1.

[1] Urey and Greiff, J. Am. Chem. Soc. **57**, 321 (1935); H. C. Urey and A. H. W. Aten, Jr., Phys. Rev. **50**, 575 (1936); Urey, Huffman, Thode and Fox, J. Chem. Phys. **5**, 856 (1937); Thode, Gorham and Urey, J. Chem. Phys. **6**, 296 (1938).

[2] H. G. Thode and H. C. Urey, J. Chem. Phys. **7**, 34 (1939).

a single column. In order to produce higher concentrations of $N^{15}$ Thode and Urey designed a cascade system of columns such that a smaller second column operates on the product from the first and a third column operates on product from the second. This system will come to a steady state producing high concentrations of $N^{15}$ in much less time than a single column of equal length but the same size throughout.

The three columns of the cascade reached a maximum concentration of 72.8 percent $N^{15}$ in four weeks of continuous operation. This represents a 702-fold change in the ratio of the nitrogen isotopes. The columns transported one gram of $N^{15}$ per 24 hours, an amount 1000 times that transported by the Hertz cascade diffusion method. In one run Thode and Urey produced 8.8 grams of 72.6 percent $N^{15}$, an amount sufficient for many investigations of physical properties of $N^{15}$ and its compounds. In addition large quantities of material were produced having ten times the natural concentration of $N^{15}$ or better. This material is very valuable in the biological tracer work now in progress.

**Photographic Theory** The grains of a photographic emulsion, flat microscopic crystals of silver halide, are distributed haphazardly throughout the thickness of the emulsion layer. Owing to the gradual absorption of radiation in traversing the emulsion, the grains placed at a greater depth receive a weaker exposure than those spread at or nearer to the upper surface of the layer. This changes perceptibly the photographic density (blackening) produced by a given total exposure. The contribution to density due to a single grain depends essentially on its size (area), apart from its intrinsic sensitivity and since in practice every emulsion contains a wide range of grain sizes, the elementary contributions have to be summed or integrated over all depths as well as over all

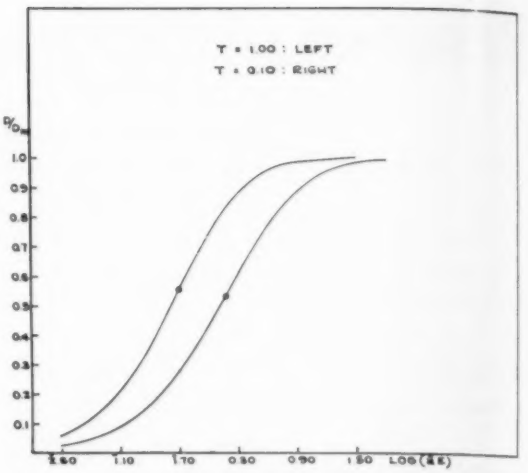

FIG. 1.

sizes. A recent investigation by Dr. L. Silberstein,[1] based on his quantum theory of photographic exposure, shows that the integral can be evaluated in finite form for a size-frequency distribution of the exponential type, leading to a compact formula for the photographic density as function of the exposure, with the transparency ($T$) of the coated plate as parameter. This formula represents closely enough a number of observed sensitometric curves (density plotted against the logarithm of exposure). The effect of the gradual absorption may be seen from the diagram (Fig. 1). The curve on the right corresponds to a transparency $T=0.1$ and that on the left, *caeteris paribus*, to the ideal case of $T=1$ or perfect transparency. Besides the obvious general depression of density there is a perceptible change of shape, and especially slope, of the sensitometric curve. A comparison of the theoretical formula—particularly under the assumption that the absorption of two light-quanta, instead of one, is the minimum required for the developability of a grain—with observed sensitometric curves leads to consistent determinations of intrinsic sensitivity.

[1] L. Silberstein, J. Opt. Soc. Am. **29**, 67 (1939).

# New Books

**Tensor Analysis of Networks.** GABRIEL KRON. Pp. 635 +xxiv, 15×24 cm. John Wiley & Sons, New York, 1939. Price $7.50.

The book deals primarily with the subject of matrix and tensor *algebra* in a language which is simple and easily understood by the reader who does not possess the advantages of a special mathematical training. Since a mathematical treatment of the subject is thus precluded, the presentation must content itself with a parade of symbols, rules, operations and concepts. The reader receives a good exposure to all the terminology and mathematical jargon peculiar to this subject.

Network theory is used as a vehicle for illustrating the application of this branch of mathematics to engineering problems. The systematic nature of the mathematical method is claimed to be particularly effective in dealing with such problems as are encountered in multi-winding transformers, armature windings, and polyphase networks under conditions of unbalanced operation.

The reader who is unfamiliar with the state of development of the art of network theory prior to the advent of tensor analysis in this field, gains the impression that this systematic procedure is new and a unique characteristic of the tensor viewpoint. In reality the novel features introduced by the tensor algebra are confined for the most part to the peculiarities of the notation and terminology which are used. This erroneous impression is caused in part by the absence of specific references in the text to the literature on network theory. A bibliography is provided at the end of the volume, but even this lacks a number of pertinent contributions to the earlier literature of matrix algebra as applied to network theory, for example, the work of Feldtkeller and Strecker on the analysis of vacuum tube amplifier circuits (1930), and that of Baerwald on *2n* terminal-pairs (1931).

Although the chief aim of the volume is to demonstrate the effectiveness of the tensor method of approach in network theory, the latter is almost obscured by the sheer weight of the tensor mechanism itself. For the reader who is looking for a treatment of network theory the book is hardly suitable. In fact, to appreciate the value of the tensor method it is necessary that the reader have a fairly thorough understanding of fundamental network principles before consulting this book.

In the discussion of network analysis in terms of the so-called "mesh-currents" or "junction-pair voltages," the author fails to mention the important artifice of transforming voltage sources into equivalent current sources and vice versa. Instead, when dealing with networks in which both voltages and currents are impressed, he uses an approach based upon what he calls the "orthogonal network." His example of such a case on pp. 423–425 can by inspection be immediately reduced to a simple two-mesh or two-node problem which is solved in a few lines as compared to the two pages of tensor manipulations which he gives.

In the final chapter which is entitled "The Synthesis of Networks," the author works out the conditions which the coefficients in the equilibrium equations of a network must satisfy in order that certain currents or voltages may become independent of the applied voltages and the load impedances. He then gives in tensor language a discussion of the method of obtaining equivalent networks by means of linear transformations and points toward the greater generality of his formulation by remarking among other things that this transformation matrix ("synthesis tensor") is not restricted (as are those of Cauer and Howitt) by the condition that it be *real*. However, unless the transformation matrix *is* real the quadratic forms for the energy functions do not remain real and positive, and the transformed network is not physical and hence is of no practical interest! The whole question of physical realizability, which is the crux of the synthesis problem is dismissed with hardly a gesture. One glance at the "synthesis tensor," Eq. (23.67) on p. 618, for the simple problem of Fig. 23.9 on p. 616 reveals the inadequacy of the author's grasp of what network synthesis implies. In the light of what the problem of network synthesis is generally understood to mean, one must conclude that there is no material of practical value in this chapter.

The one significant contribution which the author makes is the introduction of the "connection tensor" into the mechanism of setting up the equilibrium equations for a network. In this way he is able to write a single tensor equation which is applicable no matter what the number or interconnection of the network branches may be. The connection tensor characterizes the geometrical form of the network or device. This unifies the theory of apparently isolated problems. On this ground the author claims, for example, that the salient-pole alternator and the a.c. commutator motor have the same theory because they have the same form of equilibrium equations when written in tensor notation, whereas the usual textbooks treat these devices by means of individual theories. While the first part of this argument may be granted, it is nevertheless true that the theory of a device lies not in the general underlying equilibrium equations but in the detailed interpretation of them.

In spite of some of the above remarks, I believe that the book has real merit if read and interpreted in the proper spirit. Although the tensor viewpoint in network theory has as yet not been instrumental in the further fundamental development of the network art, it gives promise of becoming useful in the future and therefore certainly deserves recognition as an additional tool. As a first presentation of this subject to an engineering audience the book merits recognition (particularly since our colleagues the mathematicians seem so far to be either unwilling or incapable of producing something readable in this field) and we should feel grateful to the author for all the labor which he must have put into the preparation of this work.

E. A. GUILLEMIN
*Massachusetts Institute of Technology*

**The Alloys of Iron and Nickel. Vol. I. Special-Purpose Alloys.** J. S. MARSH. Pp. 593+xii, Figs. 290, 15×23 cm. McGraw-Hill, New York, 1938. Price $6.00.

This is the tenth of a series of monographs on alloys of iron sponsored by the Engineering Foundation. The aim of the book, as stated by the Committee on page vi is to "provide a reliable foundation for further research and supply to the practical metallurgist, steel worker, foundryman and engineer the essential information now scattered through more than 2000 journals and textbooks in many languages."

In the pursuit of this aim much has been included which is of secondary interest to the physicist, but where his interest is keenest he will find abundant information to justify purchase. The discussion of magnetism is especially detailed. The reviewer has been interested in this alloy system for eighteen years, principally because of its magnetic peculiarities, and has attempted to keep up with new information as it appeared. Upon comparing his own list of references with the 619 presented in the present monograph the completeness of coverage in the new review is at once apparent. To make a quantitative statement on this point, there are about 550 names in the Name Index, and only about 80 names would have to be added to index the combined lists. (This omits new names appearing in 1938 and 1939.) A spot inspection of the papers not mentioned here shows that many of them are secondary in nature, such as reviews or discussions, or papers in which properties of iron-nickel alloys are reported along with those of quite different materials, so that their inclusion is incidental.

In one respect only do omissions seem to have been deliberate and, in the opinion of the reviewer, ill-advised. Nothing is said about the electrodeposition of iron-nickel mixtures, the properties of such deposits, or the relatively simple heat treatments which may be necessary for rendering them homogeneous.

The author's own particular interest in phase diagrams is especially apparent in his discussions of several ternary systems. In the physical, as distinguished from the physico-chemical, sections the text is not nearly so critical, conflicting viewpoints being presented with less guidance for the reader's choice.

It is hard to say too much in praise of the care and precision with which the material has been assembled and arranged. It is easy to find what has been done, and further reference to original monographs will very rarely be necessary. This is especially true because tabular and graphical extracts (the latter often better than in the original publications) are constantly given. The book is not meant to be read straight along, but many of its sections are written so smoothly that the fundamental jerkiness of linked abstracts is hardly noticeable.

It is interesting that this book, and the only other with which comparison is inevitable* are both products of industrial rather than academic enterprise. The corporate engineer, in fact, is the only individual who can afford, nowadays, to know all about a limited subject.

L. W. MCKEEHAN
*Sloane Physics Laboratory,*
*Yale University*

* O. V. Auwers, on magnetic and electrical properties of iron and its alloys. See review, J. App. Phys. **10**, 186 (1939).

**Gas Analysis.** A. MCCULLOCH. Pp. 166, Figs. 38, 14½×22 cm. H. F. and G. Witherby, Ltd., London, 1938. Price 7s. 6d.

The author states that his *Gas Analysis* was written primarily to meet the need for a small book on gas analysis suitable for students in fuel technology. It consists of six chapters as follows: I. Introduction. II. The Absorbents used in Gas Analysis. III. The Determination of Hydrogen, Carbon Monoxide and Saturated Hydrocarbons by Combustion. IV. Gas Analysis Apparatus. V. Miscellaneous Determinations. VI. The Calorific Value of Gases. Methods for the determination of the various constituents of fuel gases are described and the manipulation of five common types of gas analysis apparatus is explained. The book contains a twelve-page appendix of useful tables, name and subject indices. No attempt is made to cover the entire field of gas analysis.

The selection of methods is well made, especially for a student in Great Britain. The descriptions are clear and sufficiently detailed in most cases so that an accurate trial of the method could be carried out. The inclusion of several typical analyses and laboratory reports adds much to the value of the book as a text. The addition of material on the use of a simple gas buret, the use of the gas density balance, the determination of the humidity of gases, and the construction of a wet test gas meter would be desirable. Likewise, a brief statement of the thermal conductivity method of gas analysis and the use of the gas interferometer could be added advantageously. From the point of view of students in the United States, a brief description of the apparatus of M. Shepherd,[1] that of Burrell and others,[2] methods of the chemists of the United States Steel Corporation for the sampling and analysis of gases,[3] that of Podbielniak[4] and also of the National Bureau of Standards method for total sulfur[5] would increase the usefulness of the book.

In any case it should be stated that the first edition of *Gas Analysis* by A. McCulloch is a worth while contribution to the textbook literature in the field and a practical reference book, especially for those who do not have access to the more extensive treatises on the subject.

C. C. MELOCHE
*University of Michigan*

[1] M. Shepherd, Nat. Bur. Stand. J. Research **6**, 121 (1931).
[2] Bur. Mines Bull. 197 (1926).
[3] Pittsburgh, Pa., (1927), p. 8.
[4] Podbielniak, Ind. Eng. Chem., Anal. Ed. **3**, 177 (1931).
[5] Circular Nat. Bur. Stand. No. 48, p. 133.

# Here and There

### Acoustical Society of America

The Acoustical Society of America will hold its tenth anniversary meeting at the Hotel Pennsylvania in New York City on Monday and Tuesday, May 15 and 16, 1939. The following interesting program has been arranged:

1. A Symposium on the Measurement and Application of Absorption Coefficients.
   - Statement of the Problem—F. V. Hunt, Harvard University
   - Measurements in the Reverberation Chamber—P. E. Sabine, Riverbank Laboratories
   - Measurements in the Field—G. T. Stanton, Electrical Research Products, Inc.
   - Open Discussion led by V. L. Chrisler, National Bureau of Standards, and J. Parkinson, Johns-Manville Sales Corporation.
2. Architectural Acoustics, Its Past and Its Possibilities. P. E. Sabine, Riverbank Laboratories.
3. A Modern Concept of Acoustical Design. C. C. Potwin and J. P. Maxfield, Electrical Research Products, Inc.
4. The Role of the *Journal of the Acoustical Society*. F. R. Watson, University of Illinois.
5. An Ear to the Future. V. O. Knudsen, University of California at Los Angeles.
6. A Demonstration of Combination Tones. Sir William Bragg, The Royal Institution, London.
7. Conclusions from Further Measurements of Old and New Violins. F. A. Saunders, Harvard University.
8. Remaking Speech. Demonstrated by its Instantaneous Analysis and Synthesis—Homer W. Dudley, Bell Telephone Laboratories.
9. Demonstration Lecture on Auditory Patterns. Harvey Fletcher, Bell Telephone Laboratories.

★

### Mathematical Biophysics

The first number of a new booklet on *Mathematical Biophysics* has just been issued. It is published as a supplement to *Psychometrika*. It is edited by Dr. N. Rashevsky of the University of Chicago. The first issue contains papers on "Mathematical Biophysics of Cell Respiration," "Biological Periodicities," "Mechanism of Cell Division," "Mechanics of Viscous Bodies and Elongation in Ellipsoidal Cells," "Mathematical Biophysics of the Cell," and "Rashevsky's Theory of the *Gestalt*." This publication seems to fulfill a very definite need and should be very valuable to those interested in mathematical biophysics.

### Metropolitan Section of the APS

The program of the meeting of the Metropolitan Section of the American Physical Society held at 2:30 P.M. on Friday, March 24, in the Pupin Physics Laboratories of Columbia University was as follows:

Present Status of the Analysis of Atomic Spectra—A. G. Shenstone.

Cosmic Rays: The Primary Rays and the Phenomena of showers—K. K. Darrow.

Cosmic Rays: The Mesotron—Enrico Fermi.

★

The Electrochemical Society will hold its Columbus meeting at the Deshler-Wallick Hotel from April 26 to April 29, 1939. There will be two important and timely symposia on "Organic Electrochemistry" and "Refractories for the Electrochemist."

★

Dr. R. N. Varney, Assistant Professor of Physics at the Washington University, spoke to the Physics Colloquium of the University of Missouri on "The Ionization of Gases by Ions and Atoms." Dr. Varney joined the staff of the University of Washington in September, 1938.

★

Dr. E. J. Schremp, also of the Physics Department of Washington University, spoke to the Physics Colloquium of the University of Missouri on "Recent Developments in Electrodynamics." Dr. Schremp came to the Physics Department of the Washington University from the Massachusetts Institute of Technology in September, 1937.

★

*Science* reports that among the men elected as fellows of the Royal Society at the meeting held at Burlington House, London, on March 16 were:

M. Born, Tait Professor of Natural Philosophy, University of Edinburgh, distinguished for his work in many branches of mathematical physics and particularly for his contributions to quantum theory and its applications to physics and chemical physics.

A. J. Bradley, Assistant Director of Research in Crystallography, Cavendish Laboratory, Cambridge, distinguished for his methods of applying x-ray crystallography to elucidate the structure of metals and particularly the gamma-phase and order and disorder in alloys.

G. W. C. Kaye, superintendent, Department of Physics, National Physical Laboratory, distinguished for his pioneer work in x-ray measurements and for his studies on acoustics and physical constants; has rendered valuable service to the Radium Protection Committee and the National Radium Commission.

E. J. Williams, Professor of Physics, University of Wales, Aberystwyth, distinguished for his researches on the passage of electric particles through matter, and on individual collision processes, which have provided evidence for the existence of the heavy electron.

### Summer at University of Chicago

*Symposium on Liquids and Polyatomic Molecules.* The Department of Physics and Chemistry will cooperate in offering a symposium on liquids and polyatomic molecules from June 21 to June 24. This will deal with recent developments in regard to the structure and optical properties of liquids and of polyatomic molecules and will be conducted by Professors Franck, Harkins and Mulliken.

*Symposium on Cosmic Rays.* A symposium on cosmic rays, conducted by Professor Arthur H. Compton, will be held from June 26 to June 28.

*Conference on the Calculus of Variations.* Under the direction of the Department of Mathematics a conference on the calculus of variations will be held from June 27 to June 30, with a number of invited addresses by members of the Faculty of this and other universities on topics connected with the calculus of variations in which the speakers have been especially interested.

★

### Priestley Lectures

The Pennsylvania State College celebrated the two hundred and sixth anniversary of the birth of Joseph Priestley with the presentation of the thirteenth annual series of Priestley Lectures on March 20 to 24. The lectures, a series of five, were given this year by Dr. Kenneth S. Cole, Associate Professor of Physiology at the College of Physicians and Surgeons, Columbia University.

Joseph Priestley was born in England in 1733 and did most of his work in chemistry in that country. His chemical investigations were carried out quite aside from his regular duties as a clergyman. Although he did not begin his scientific work until after he had reached the age of thirty, his enthusiasm and talent for experimental devices overcame his lack of previous training and unfamiliarity with chemistry in general and he became one of the outstanding chemists of his time. He is known primarily for his most important discovery of oxygen in the air and for the preparation of the first pure oxygen. His first recognition came, however, in 1773 when he was awarded the Copley Medal for correlating the then known facts concerning carbon dioxide and recommending that a solution of this gas in water (our present "soda water") be carried by sailors on long voyages for the prevention of scurvy.

Toward his later years Priestley became quite unpopular in England because of his liberal views toward religion and the American and French Revolutions. Because of this ill-feeling he emigrated to America in 1794 and built a home at Northumberland, Pennsylvania, where he continued his experimenting and writing until his death. His Northumberland home was purchased in 1919 by the alumni of the Department of Chemistry of The Pennsylvania State College and a museum built nearby as a memorial to Priestley's contributions to early American chemistry.

In 1926 the members of the faculty of the Department of Chemistry inaugurated a series of lectures known as the Priestley Lectures. Since 1931 the lectures have been sponsored by the local chapter of Phi Lambda Upsilon, national honorary chemical fraternity, with the cooperation of the Department of Chemistry. The lectures, therefore, now constitute a living memorial to Joseph Priestley.

The lectures are given each year by an authority in a field related to that in which Priestley's work falls, physical chemistry. The lecturers for the past five years have been Dr. Ross A. Gortner of the University of Minnesota, Dr. Matthew A. Hunter of the Rensselaer Polytechnic Institute, Dr. Warren K. Lewis of the Massachusetts Institute of Technology, Dr. G. H. A. Clowes of Eli Lilly and Company, and Dr. Robert F. Mehl of Carnegie Institute of Technology.

Professor Cole, this year, discussed the inter-relationships between physical chemistry and cell membranes. His lectures dealt with the properties of the cell membranes which have been determined by the methods of physics and physical chemistry. The general topic was subdivided into the following parts for the five lectures: Membrane Problems; Membrane Permeability; Membrane Impermeability; Membrane Activity; and Membrane Structure. The lectures were given in the Auditorium of the Home Economics Building at State College, Pennsylvania, beginning at 7:30 P.M. on the evenings of March 20, 21, 22, 23 and 24.

★

### Sigma Pi Sigma

Sigma Pi Sigma, the national physics honor society, held its convention on April 6, 7 and 8 at Columbus, Ohio, with the Ohio State University Chapter as host. Delegates from over thirty active chapters attended the business and scientific sessions, which concluded with an inspection trip to the Perkins Observatory. Dr. R. C. Colwell, of West Virginia University, the retiring president, delivered the presidential address on "Electromagnetic Waves and Radio Signals." After being received into honorary membership in the society, Dr. Paul E. Klopsteg, of the Central Scientific Company, spoke at an open meeting on "Archery, a Physicist's Hobby." At a panel discussion, Dr. M. N. States, assisted by Dr. W. P. Davey, Dr. W. E. Forsythe and others presented various phases of problems dealing with the placement of graduates in physics.

The Convention authorized the expansion of the services of the Placement Board of the Society and its establishment upon a permanent basis. This board will serve as an agency to bring to the attention of prospective employers of physicists the availability of certain members of the society and will function as a general clearing house for information regarding the placement of graduates in physics.

The report of the Executive Secretary to the convention indicated that the society has a total membership of 2435 and an active-chapter membership of 650.

Officers elected at the close of the convention were: *President*, Dr. F. C. Blake, Ohio State University; *Vice President*, Dr. Joyce C. Stearns, University of Denver; *Executive Secretary*, Dr. Marsh W. White, The Pennsylvania State College.

### Purdue Summer Session

Professor Werner Heisenberg of the University of Leipzig will be Visiting Professor at Purdue University during the Summer Session, from July 1 to July 22. Professor Heisenberg will lecture on problems of nuclear physics and cosmic rays. Those interested in attending should communicate with the Department of Physics to obtain information regarding available accommodations on the campus.

★

### International Meeting on Physics

An International Meeting on Physics will be held in Zurich, Switzerland, from September 4 to September 16, 1939, in the Physical Building of the Federal Institute of Technology, 35 Gloriastrasse, Zurich 7, in connection with the Swiss National Exhibition. The program is as follows:

**Section I. Nuclear Physics**

September 4 to 9, 1939

*Chairman:* P. Scherrer, Federal Institute of Technology, Zurich.

Main lecturers:
N. Bohr, J. Chadwick, H. Euler, O. Hahn, W. Heisenberg, F. Joliot, R. A. Millikan, F. Rasetti.

**Section II. Physics of the Solid Body**

September 4 to 9, 1939

*Chairman:* P. Niggli, Federal Institute of Technology and University of Zurich.

Main lecturers:
A. E. van Arkel, P. Debye, R. A. Fowler, R. de L. Kronig, G. Joos, L. Pauling, W. Pohl.

**Section III. Technical Physics**

September 11 and 12, 1939

*Chairman:* F. Fischer, Federal Institute of Technology, Zurich.

Main lecturers:
J. H. de Boer, L. Brillouin, E. Brüche, R. Houwink, G. Masing, R. Nitsche, W. Schottky.

**Section IV. Television**

September 13 to 15, 1939
At the same time:
2nd International Television Meeting

*Chairmen:* F. Fischer and F. Tank, Federal Institute of Technology, Zurich.

Main lecturers:
R. Barthélémy, A. D. Blumlein, K. Küpfmüller, R. Möller, F. v. Okolicsanyi, F. Schröter, V. K. Zworykin.

**Section V. High Frequency**

September 16, 1939
At the same time:
5th High-Frequency Meeting of the "Association Suisse des Electriciens"

*Chairman:* F. Tank, Federal Institute of Technology, Zurich.

Main lecturers:
E. M. Deloraine and T. L. Eckersly.

Besides the main lectures time will be provided in every section for a certain number of smaller papers of 30 minutes each. Registration of these papers must be made before May 31, 1939, with the Secretary of the International Meeting on Physics, 41 Gloriastrasse, Zurich 7, Switzerland.

★

### Summer at the University of Pittsburgh

The University of Pittsburgh announces a second Summer Session on the Physics of Metals to be held from July 6 to August 11. This summer session is a cooperative effort on the part of physicists and metallurgists to bring out recent progress in the physics of metals and to discuss possible applications in the field of metallurgy. The following tentative schedule of courses has been arranged:

Introductory Electronic Structure of Metals, JOHN C. SLATER
Elementary Atomic Physics, M. F. MANNING
Modern Theory of Solids, WILLIAM SHOCKLEY
Electric and Magnetic Properties of Metals, FREDERICK SEITZ
Introductory Statistical Mechanics, E. U. CONDON
Theory of Atomic Vibrations, J. C. SLATER

A booklet will be ready shortly describing these courses in detail and may be obtained by writing to Dr. E. Hutchisson, Head of the Physics Department, University of Pittsburgh, Pittsburgh, Pennsylvania.

★

### Westinghouse Research Fellowships

Announcement of appointment of the second group of five Westinghouse Research Fellows has been made by the Westinghouse Electric and Manufacturing Company. The first group of five was appointed last year, and all of the group have been reappointed for a second year of fundamental research work at the Westinghouse Research Laboratories in East Pittsburgh.

The new appointees are:

*Dr. William A. Johnson*, who will work on problems of diffusion of metals using artificial radioactive metals produced in the Westinghouse "atom-smasher" as tracers. Dr. Johnson's home is in Washington, D. C. He graduated from Lehigh University with highest honors in metallurgy in 1935, and has just completed his graduate study in the Metals Research Laboratory of Carnegie Institute of Technology under Professor R. F. Mehl.

*Dr. Alois Langer*, who will work on chemical applications of artificial radioactive isotopes. Dr. Langer comes to the Laboratories from the School of Chemistry of the University of Minnesota, where he has been engaged in research in analytical chemistry with Dr. I. M. Kolthoff, chief of the division of analytical chemistry.

*Dr. T. A. Read*, who will study the processes governing internal friction in metals. Dr. Read comes from Columbia University, where he has been doing research in the energy dissipated in metals during vibration, in collaboration with Professor S. L. Quimby and with Professor C. Zener of the College of the City of New York.

*Dr. Alden H. Ryan*, who will study the dielectric behavior of gases at ultra-high radiofrequencies, corresponding to wave-lengths of about ten centimeters. He will also conduct experiments on new methods of producing radio waves of this type. Dr. Ryan comes from Iowa State College in Ames, Iowa, where his graduate research has been devoted to study of dielectric constants at high frequencies.

*Dr. G. L. Tawney*, who will work on the fundamental processes of thermionic emission from oxide crystals, continuing basic studies in this field which he has been carrying on at Massachusetts Institute of Technology, where he has worked in collaboration with Professor W. B. Nottingham.

These five Fellows are the second group to be appointed under a plan announced by the Westinghouse Company in the fall of 1937, according to which ten young research men will be supported for fundamental research in fields broadly related to the electrical industry. These men work on basic problems not directly connected with the immediate needs of the industrial research program of the company. The first group of five, whose reappointment for a second year was announced at the same time, include three nuclear physicists, Drs. R. O. Haxby, W. E. Shoupp, and W. E. Stephens, who are working with Dr. W. H. Wells on the large atom smasher, together with Dr. J. A. Hipple, who has constructed a mass spectrograph for molecular structure studies, and Dr. Sidney Siegel, who is studying the effect of the order-disorder transition on the elastic properties of single crystals of copper-gold alloys.

Work of the Fellows is carried on under the general supervision of Dr. E. U. Condon, Associate Director of the Westinghouse Research Laboratories.

# Contributors to This Issue

**R.** P. Johnson received his B.A. from the University of Richmond in 1929, his M.A. in Physics from the University of Virginia in 1930 and his Ph.D. from the Massachusetts Institute of Technology in 1936. From 1930 to 1931 he was employed by the Geophysical Research Corporation; from 1931 to 1933 he was an instructor in mathematics at the University of Richmond and since 1936 he has been with the Research Laboratory of the General Electric Company.

**C**aptain S. F. Varian was a graduate student at California Polytechnic Institute. He was a commercial pilot for fifteen years and from 1929 to 1936 was a Captain with Pan American Airways, flying between Brownsville, Texas and the Panama Canal. He is now a research associate at Stanford University.

**R**ussell H. Varian received his B.A. degree from Stanford University in 1925, his M.A. in 1927. From 1929 to 1932 he was with Farnsworth Television Corporation.

**R.** B. Nelson received his B.S. in physics from the California Institute of Technology in 1935 and his Ph.D. in 1938 from the Massachusetts Institute of Technology. He is now employed by the RCA Manufacturing Company at Harrison, New Jersey.

**M**iklós Hetényi obtained his engineering diploma from the Technical University of Budapest in 1931 and, after spending several years in the design of Danube bridges, came to this Country under the Jeremiah Smith Fellowship in 1934. He obtained his Ph.D. degree in Engineering Mechanics at the University of Michigan in 1936, where he became a Horace H. Rackham Fellow for 1936-37. Since 1937 he has been engaged at the Westinghouse Research Laboratories.

R. H. Varian

S. F. Varian

M. Hetényi

R. B. Nelson

# Contributed Original Research

## A High Frequency Oscillator and Amplifier

RUSSELL H. VARIAN AND SIGURD F. VARIAN
*Stanford University, California*
(Received January 6, 1939)

A d.c. stream of cathode rays of constant current and speed is sent through a pair of grids between which is an oscillating electric field, parallel to the stream and of such strength as to change the speeds of the cathode rays by appreciable but not too large fractions of their initial speed. After passing these grids the electrons with increased speeds begin to overtake those with decreased speeds ahead of them. This motion groups the electrons into bunches separated by relatively empty spaces. At any point beyond the grids, therefore, the cathode-ray current can be resolved into the original d.c. plus a nonsinusoidal a.c. A considerable fraction of its power can then be converted into power of high frequency oscillations by running the stream through a second pair of grids between which is an a.c. electric field such as to take energy away from the electrons in the bunches. These two a.c. fields are best obtained by making the grids form parts of the surfaces of resonators of the type described in this Journal by Hansen.

### I. INTRODUCTION

IT has long been realized that apparatus for transmitting and receiving electromagnetic oscillations at wave-lengths of the order of 10 cm or shorter should lead to the accomplishment of a large number of useful objectives, because wave-lengths of this order would permit concentration of the radiation into rather sharply defined beams. Such waves have been produced in many ways since the time of Hertz, and can be produced readily by a spark transmitter and in other ways; but the perfection of the three-electrode tube, and in particular the ease with which it obtains great amplifications, has raised our standards so far, at least for low frequencies, as to create a hope for similar apparatus for ultra-high frequencies. It is the purpose of the present paper to describe a new type of electronic device which has made progress in this direction.

The reasons for certain important features of this device may be seen most readily after a brief discussion of some of the difficulties encountered by the triode at very high frequencies. The fundamental difficulties have been of two kinds: with the resonant circuits and with the tube itself.

As a resonant circuit the ordinary coil and condenser become unsatisfactory as the frequency is increased, not only because it becomes too small to be mechanically convenient but even more because the losses become too great and therefore the shunt impedance becomes too low. Another related and yet partially independent difficulty is the decline in frequency stability as the losses increase. These difficulties can be, and are, partially avoided by using such resonators as concentric lines; but because of limitations due to leads and other reasons the resonant circuit often remains a limiting factor. Improvement in resonant circuits is, therefore, of primary importance.

Turning to difficulties with tubes, it is always found, with any given triode, that, as the operating frequency is increased too far, the efficiency declines and eventually the decline becomes so rapid that in a rather short range of frequency the efficiency drops from a usable value to zero. It has been found that this difficulty is associated with the transit time of the electrons. Whenever the time of transit from filament to plate becomes appreciable by comparison with the time of a quarter-cycle, the tube fails to act in the normal way. There are two obvious methods of attack: to increase the plate voltage,

and to decrease the physical size of the tube. The former of these methods cannot be carried far; but the latter method has made tubes now commercially available for work at fairly high frequencies. The difficulties associated with this

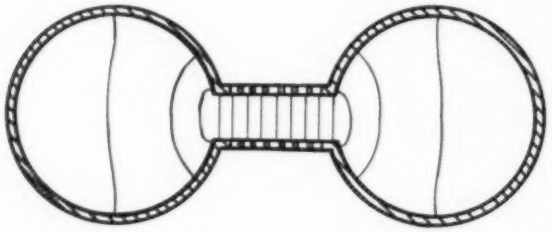

FIG. 1. Cross section of a copper enclosure, useful as a resonator. A qualitative representation of the electric field corresponding to the mode of oscillation used is also given. The horizontal dotted lines represent grids which should be of copper or other good conductor, and which should be designed so as to resist the current flow as little as possible.

method, however, are serious: first because of the mechanical troubles in producing the tube, and, much more important, because each decrease in size decreases the power capacity. It would seem therefore that there is a practical limit to useful results along this line. Accordingly, it becomes necessary to try another plan: not to attempt elimination of the effect of transit time, but to turn it to constructive use. The two objectives in this work, therefore, are first, the application to this problem of a new type of resonator, and second, a constructive use of the transit time.

## II. The Resonators, and Excitation by Cathode Rays

Considering first the resonators, we apply here the results obtained by Hansen,[1] who had considered the resonant properties of practically closed metal vessels, like those sometimes called *hohlraums*. In our laboratory, these have been called "rhumbatrons," from the Greek word "rhumba," meaning rhythmic oscillation, and the familiar termination "tron," making the name mean the place where these rhythmic oscillations occur. Hansen obtained mathematical results on frequencies and power consumption for shapes of sufficient variety to make rough estimates possible for many other cases.

For such resonators there are no quantities corresponding exactly to the familiar self-inductance $L$, resistance $R$ and capacitance $C$ of an ordinary circuit; and there are several essentially different but almost equally good ways of defining quantities to correspond roughly to them. By using any of these ways, and letting $Q=L\omega/R$ as usual,* any simple non-re-entrant rhumbatron, such as a spherical one, has a $Q$ of the order of $\lambda/\delta$, where $\lambda$ is the wave-length in free space and $\delta$ is the skin depth in the metal of which the rhumbatron is made. The quantity corresponding to shunt impedance, by any reasonable definition, is then expressible in absolute electromagnetic units as something of the order of $Qc$, where $c$ is the velocity of light, $3\times10^{10}$ cm/sec. Since $Q$ is a pure number, the conversion to practical units affects only $c$, which becomes 30 ohms. If $\lambda=10$ cm and the metal is copper, $(\lambda/\delta)=5.88\times10^4$; so such shapes give high values to $Q$ and to the shunt impedance. For reasons to be explained below, the shapes actually used are re-entrant, as, for example, in Fig. 1; and then $Q$ and the shunt impedance are somewhat reduced but their values are still very high.

Hansen proposed to use such resonators, excited by any feasible means, to accelerate electrons by running them through the resonator in the general region and direction of the strongest electric field. So a reversal of phase relations gives the opposite result, the electrons being decelerated and the energy they lose being transferred to the field. Thus to excite our resonator we make holes or grids in two of its opposing walls adjacent to the region of high electric field strength, and pass through these grids and this field a periodically changing stream of electrons, the changes being so timed that more electrons pass when the field is such

[1] W. W. Hansen, J. App. Phys. 9, 654 (1938), and much information imparted in private conversation.

* This may sound as if there are various definitions of $Q$ possible, each leading to a different numerical value. What is intended, rather, is that this is an equation of condition, which, taken along with the equation $LC\omega^2=1$ forces us, on choosing some particular definition of, say, $L$ to use with this definitions of $C$ and $R$ which will make the lumped constant "equivalent circuit" have the same frequency and the same damping ratio as the actual rhumbatron. This means that, whatever definition of $L$ one starts with, $Q$ is always defined as $2\pi$ times the ratio of the energy stored to the energy lost per cycle.

as to take energy from them than when the field is reversed. The reason why a sphere, for example, is not a suitable shape of rhumbatron is that its wave-length is only about 1.14 times its diameter; so even if an electron had a speed equal to that of light, it would never get through the sphere before the field reversed. For best operation, the path of the electron in the resonator must not be much longer than $\beta\lambda/2$, where $\beta=v/c$ and $v$=electron velocity, and it seems best to have the path still shorter. We therefore use as a resonator a copper enclosure of shape generally similar to that of Fig. 1.

It will be noted that no use is made of high frequency lead wires, nor is there any solid dielectric. Thus we obtain the full benefit of the desirable qualities of the resonator. Also, it should be specially noted that there is no radio-frequency field outside the resonator, and therefore no radiation, until we add such accessories as are needed for producing the radiation desired for practical uses.

## III. Transit Time and Bunched Cathode Rays

The requirement for intermittent cathode rays, just described, cannot be readily met by grid control as in a triode for the reasons stated in our introduction, in connection with transit times. Consequently it leads back to the second problem stated at the conclusion of our introduction; namely, that of finding a constructive use for the transit time. The idea of constructive use of transit time, in general, is not new, since for example it appears in the magnetron and Barkhausen-Kurz oscillators. In the present case, however, the method of using this time is different, being more adapted to the present problem.

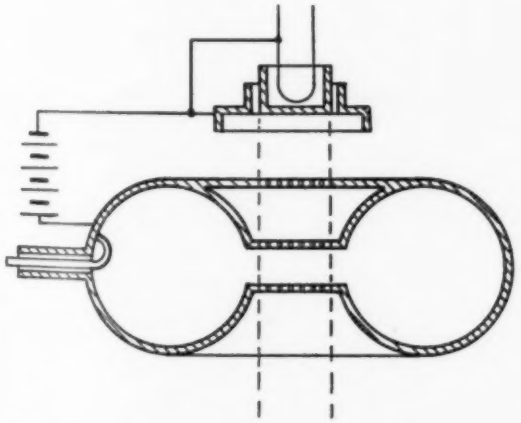

Fig. 2. Diagrammatic representation of a rhumbatron, like that of Fig. 1, a battery, and a cathode which emits a beam of electrons indicated by the parallel dotted lines. Also shown is a concentric line and a coupling loop for supplying radiofrequency power which maintains a radio-frequency field inside the rhumbatron. This field alternately accelerates and retards the electrons passing through.

This method involves the use of an auxiliary rhumbatron, in a way shown diagrammatically in Fig. 2. Here the electrons from the cathode are accelerated by the electrostatic field produced by the battery. In the form shown here, using grids and straight beams, rather than holes and focused beams, the first grid serves to straighten the lines of force of this field. Beyond it the electrons pass through a field-free space to the second grid, and then through the high frequency field of the rhumbatron to the third grid. The latter field is not strong enough to change the speed of an electron by more than a small or very moderate fraction of its speed at the first or second grid. So the current carried by the cathode rays not only has the same value at all points in space from the cathode to the second grid, but also nearly the same to the third grid.

Beyond the third grid, however, the changes of speed have important effects. These are understood best by first considering an electron which passes the center of the high frequency field just as that field is changing from opposing to helping electrons. At the third grid, this electron has practically the same speed as at the second; but another electron which passed the center of the field a few electrical degrees earlier has had its speed reduced; and a third one, passing a few degrees later, is going faster. If there is plenty of field-free space beyond the third grid, these differences in speed cause the electrons ahead and behind the one of unchanged speed to draw nearer to it. Another electron of unchanged speed, a half-cycle earlier or later, has its neighbors draw away from it. Consequently at a suitable distance from the third grid the stream contains bunches of electrons denser than the stream at the third grid and separated by regions less dense.

This stream is of just the sort required for driving the oscillations in the rhumbatron dis-

cussed in Section II. Therefore, if this stream is sent through such a rhumbatron as that, and if that rhumbatron is oscillating in the proper

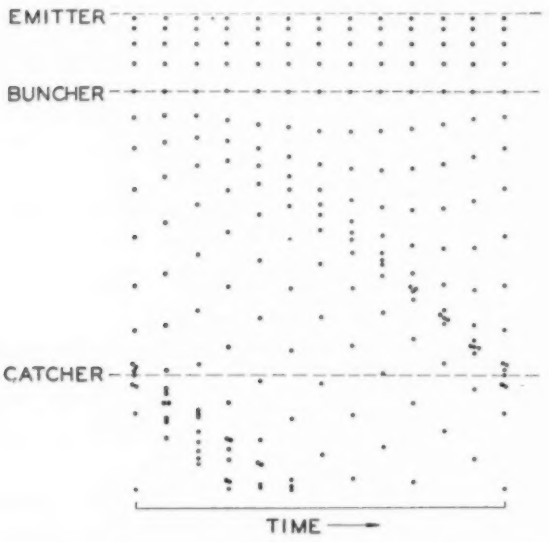


FIG. 3. Sequence of diagrams showing, for 12 times equally spaced throughout one cycle, the positions of chosen typical electrons (dots) in the beam shown in Fig. 2. As to phase, the first vertical row of dots shows the positions of the electrons at a time when the field in the "buncher" is zero and is coming to be in the direction to increase the speeds of the electrons. Horizontal lines show the positions of the cathode and the buncher rhumbatrons. A suitable place for the catcher is designated by the horizontal dotted lines.

phase to retard the electrons in the bunches, and if its oscillating field is strong enough to take more energy from the electrons than was given them by the rhumbatron of Fig. 2, the apparatus as a whole converts part of the d.c. power of the cathode rays into high frequency a.c. power.

Such an apparatus we call a "klystron," from the Greek verb "klyzo," expressing the breaking of waves on a beach. The rhumbatron in which the electrons are given their first modulation of speed is called the "buncher," and the one into which the bunches "break" is called the "catcher" —though it must be noted that the electrons may go through the catcher, if both its surfaces are grids, and that what it "catches" is not primarily current but power.

To show diagrammatically the character of these bunches, in Fig. 3 we have reduced the spacing of the grids in the buncher to zero, and likewise in the catcher, and drawn vertical columns of dots each representing a line of electrons in the places they occupy at one instant, and different columns representing such lines occurring at different instants throughout the cycle. To catch the most power, the catcher must satisfy three requirements: it must be placed where the electrons are in bunches of a certain best form, to be defined later in a paper by D. L. Webster; it must oscillate in the right phase; and the strength of the oscillations must be such as to reduce the electrons in the centers of the bunches just to rest. Under these conditions, as Webster will prove, with ideally perfect grids and other parts, it should convert 58 percent of the power of the cathode rays going through it into high frequency power. Practically, of course, we cannot claim to reach this ideal efficiency, but the efficiency is good.

As the klystron has been described here, with the buncher driven by some independent source of power, such as an antenna receiving a signal, it is evidently an amplifier; but to convert such an amplifier into an oscillator, we need only take a small part of the oscillatory power in the catcher and use it to excite the buncher. The phase relations must, of course, be correct; and if not otherwise adjustable electrically the proper phasing may be simply obtained by

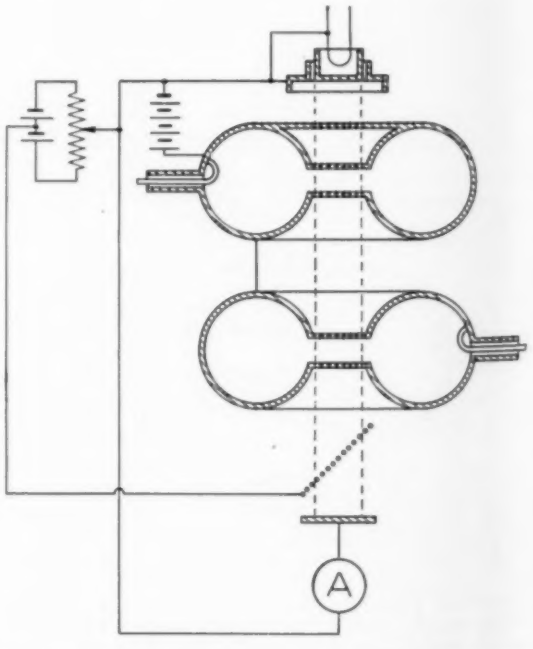


FIG. 4. Diagrammatic representation of radiofrequency amplifier and detector.

varying the mean speed of the electrons, by varying the P.D. between the cathode and the first grid. And, of course, a klystron almost converted from an amplifier to an oscillator makes a good regenerative amplifier.

Another point of interest in connection with the amplifier relates to the energy of the electrons after they have passed through the second rhumbatron. A substantial majority of the electrons give energy to the catcher; therefore they pass the last grid at lower speeds than that at which they passed the first grid. Also, it is unavoidable that a small minority of the electrons go through the catcher during the wrong half of the cycle and acquire more speed. Thus any device which sorts electrons according to their speed may be placed after the last grid of the catcher and be used as a detector. Perhaps the simplest such is a grid nearly at cathode potential. When there is no signal input almost all the electrons go through it. Then if there is a signal to the buncher, the buncher bunches the electrons, which in turn builds up a field in the catcher, and this field slows down some of the electrons so that they can no longer go through the detector grid: this causes a decrease in the current to any collector beyond the grid. Such a device is shown in Fig. 4. Alternatively, the grid may be biased so that with no signal the electrons just fail to pass, and a signal then causes an increase in the collector current.

Thus we have shown how amplification, oscillation, and detection may be achieved. Modulation may be obtained by varying the beam current; also by varying the cathode potential and so making the phase relations come nearer to or farther from the ideal ones noted above; and there are many alternative methods growing out of these.

## IV. Practical Details of a Typical Klystron

In this section we describe certain constructional and design details that might not be obvious. For the most part these relate to a particular early oscillator which worked at about 13 cm and which is shown in Fig. 5, but information obtained from other apparatus has been included. Also, in Fig. 6 we have shown a photograph of various parts of interest.

First we may note the means needed to obtain the columnar beam of electrons assumed above. Electrons are drawn from a plane oxide-coated emitting surface *A* through a plane grid of tungsten wires *B*. Were it not for space charge, the field between these two planes would be straight and the electrons would all leave in the same direction. But there is space charge, and to compensate for this ring *C* is added in an endeavor to keep the field due to the electrodes plus that of the space charge approximately straight.

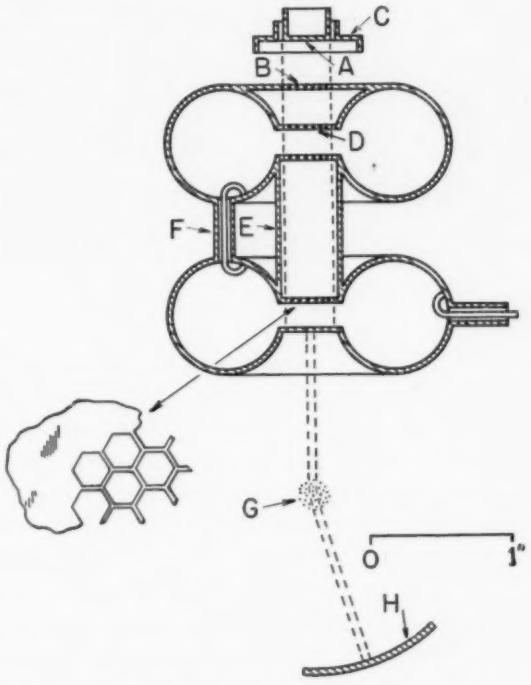


FIG. 5. Scale drawing of essential parts of a typical klystron oscillator. The vacuum envelope, means for tuning, means for varying the feedback and various unimportant details have been omitted.

After passing through grid *B* the electrons pass through three, and in many other cases four, grids, the first of which is *D*. These grids must have high electrical conductivity to avoid spoiling the resonators; they must have high heat conductivity to dissipate the energy derived from the electrons striking them; and they should have as little projected area as possible to keep the number of electrons intercepted at a minimum. In an effort to satisfy these requirements we have sometimes made the grids of honeycomb form as

shown in the detail. They are drilled and filed from copper $\frac{1}{16}''$ thick and are perhaps the most tedious parts to make in the whole apparatus.

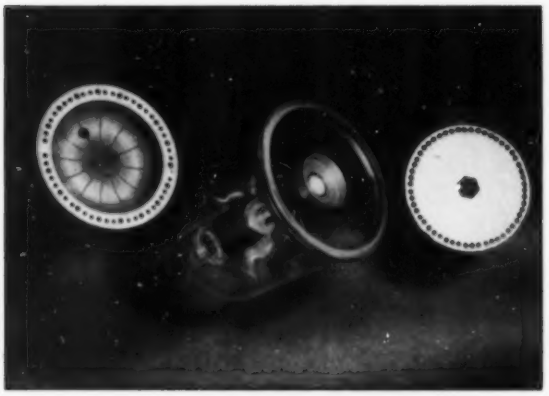

FIG. 6. Photograph of typical cathode, grid and rhumbatron.

The "lattice constant" of the grid is determined by the requirement that the radio-frequency field along the electron path should usually change from zero to full value in a distance short compared to the distance traveled by an electron in one half-cycle. The meaning of "short" will be discussed more precisely in a forthcoming paper by Hansen.

The distance between two grids of the same rhumbatron is usually less than the distance traveled by an electron in one half-cycle. For the buncher this would be $\beta\lambda/2$; but in the catcher some of the electrons are slowed nearly to rest, so that $\beta\lambda/4$ is a closer approximation. In practice the latter spacing is used for both so that the rhumbatrons can be made nearly identical, so as to simplify tuning. Smaller grid spacings can be used, but with some impairment of the shunt impedance.

The two rhumbatrons are connected, mainly for mechanical reasons, by a tube $E$ whose length is determined by a compromise between the following opposing considerations. First, the shorter the tube, the less distance the electrons have in which to bunch, with the result that, for best bunching, they must be given a larger spread in velocity. This, on the other hand, tends to reduce the efficiency because: (a) more power is required to drive the buncher as the buncher voltage is increased; and (b) since no electrons should be thrown backward in the catcher, only the slowest ones can be stopped, and so a larger spread in velocities means more loss of energy due to incomplete stoppage of the faster electrons. On the other hand, a large bunching distance increases the difficulty of getting a large fraction of the beam into the catcher. In practice the compromise chosen is not critical, and the apparatus works well over a large range of distance.

The exact shape of rhumbatron best suited for the present purpose is not known but the shape shown works well and is convenient to manufacture.

Since the $Q$ of the resonators is high (about 1000) it is not easy to build them sufficiently nearly identical to resonate nearly enough to the same frequency without tuning. One of the simplest methods of tuning is that shown, in which the rhumbatron is slotted (along the lines of current flow) and then deformed elastically by a screw. The exact mechanism for doing this is not shown as it is felt that different experimenters will prefer different mechanisms.

The same idea applies to the vacuum envelope and pumping system, which are not shown, and also to the mechanism for rotating the concentric line which carries loops projecting into the rhumbatron. The purpose of this latter is, of course, to feed power back from the catcher to the buncher.

Power may be taken from the catcher for radiation or other uses by a concentric line; or, for radiation, the power may be taken out by simply boring a hole in the catcher.

The energy supply or "plate voltage" has one terminal connected to the cathode parts $A$ and $C$ and the other to the assembly of rhumbatrons, grid $B$, etc. Choice of a suitable voltage is governed by the following considerations. As the voltage is raised, at constant power, the needed current decreases and the needed shunt impedance increases, perhaps beyond what can be had. On the other hand, as the voltage is decreased, troubles with spreading of the beam by space charge increase. Clearly the proper voltage depends on the power output desired and other factors; but here also conditions are not very critical. For example, it is possible to use many different voltages, from 300 to 4000, on a single klystron oscillator.

Finally we have shown a device that is not essential but very convenient, namely, an oscillation indicator. This consists of a magnetic field $G$ produced by a small permanent magnet (not shown) through which a narrow pencil of electrons from the catcher pass enroute to the fluorescent screen $H$. When the rhumbatrons are not oscillating the electrons all have the same velocity and make a single spot on the screen. When oscillations occur some of the electrons are retarded and others accelerated by the field in the catcher, and so the spot spreads into a line. This device is exceedingly convenient because of its quick responses. Also, by observing the pattern on the screen one may obtain qualitative information about the bunching.

## V. Summary

The most important requisites for a klystron amplifier are as follows:

(1) Efficient resonators, such as rhumbatrons, with holes or grids permitting cathode rays to go through them along the lines of force of their electric fields;

(2) A beam of cathode rays going through both resonators and carrying power enough to make the catcher oscillate more powerfully than the buncher.

For a klystron oscillator, the requirements are those of the amplifier and in addition:

(3) A coupling loop or some practically equivalent line feeding power from the catcher to the buncher;

(4) A P.D. between the cathode and the rhumbatrons such that the bunches arriving at the catcher are not too far out of phase with the field within it.

*Note added in proof.*—Below are three references closely related to the above article which have come to our attention since the article was written. One of these has appeared since this article was submitted. A. Arsenjewa-Heil and O. Heil, Zeits. f. Physik, **95**, 752–762 (1935); E. Brüche and A. Recknagel, Zeits. f. Physik, **108**, 459–482 (1938); W. C. Hahn and G. F. Metcalf, Proc. I. R. E. **27**, 106–116 (1939).

---

# Studies in Lubrication

## IV. The Experimental Variation of the Coefficient of Friction with the Strength of the Lubricant Source for a Complete Journal Bearing

F. Morgan and M. Muskat
*Gulf Research & Development Company, Pittsburgh, Pennsylvania*
(Received December 1, 1938)

The experimental study of the lubrication of a complete journal bearing has been extended, emphasis being placed upon the role played by the position and strength of the lubricant source upon the coefficient of friction. As predicted theoretically, the friction on the bearing has been found to increase with increasing source strength and to be somewhat higher when the source is at the crown than when at the base (region of highest load) of the bearing. It has also been found that when the source is at the base, where it aids the journal rotation effects in supporting the load, the bearing may be successfully operated at much lower speeds and higher loads than when it is at the crown without encountering the usual thin film phenomena. Moreover, for this case, there exists a critical value of the source strength at which the journal and bearing are concentric and the coefficient of friction is given by the simple Petroff theory. The experimental results confirm qualitatively all the predictions of the hydrodynamic theory previously developed. Quantitatively, experiment and theory also agree for small values of the source strength and high values of the Sommerfeld variable, and especially when the source is at the base of the bearing, the discrepancies becoming marked in regions where the approximations of the theory are inherently inadequate.

## Introduction

While rather definite rules have for a long time been accepted by industry for the most advantageous location of the source of lubricant for full journal bearings, they apparently are, for the most part, of an empirical nature, and little information[1] is available con-

[1] G. Welter and W. Brash (General Discussion of Lubrication and Lubricants, The Institution of Mechanical Engineers, October, 1937) have found that when the usual lubrication of a journal bearing is supplemented by high

cerning the effect of the strength of the source upon the operating characteristics of such bearings.

In the first paper[2] of this series hydrodynamical considerations were utilized to show the effect of a variation of the pressure of the source upon the coefficient of friction of a finite journal

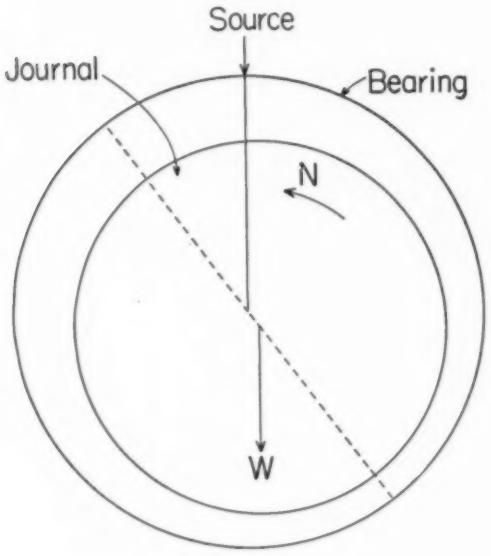


FIG. 1.

bearing, and the existence of this effect was demonstrated qualitatively by the experiments described in the second paper.[3]

Since the original analysis was restricted to cases where the lubricant source is set 90° in advance of the maximum film thickness, the hydrodynamic theory was then extended in Part III[4] so as to apply to the thick film lubrication of finite journal bearings with arbitrary positions of the lubricant source, and for bearing lengths equal to or greater than one-half the bearing perimeter. In applying the theory, however, each position of the source has to be treated separately, and the actual calculations were made only for the cases where the source is at the crown or base of the bearing.

The theory clearly shows that the Sommerfeld variable, $S=(r/c)^2\mu N/P$—where $r$ is the journal radius; $c$, the radial clearance; $\mu$, the lubricant viscosity; $N$, the journal speed; and $P$, the load per unit of projected bearing area—does not uniquely determine the coefficient of friction, but that the latter also depends upon the dimensionless lubricant source strength, which may be represented by

$$q_0=3\mu Qr^2/\pi c^3W,$$

where $W$ is the total load, and $Q$ is the actual rate of lubricant flow through the bearing. It also indicates that when the lubricant source is in the loaded portion of the bearing a critical value of $q_0$ exists for which the journal and bearing are concentric for all values of the Sommerfeld variable. At this critical value, which depends upon the bearing length, the coefficient of friction is given by the Petroff equation ($(r/c)f=2\pi^2S$), and the curve of $f$ *vs.* $\mu N/P$ is consequently a straight line which passes through the origin of coordinates. Moreover, all of the $(r/c)f$ *vs.* $S$ curves obtained by keeping $q_0$ constant were shown to approach the Petroff line as an asymptote when $S$ becomes large regardless of the position of the source. In case the source is in the loaded portion of the bearing, these curves also pass through the origin of coordinates.

In the first experimental paper of this series it was also shown that for low values of the lubricant source pressure the curve of friction coefficient *vs.* Sommerfeld variable in the thick film region lies on a straight line passing through the origin. In this paper these results will be extended with regard to the roles played by both the strength and position of the lubricant source upon the friction coefficient curves, and the latter effects will be compared with those predicted theoretically.

## EXPERIMENTAL ARRANGEMENT

The experimental apparatus was practically the same as that already described,[3] except that copper tubing was so placed about the bearing that lubricant could be introduced either in the loaded or unloaded portion, that is, at the base

pressure lubrication supplied in the region of highest load the frictional resistance at starting is very much reduced. They apparently made no attempt, however, to study the variation of the coefficient of friction with the strength of the lubricant source under conditions of uniform operation.

[2] M. Muskat and F. Morgan, J. App. Phys. **9**, 393 (1938).
[3] F. Morgan and M. Muskat, J. App. Phys. **9**, 539 (1938).
[4] M. Muskat and F. Morgan, J. App. Phys. **10**, 46 (1939).

or crown of the bearing. The case[5] in which the source, which determines the polar axis, is at the crown is illustrated by Fig. 1. In order to secure better torque characteristics at extremely low speeds, a sliding gear transmission was introduced between the Graham variable speed transmission and the journal. Vibration was greatly reduced by mounting the driving mechanism on rubber on a separate base, the journal being driven through two universal joints. The bearing length was 9.75 in. and its radius 1.75 in., giving a ratio of length to perimeter of 0.88. The ratio $r/c$ of journal radius to radial clearance was 1470.

The flow was determined by collecting the oil, that had passed through the bearing, in a burette. Since the flow, after leaving the bearing, was due entirely to gravity, the possibility of some error was introduced because of local variations in various parts of the collecting apparatus. The consistency of the observed results, however, indicates that this error was not appreciable.

In all of the measurements described in this paper Gulfgem Oil A (viscosity 12.6, centipoises at 80°F) was used as the lubricant.

As in the previous experiments, the temperature was measured by a single copper-constantan thermocouple set in the bearing surface, 180 degrees from the source. The speed of rotation of the journal varied from about $\frac{1}{16}$ to 50 r.p.m.

In the first measurements the source pressure was kept fixed while the Sommerfeld variable, $S$, was varied by changing the speed of rotation of the journal. It soon became evident, however, that curves of $(r/c)f$ *vs.* $S$ for fixed values of flow could not readily be obtained by that procedure, because when $S$ was varied the eccentricity of the system changed also and this was followed by a change of lubricant flow. In order then to secure curves for fixed $q_0$, $S$ was treated as a parameter, and data were taken showing the variation of the coefficient of friction as a function of $q_0$ for various values of $S$. From these plots, curves of $(r/c)f$ *vs.* $S$ for several values of $q_0$ were constructed. In order to keep $S$ practically constant, changes of viscosity due to changes in room temperature were compensated by changes in the speed of the journal. The coefficient of friction was then further corrected, for slight variations in $S$, by assuming that the Petroff formula was valid for a small range, so that $(r/c)\Delta f$ could be expressed by $2\pi^2\Delta S$.

As an alternative the source pressure, $p_i$, could have been utilized instead of $q_0$ in the development of the theory. The use of $q_0$ was retained, however, so as to avoid the introduction of the radius of the source of lubricant, a factor depending upon the geometry of the particular system, which appears in the equations connecting the strength of flow and the source pressure.

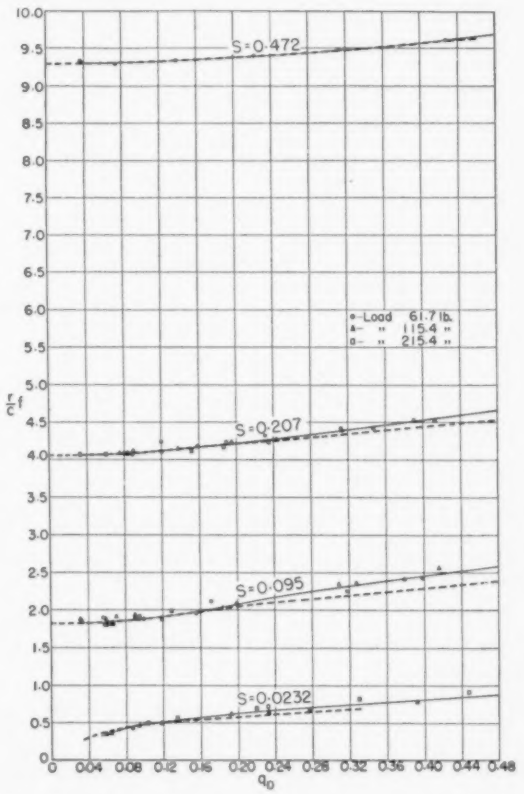


FIG. 2. The variation of the friction coefficient with the dimensionless flux strength of the lubricant source for a journal bearing fed at the base (loaded part) of the bearing. Dashed curve—theoretical. Torque measured on the bearing. $S$ = Sommerfeld variable.

## EXPERIMENTAL RESULTS

The solid lines of Fig. 2 show the effect of the variation of $q_0$ upon the coefficient of friction for

[5] Actually, in the experiments, the source was in the loaded part when at the highest point because the bearing carried the load. The change has been made in order to be consistent with the geometry previously chosen, which, in turn, agrees with that ordinarily found in the literature.

$S=0.472$, 0.207, 0.095, and 0.0232, the torque being measured on the bearing. The source was in the loaded portion of the bearing. Fig. 3 likewise shows the results obtained, for $S=0.399$, 0.207 and 0.095, when the source was in the

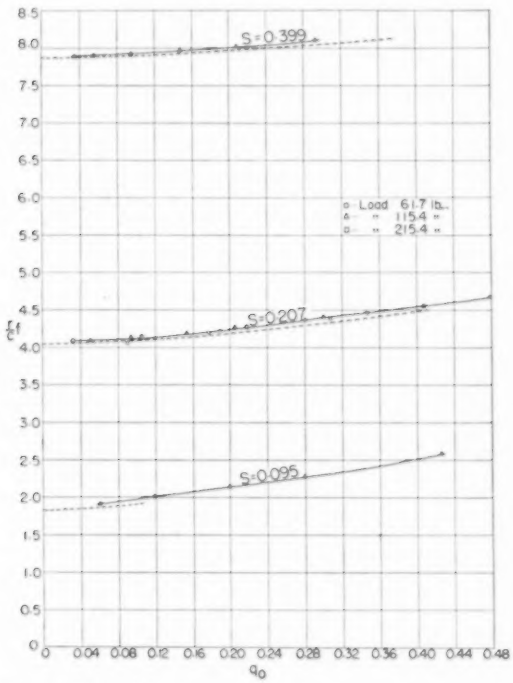


FIG. 3. The variation of the friction coefficient with the dimensionless flux strength of the lubricant source for a journal bearing fed at the crown (unloaded part) of the bearing. Dashed curve—theoretical. Torque measured on the bearing.

unloaded portion of the bearing, 180° from the previous position.

The plotting of $(r/c)f$ against $q_0$, which is essentially the product of the viscosity and the flow per unit load, was suggested originally by the theory, which showed that the flux strength, rather than the quantity of lubricant itself, is the fundamental variable.* This result might have been anticipated because the effectiveness of the source in bringing about a displacement of the journal relative to the bearing must obviously be dependent upon the load. Moreover $q_0$ is a dimensionless quantity while $Q$ is not. It is, however, interesting to compare one of these curves with the components obtained by plotting $(r/c)f$ against $\mu Q$, rather than against $q_0$. In Fig. 4, the curve for $S=0.207$ of Fig. 2 has been replotted in this manner. It will be evident at once that, although the deviation from the average curve is quite large in the case of many of the points in Figs. 2 and 3, considerable justification exists for the adoption of the flow per unit of load as the fundamental variable.

In view of the fact that in some of the plots of Figs. 2 and 3 the data for the three different values of the load do seem more or less to separate themselves into three different curves, it might appear that some further correction term should be introduced in order to compensate adequately for the variation in load. However, since no such definite trend is observable in all cases, this variation must be largely due to experimental error. Moreover this assumption is easily justified because the deviation of almost any point from the curves shown is well within the experimental error. Thus in the case for $S=0.207$ of Fig. 2, the maximum deviation of any single point from the average curve is about one percent. This corresponds to about one gram on the scale pan and is of the order of the uncertainty in the torque determination. For lower values of $S$ the average percent deviation from the mean is larger. The increase of friction due to lubricant flow is also larger, but since the absolute value of the friction coefficient is much smaller the greater fluctuations in the data are still within the experimental errors.

Conditions might appear to be more favorable for accurate observations in case the load were increased, since for the same value of $S$ the speed of rotation and consequently the torque would be increased accordingly. This, however, is not the case. Although an increased torque is favorable to greater accuracy of torque readings, $q_0$ is at the same time reduced because of the additional load, and the total effect to be observed becomes smaller.

The broken lines of Figs. 2 and 3 are the curves predicted by the theory for the corresponding values of $S$. All are for $\bar{w}$, the ratio of

* An interesting physical interpretation of $q_0$ is obtained by introducing the Sommerfeld variable $S$ and the volume of the clearance space $V$. It then may be shown that:

$$q_0=3SQ/VN.$$

Thus $q_0$ may be expressed as $3S$ multiplied by the number of complete changes of lubricant per revolution of the journal, even though not all the lubricant will be replaced uniformly.

the bearing length to its perimeter, equal to 0.88.

Figures 5 and 6, which show $(r/c)f$ as a function of $S$ for various values of $q_0$, were constructed by reading the values of $(r/c)f$ from the curves of Figs. 2 and 3 for several values of $q_0$ up to and including 0.4.

Due to crowding and overlapping, only the experimentally determined curves are shown. The solid circles represent readings that have been taken from Figs. 2 and 3 in the above manner.

The curves of Fig. 5 have been extrapolated to the origin of coordinates even though some contact between the journal and bearing was observed when $q_0$ and $S$ were very small. If the journal and bearing were perfectly round and smooth, theory predicts that the curves should follow the trend indicated. The curves of Fig. 6 were broken off at the lower end because additional points could not be obtained without possible damage to the journal and bearing.

The open circles and crosses in Fig. 5 correspond to friction data that were taken by varying $\mu N/P$, keeping $q_0$ practically constant at the critical value at which the load, according to the theory, should be just supported by the applied lubricant pressure. Under such conditions the journal and bearing should be concentric and the friction curve should be a straight line, through the origin of coordinates, of slope $2\pi^2$. As in the previous paper[3] the value of $r/c$ required for this slope is 1470. It was not found possible, at the very low speeds, to keep the lubricant flow rigorously at the required value. Moreover, in this region the flow was not quite the same for clockwise as for counterclockwise rotation. These probably are the reasons why the deviations of the points from the straight line are greater at very low values of $S$.

## Discussion of Results

Although the curves are largely self-explanatory and the observed results are, for the most part, in good agreement with those predicted theoretically, there are some inferences that may perhaps be worthy of note and some differences between the experimental results and the theoretical predictions that should be pointed out.

Thus when the source is in the loaded part of the bearing, a critical value of the source strength ($q_0=0.091$ for a bearing in which $\bar{w}=0.88$) at which the load is entirely supported by the pressure due to the source is predicted by the theory. Actually, however, this value did not appear to be sufficiently large in some cases. When $S$ was steadily reduced, under these conditions, contact between the journal and bearing apparently occurred at about $\frac{1}{3}$ r.p.m. This became evident by a sharp reduction in electrical resistance and a sudden large increase of torque during a certain part of each revolution. After the source pressure was increased, contact no longer occurred. At $q_0=0.324$, rotation at $\frac{1}{16}$ r.p.m. could apparently continue indefinitely. At this speed the friction torque was too small to be measured.

These results indicate that it is possible by a proper choice of the position and strength of the source to operate a journal bearing under thick film conditions of lubrication at any value of the Sommerfeld variable. This is in direct contradiction to the results usually found in the literature where a rise of the coefficient of friction with decreasing $S$ is almost always shown

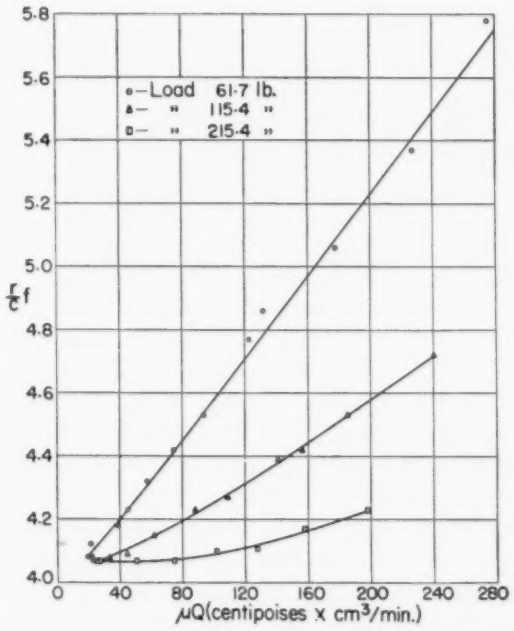


Fig. 4. The variation of the friction coefficient with $\mu Q$ (viscosity × lubricant flow) for a journal bearing fed at the base (loaded part) of the bearing. $S=0.207$.

at very low values of $S$. Moreover, under such conditions the coefficient of friction must also remain finite for the case in which the torque is measured on the journal because the difference

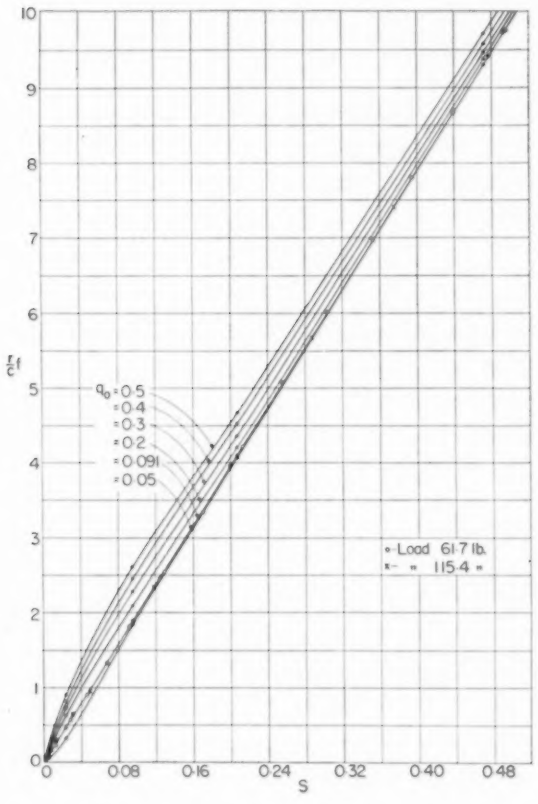


FIG. 5. The variation of the friction coefficient on the bearing with $S$ for a journal bearing fed at the base of the bearing. $q_0$ = dimensionless flux strength. Solid points represent readings taken from Fig. 2.

between the coefficient of friction for the torque measured on the journal and the coefficient for the torque measured on the bearing cannot be greater than $c/r$.

While the agreement between the observed results and the theoretical predictions in Figs. 2 and 3 is, in general, satisfactory for low values of $q_0$ and high values of $S$, the deviations become greater at large values of $q_0$ and small values of $S$. Moreover, the agreement, in case the source is in the loaded part of the bearing, is better than when it is in the unloaded part where the eccentricity is, in general, larger. These results immediately suggest that the second approximation of the analytical theory is not sufficient in case $q_0$ exceeds about 0.25 for an eccentricity of 0.5 or more. It is believed, however, that this is only a part of the actual explanation, and that irregularities and non-uniformity in the journal and bearing lead, in a considerable degree, to experimental errors which tend to exaggerate the deviations at large values of $q_0$ and small values of $S$. Inaccuracies in the journal or bearing could also, no doubt, account for the excessively high value of flow that was found necessary to float the journal at extremely low speeds.

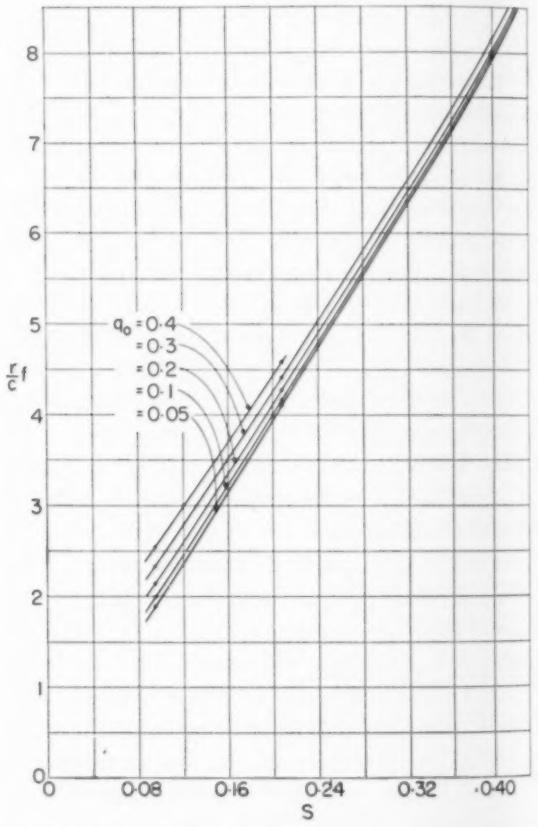


FIG. 6. The variation of the friction coefficient on the bearing with $S$ for a journal bearing fed at the crown of the bearing. $q_0$ = dimensionless flux strength. Solid points represent readings taken from Fig. 3.

A comparison of the experimental and theoretical curves of Figs. 2 and 5 for the source of lubricant in the loaded portion with those of Figs. 3 and 6 for the source in the unloaded part of the bearing shows that the coefficient of friction for thick film lubrication is, in general, a little higher for the same values of $S$ and $q_0$

when the source is in the unloaded portion. At very low values of $S$, however, the position of the source has a much greater effect upon the coefficient of friction. In fact, tendencies toward seizure were always observed for $S<0.05$ when the source was in the unloaded portion of the bearing, although operation could be continued indefinitely for $S=0.01$ with the source at the base. This, of course, was due to the fact that when the source is at the base of the bearing it helps to support the load and the journal eccentricity is consequently less than that obtaining when the source is at the crown.

Although the curves of Figs. 5 and 6 show the variation of the coefficient of friction with $S$ and with $q_0$ in a satisfactory manner, it is instructive to study the behavior of the torque as a function of the load. It is evident immediately that a plot of the reciprocal of $S$ as abscissa and of the torque as ordinate will essentially be one of torque *vs.* load. Such curves may easily be plotted from observed data, but a simple observation makes the plot possible from the customary curve of coefficient of friction *vs.* $S$. Thus, by definition, we have

$$\frac{r}{c}f=\frac{r}{c}\frac{T}{r\cdot W},$$

where $T$ is the torque and $W$ the load. Also,

$$\frac{1}{S}=\frac{c^2}{r^2}\frac{P}{\mu N}=\frac{c^2}{2r^3\mu NL}W.$$

Hence, for any point on the $(r/c)f$ *vs.* $S$ curve the ratio:

$$\frac{\text{ordinate}}{\text{abscissa}}=\frac{(r/c)f}{S}=\frac{c}{2r^3L\mu N}T.$$

Curves of the above ratio (ordinate/abscissa) against $1/S$ are thus equivalent, in the case of a particular bearing and for constant values of viscosity and speed, to plots of torque *vs.* load.

In Fig. 7 several curves that were obtained in this manner are shown. Curves 1 and 5, respectively, correspond to the Sommerfeld curve for the torque on the journal and the Harrison curve for the torque on the bearing. The horizontal straight line at $T=(4\pi^2/c)r^3L\mu N$ is for the Petroff case where the torque is independent of the load. Curves 2 and 4 were obtained from the curves for $q_0=0.5$ and 0.05 of Fig. 5.

As $1/S$ has been plotted as the abscissa, cases of fairly complete lubrication may be expected

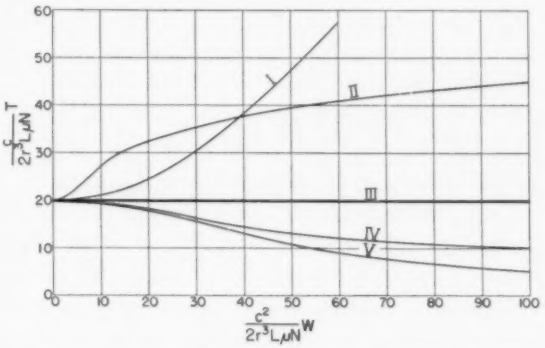


FIG. 7. The variation of the friction torque ($T$) with the load ($W$) for full journal bearings. I, Torque on the journal of a journal bearing of finite length according to the Sommerfeld theory. II, $\bar{w}=0.88$; $q_0=0.5$. Torque on bearing. Source at base. III, Petroff line. IV, $\bar{w}=0.88$; $q_0=0.05$. Torque on bearing. Source at base. V, Torque on the bearing of a journal bearing of infinite length according to the Harrison theory. $c$=radial clearance; $r$=journal radius; $L$=bearing length; $\mu$=lubricant viscosity; $N$=journal speed; $\bar{w}$=bearing length/bearing circumference; $q_0$=dimensionless flux strength. Curves II and IV were calculated from Fig. 5.

to lie well to the left on the curves of Fig. 7. In fact for $S=1$, the curves shown do not differ appreciably from each other or from the Petroff curve. This is because rotational effects predominate in this region in all of the cases illustrated.

In the thin film region, however, i.e., large values of load, the character of the torque *vs.* load curve depends entirely upon the curvature of the friction coefficient *vs.* $S$ curve. Thus if the latter curve is everywhere concave upward with a positive friction axis intercept, or has a minimum of the type usually found with practical lubricant testing machines or of that given by the Sommerfeld theory, the torque will rise monotonically as the load is increased. If the friction coefficient curve is concave downward in the thin film region and passes through the origin, as the curves of Fig. 5 do for $q_0>0.1$, the torque will rise and approach a constant value as the load increases. On the other hand, if the friction coefficient curve passes through the origin but is concave upward in the thin film region, as are the curves of Figs. 5 for $q_0<0.1$, the torque will fall to a constant value

as the load is increased. And in the special case where the tangent at the origin is zero, the torque will ultimately vanish as the load is indefinitely increased, as in the case of the Harrison curve.

The line of constant torque corresponds to the case in which the journal and bearing are concentric for all values of $S$. This condition may be realized experimentally, when the source is in the loaded part, by adjusting the flux strength to the critical value for each load.

Comparison between the observed and calculated source pressures for given values of lubricant flow may be made most easily when the flux strength has the critical value, that is when the pressure due to the source is just sufficient to carry the load. In this case the journal and bearing are concentric, the eccentricity is zero, and the pressure above atmospheric is given[4] by:

$$p_i=\frac{W(1+\mathrm{ctnh}^2\, w_0/2)}{8\pi r^2}\times\left[w_0-2\log \bar{r}-4\sum_1^\infty \frac{1}{n(1+e^{2nw_0})}\right],$$

where $W$ is the total load; $w_0$, the ratio of bearing length to journal diameter; $r$, the journal radius; and $\bar{r}$, the ratio of source radius to journal radius. Thus for a load of 115.4 lb., and for $w_0$, $r$, and $\bar{r}$ equal to 2.76, 1.75 inches, and 0.0937, respectively, the calculated value of the pressure is 26 lb./in.$^2$ The observed value in that case was actually 25 lb./in.$^2$

Finally, attention should be called to the fact that in these experiments the rotational velocities and loads were small so that the temperature rise of the bearing due to shearing of the oil film was scarcely detectable. Air bubbles in the oil at the ends of the bearing were frequently the source of much concern, although they usually disappeared before any measurements were made. Several unsuccessful attempts were made to obtain some correlation between the appearance of these bubbles and the occurrence of a pressure gradient tending to produce a flow of lubricant toward the center of the bearing. While the theory indicates that the probability of the occurrence of unfavorable pressure gradients is much higher when the source is at the crown than when at the base of the bearing, no appreciable difference could be detected experimentally. This, of course, does not necessarily mean that the film was complete in both cases. The possibility still exists that the greater eccentricity necessary to obtain the same load carrying capacity in the case of an incomplete film might compensate for any decrease in friction due to the limited extent of the lubricating film. It seems more probable, however, that with the small loads of these experiments the film was complete at all times.

## Summary

Although a detailed quantitative agreement between theory and experiment cannot be claimed, there can be no question but that the experimental results are at least in qualitative agreement with the essential features of the theoretical predictions.

These are that: (1) a monotonic increase of the friction coefficient occurs when the pressure of the lubricant source is increased; (2) all of the curves for various values of source strength approach the Petroff line as an asymptote at high values of $S$; (3) in case the lubricant source is in the loaded portion of the bearing the curves pass through the origin of coordinates and no thin film region exists; and (4) at a certain value of the source strength the friction curve is a straight line when the source is in the loaded portion of the bearing.

Finally, the position of the source of lubricant has been found to have considerable effect upon the practical operation of a journal bearing, particularly at low values of $S$.

The authors are indebted to Dr. Paul D. Foote, Executive Vice President of the Gulf Research & Development Company, for permission to publish this paper and to Mr. D. W. Reed for assistance in performing the experiments.

# Luminescence During Intermittent Electron Bombardment

R. B. Nelson,* R. P. Johnson and W. B. Nottingham†
*Research Laboratory, General Electric Company, Schenectady, New York*
(Received January 3, 1939)

The dynamic luminescence characteristics of five samples of commercial phosphors excited intermittently by electron bombardment have been studied. The decay of artificial willemite follows closely a simple exponential law, except for a rapid fall during the first three milliseconds after bombardment, the prominence of this component increasing with the current density. An attempt is made to correlate the observed dependence of build-up rate on current density with the phenomenon of current-saturation under continuous bombardment. A sample of calcium tungstate follows changes in the intensity of excitation within 100 microseconds, the resolving time of the apparatus. Two samples of ZnS·Ag and one sample of ZnS·CdS·Ag decay more rapidly the higher the intensity of excitation. The initial rate for ZnS·Ag is greater than would be predicted for a simple bimolecular reaction, and cannot plausibly be explained by non-uniformity in the initial distribution of reactants in a bimolecular reaction. The ZnS·CdS·Ag decays initially according to a simple bimolecular law.

## I. Problem and Experimental Method

The course of the luminescence of a phosphor toward a new equilibrium value, after a change in the intensity of the exciting agent, is an important datum for any theory of fluorescence. The information yielded by decay curves and build-up curves supplements that obtained by studying how the luminescence under continuous excitation varies with the chemical and physical composition of the phosphor, with its temperature, and with the nature, energy, and rate of arrival of the exciting particles. The behavior of phosphors under intermittent electron bombardment, which is the subject of this investigation, has also considerable technical interest.

Five samples of commercial phosphors, furnished by the RCA Manufacturing Company, have been studied: an artificial willemite, $2ZnO \cdot SiO_2 \cdot Mn$, luminescing green; two identical samples of ZnS activated with Ag, luminescing blue; a mixed sulphide, ZnS·CdS·Ag, luminescing yellow; and a calcium tungstate, presumably pure, luminescing blue. The powders are settled onto glass disks from acetone suspensions. Experiments on the luminescent and electrical properties of these same samples under continuous electron bombardment, in the tube used for the present study, have been reported.[1]

The samples are mounted off the axis of the tube (Fig. 1), to prevent contamination by material evaporated from the cathode of the electron gun.[2] The electron beam is directed by magnets to the phosphor under study. The current in the beam is controlled by the bias on the first grid $G_1$ and is measured by a galvanometer in series with the second anode, a layer of gold covering most of the inside of the tube. Measurements with the cage structure at the end of the tube have shown that the beam contains 99 percent of the current reaching the second anode. Two Fernico wires, completely shielded, are imbedded in each mounting disk and ground flush with the glass surface which is later coated;

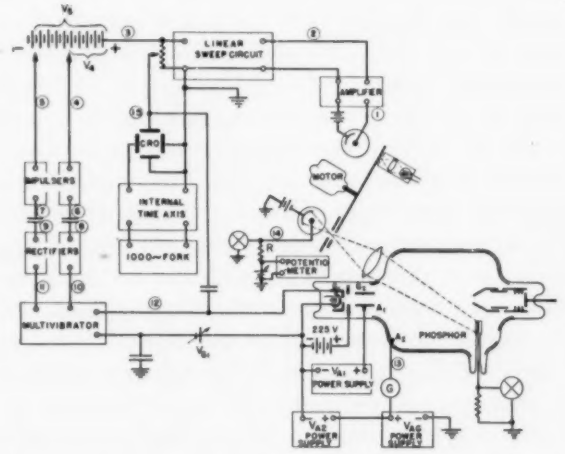


FIG. 1. Tube and circuit for studying luminescence of phosphors bombarded intermittently with electrons.

* At present, RCA Manufacturing Company, Harrison, New Jersey.

† On leave of absence from Massachusetts Institute of Technology. Some of the circuits were devised by W. B. N.; the other authors are responsible for the measurements reported here.

[1] W. B. Nottingham, J. App. Phys. **10**, 73 (1939).

[2] C. H. Bachman and C. W. Carnahan, Proc. I. R. E. **26**, 529 (1938).

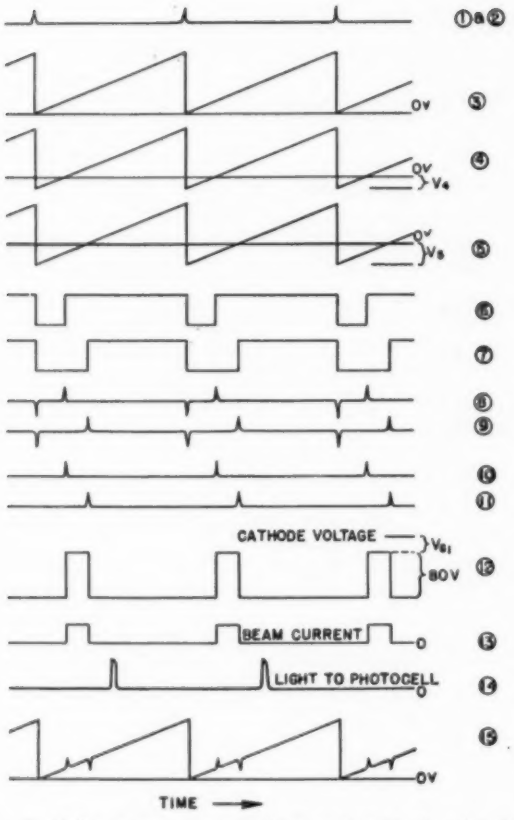


FIG. 2. Voltage waves at various points in the circuit of Fig. 1.

with these probes the potential of the phosphor with respect to ground is measured by an electrometer. For each voltage $V_{A2}$ of the cathode with respect to the second anode, the second anode is made positive with respect to ground by a voltage $V_{AG}$ just sufficient to bring the phosphor to ground potential. The difference $V_{A2}-V_{AG}$ is then the energy of the incident electrons in volts.[3]

The light from the phosphor is focused by a lens on an aperture in front of a vacuum photocell, and the average value of the photoelectric current is measured by balancing out the voltage drop in a platinum-film resistor, a Compton electrometer serving as a null indicator. That the current is proportional to the light intensity, over the range to be studied, has been established in a separate experiment.

These phosphors all follow changes in the intensity of the electron beam far too rapidly to allow consecutive readings of the light during a single cycle of build-up and decay. It is required, then, to turn the beam on and off periodically and to measure the average value of the light emitted during some short part of the total period. The total period, the fraction of the period during which the beam is on, and the phase difference between the turning on of the beam and the sampling of the light, should be separately variable. The block diagram (Fig. 1) shows how these requirements are met.

Immediately in front of the photo-cell aperture is a rotating Duralumin disk with a hole which admits light from the phosphor to the photo-cell during 1/100 of a revolution. For suppressing the electron beam periodically, a square wave of voltage from a multivibrator circuit is added to the steady grid bias on the gun. During the "on" interval this multivibrator voltage is zero, and the beam current is determined by the steady grid bias; in the "off" interval the grid voltage is carried below $-80$ v, much farther than is necessary to stop the current completely; the change from one state to the other occurs in about one microsecond.

The remainder of the circuit is for synchronizing the multivibrator oscillations with the rotating disk, and for shifting the phases. Half a revolution from the measuring photo-cell the hole passes another stop diaphragm and lets light from a

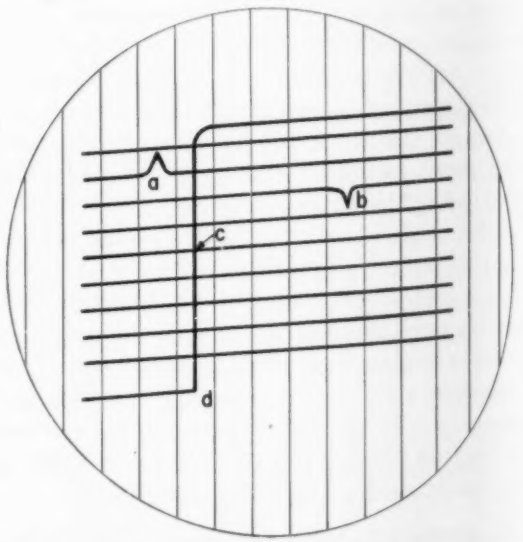


FIG. 3. Stationary monitory oscillograph pattern corresponding to the cycle of Fig. 2. (a) Beam goes on; (b) beam goes off; (c) photo-cell open; (d) end of sweep circuit cycle. By inspection, the beam persists for 0.150 cycle, and the measuring photo-cell is opened 0.160 cycle after the beam is cut off.

[3] W. B. Nottingham, J. App. Phys. **8**, 762 (1937).

lamp into another photo-cell. The resultant current pulse, after amplification, synchronizes a conventional linear sweep circuit with the disk. To the sawtooth voltage output of the sweep circuit is added a variable negative bias, so that the resultant voltage is initially negative and rises through zero at a time in the cycle determined by the negative bias. This biased wave is applied to an "impulser" circuit which has a trigger action, yielding a pulse of positive voltage when its input voltage rises through zero. This pulse turns the multivibrator on and so stops the electron beam. An identical impulser, whose sawtooth input voltage differs from that of the first only in the amount of added negative bias, turns the multivibrator off, starting the beam. Rectifier tubes prevent the negative pulses which originate in the impulsers at the end of the sweep circuit cycle from reaching the multivibrator. By changing the two biases the beam can be turned on and off at any two points in the sweep circuit cycle; the measuring photo-cell is open, of course, midway in this cycle. Fig. 2 shows the voltages at several places in the circuit of Fig. 1.

The operation is monitored continuously with an RCA Type TMV-122-B cathode-ray oscillograph. All time intervals are referred directly to the period of a 1000-cycle tuning fork oscillator, which is checked occasionally by beating the 17th submultiple of its output against the 60-cycle line voltage. This fork synchronizes the horizontal time-axis of the oscillograph at some convenient submultiple of 1000 cycles. On the vertically deflecting plates is placed a fraction of the output of the sweep circuit, to which is added, through condenser coupling, the voltage on the grid of the gun. The disk speed is held at 1/10 the frequency of the horizontal time-axis. The oscillograph pattern (Fig. 3) is then stationary, and consists of ten parallel traces and a vertical return trace, with two bumps showing where the beam is turned on and off. By inspection of the pattern, the time intervals can easily be read with an error less than one percent of the total period. Usually the shape of the beam current wave is independently monitored, on a cathode-ray oscillograph (not shown) in series with the second anode.[4]

[4] Blueprints showing these circuits in detail are available on request to the authors.

The apparatus is run at speeds from ten r.p.s., limited by flicker of the monitor pattern, up to 100 r.p.s., limited by the motor rating. Tests have shown that the resolving time is actually about one percent of the period of revolution—100 microseconds for a disk speed of 100 r.p.s.

## II. Results with Artificial Willemite

The general behavior of the willemite sample is seen in Fig. 4, where the phosphor was excited for

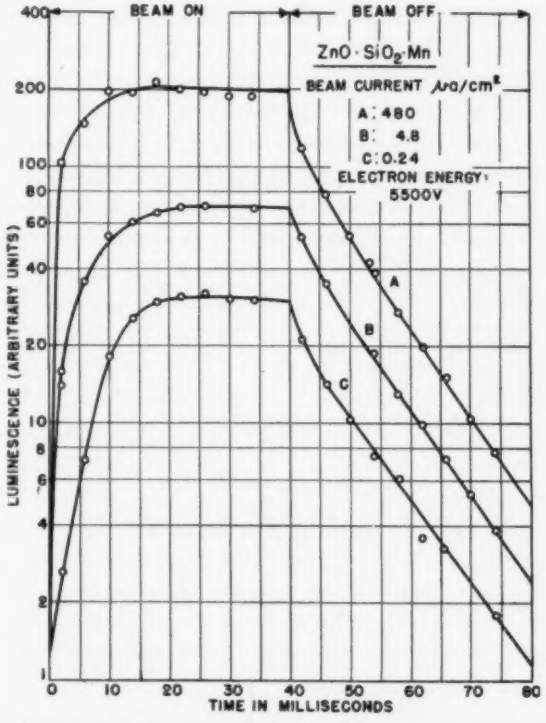


FIG. 4. Typical semi-log build-up and decay curves for artificial willemite, showing effect of changing current density. The vertical spacing is arbitrary.

40 milliseconds and allowed to decay for 40 milliseconds. The decay is approximately exponential, at a rate independent, after the first two or three milliseconds, of the current density. The rise toward the equilibrium luminescence is more rapid at the higher current densities. These same tendencies appear in Fig. 5, where the excitation period is reduced to eight milliseconds and the decay is followed for 72 milliseconds. Fig. 6 shows that the shape of the decay curve is independent of the energy of the exciting electrons. In Fig. 7, the decay during nine milliseconds, after excitation for one millisecond, is

followed in detail, and it is evident that the rapid initial decay is accentuated at the higher current density (curves A and B).[5] Curve C is added to show again that the course of the decay does not vary with the electron energy; curve D, a reproduction of part of curve A in Fig. 6, shows that it is independent of both the excitation period and the total decay period.

For this phosphor, and for all the others, a change in the color of the light during decay was sought by placing between the phosphor and the photo-cell a filter whose cut-off lay approximately midway in the emission spectrum. In all cases, the presence of a filter changed the curves only by a scale factor: the color remains constant during decay, and the photoelectric currents are a true measure of the rate of emission of quanta.

That the decay curves are nearly exponential, and nearly invariant under changes in energy,

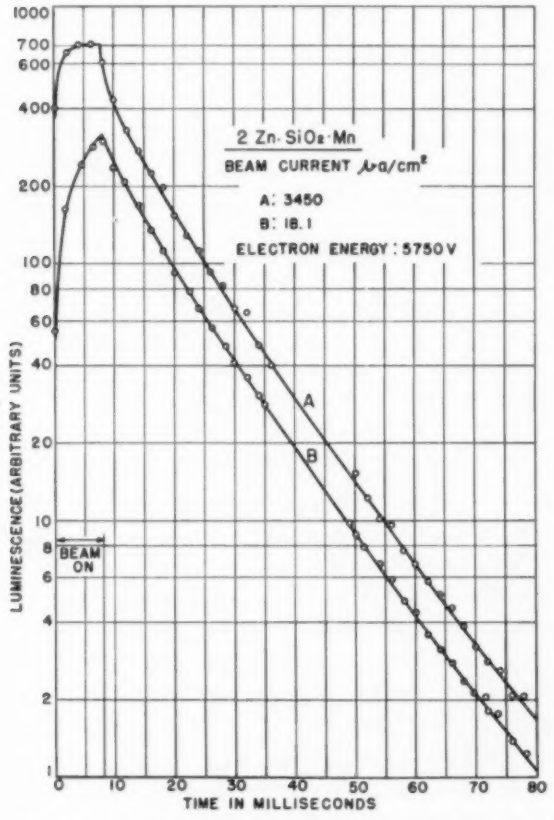


FIG. 5. Typical semi-log build-up and decay curves for artificial willemite, showing effect of changing current density. The vertical spacing is arbitrary.

[5] In this connection, see S. T. Martin, J. App. Phys. **10**, 116 (1939).

density and duration of the exciting current, suggests that at least during the first 72 milliseconds the decay process is monomolecular. The slight curvature of the semi-logarithmic plots can formally be explained by non-uniformity of the phosphor grains. Fonda,[6] using ultraviolet light for excitation, has found that the decay characteristics of synthetic willemite depend markedly on particle size. Bünger and Flechsig[7] report that single crystals of KCl·Tl phosphor show an accurate simple exponential decay. If these

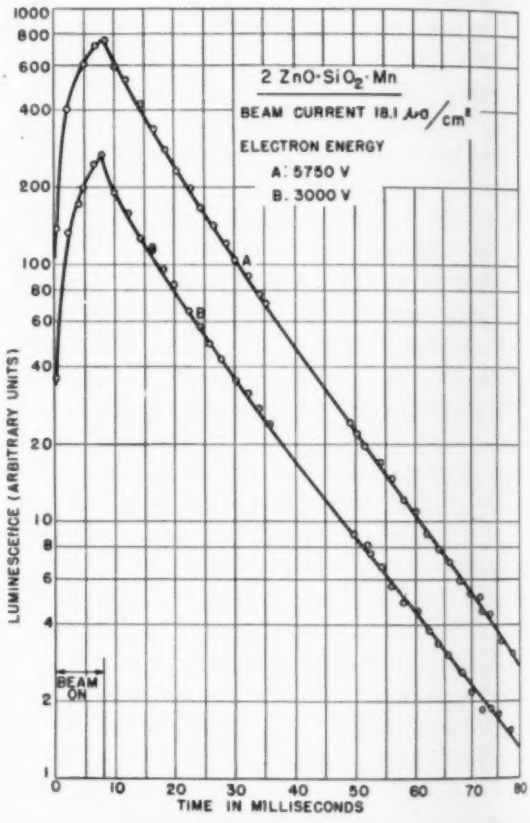


FIG. 6. Illustrating that the shape of the willemite characteristic is independent of energy of the incident electrons. The vertical spacing is arbitrary.

curves are composites of simple exponential decay curves for the individual grains, the time constants for various grains must range from about 7 to about 14 milliseconds.

The initial rapid decay, whose prominence depends on the current density, still lacks even

[6] G. R. Fonda, unpublished experiments in this laboratory.

[7] W. Bünger and W. Flechsig, Zeits. f. Physik **67**, 42 (1931).

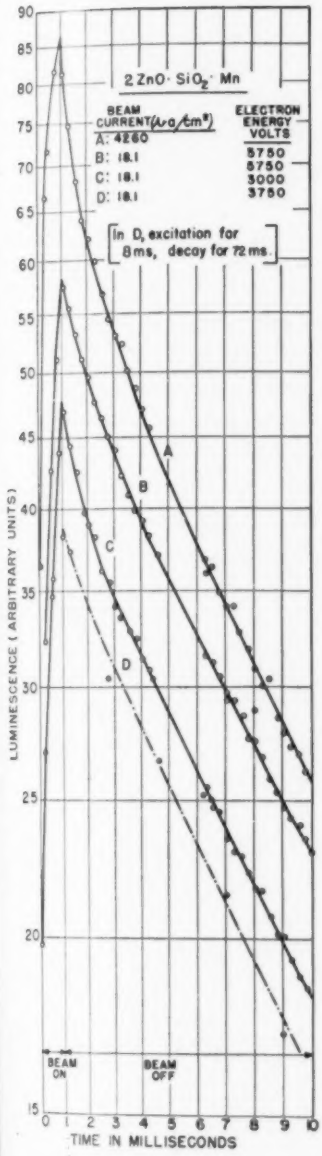


FIG. 7. Showing an initial rapid phase of the decay of willemite, prominent at high current density (curves A and B). C is added to show that the curves are independent of electron energy, D to show that they are independent of the interval of excitation and of decay. The vertical spacing is arbitrary.

formal interpretation. Heating of the phosphor during bombardment and cooling during decay cannot account for it; a rough calculation shows that the temperature rise during bombardment cannot exceed 5°C, and the day-to-day variations in room temperature, which had no effect on the decay characteristics, were greater than this.

If the decay were strictly monomolecular, and if the probability of excitation per incident electron were independent of the current density, the build-up should also follow an exponential law with the same time constant as the decay. It is known, however, that the luminescence of willemite under continuous electron bombardment increases less rapidly than the density of the exciting current and approaches a saturation value.[3] This phenomenon of current-saturation should have associated with it a dependence of the build-up rate on current density, such as appears in Fig. 4. The saturation effect is practically independent of the initial energy $E$ of the bombarding electrons—when this energy is increased the light output at every current density is multiplied by a factor proportional to $E^2$. It is consistent with these observations to suppose that the initial energy $E$ determines only the depth of penetration of the electrons, this depth being proportional to $E^2$ (in keeping with the usual theory), and that the excitation per unit length of path of the electron depends only on the concentration of excitable "centers." Assume that this concentration in the unexcited sample has the limited value $N_0$, and that each center which has been excited is unconcerned until it has reverted, with emission of light, to its ground state. Then the concentration $N_1$ of excited centers should change during bombardment according to the equation

$$dN_1/dt = kI(N_0 - N_1) - \lambda N_1,$$

where $\lambda$ is the natural decay rate (found by observing the decay after stopping the excitation), $I$ is the current density, and $k$ is a constant. Integrating this equation with $N_1(0) = 0$, and recalling that the light output is at every instant proportional to the concentration of excited centers, we find that the luminescence should build up during bombardment according to the law

$$L(t) = \mu N_1(t) = \frac{\mu k I N_0}{kI + \lambda}\left[1 - e^{-(kI+\lambda)t}\right] \qquad (1)$$

and should approach an equilibrium value $L_\infty$ given by

$$\frac{1}{L_\infty} - \frac{1}{\mu N_0} = \frac{\lambda}{\mu k N_0}\left(\frac{1}{I}\right). \qquad (2)$$

Fig. 8 shows that the current-saturation effect, for this sample of willemite, follows Eq. (2) fairly closely. However, the build-up curves, such as those of Fig. 4, follow Eq. (1) only qualitatively. If a value of $k$ is deduced from the

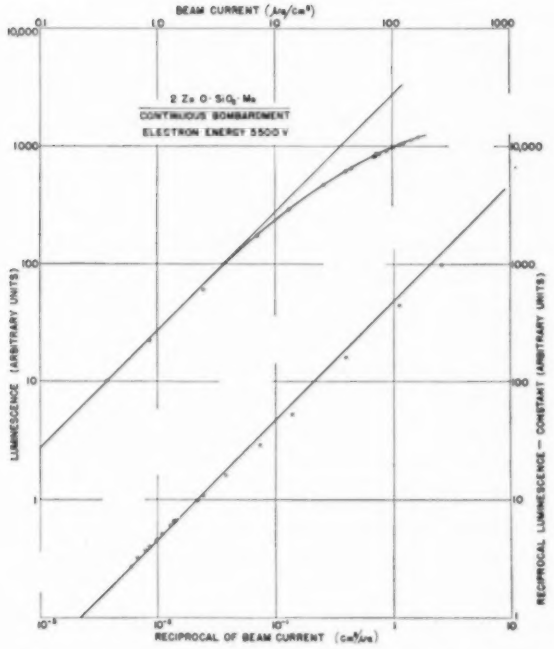


FIG. 8. (A) Current-saturation effect in artificial willemite under continuous electron bombardment; (B) the same data, plotted to show reasonable agreement with Eq. (2).

rate of build-up at high current density, then at low current density the rise is more rapid than is to be expected.

## III. RESULTS WITH $CaWO_4$

The light from the calcium tungstate sample rises to its equilibrium value within 100 microseconds (the resolving time of the apparatus, for the diaphragm sizes used) after the electron beam is turned on, and falls by a factor of at least 2000 (too low for detection with our photo-cell) within 100 microseconds after extinction of the beam.

## IV. RESULTS WITH SULPHIDES

The two ZnS·Ag samples behave alike in every respect. The rise of luminescence after the beam is turned on is too rapid to be followed with any precision. The shape of the decay curve depends strikingly on the current density (Fig. 9), the initial decay being much more rapid at higher current density. A change in energy of the incident electrons, on the other hand, makes practically no change in the shape of the curve (Fig. 10). Every ordinate is multiplied by a scale factor—the same factor by which the light output under continuous excitation is multiplied when the electron energy is changed.

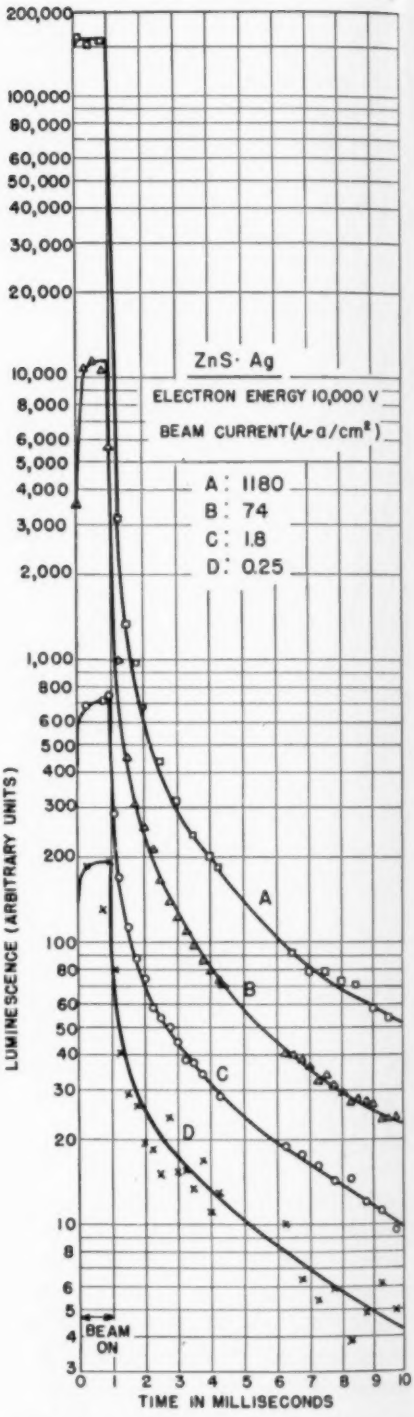


FIG. 9. Typical semi-log decay curves for ZnS·Ag, showing dependence of shape on current density. The vertical spacing is arbitrary.

That the decay curve depends in any marked fashion on current density seems to indicate inevitably that the decay rate is a function of the excitation per unit volume. The shape of the curve is not affected by a change in the energy $E$ of the incident electrons; hence the excitation per unit volume is not a function of $E$. But the luminescence, during or after excitation, does depend strongly on the initial electron energy—

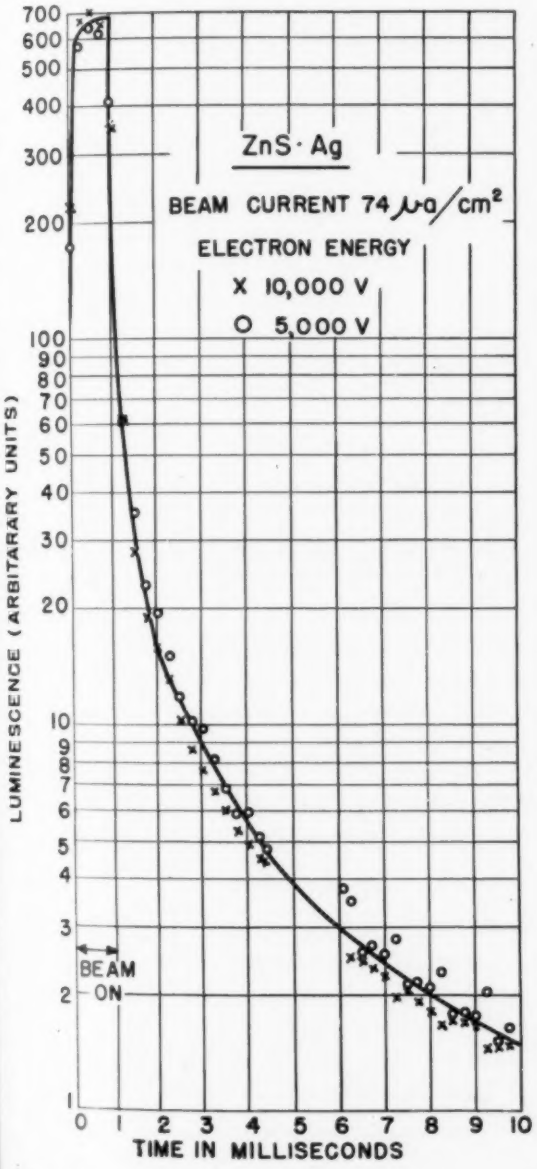


FIG. 10. Superposition to show that the decay curve for ZnS·Ag has a shape independent of the energy of the incident electrons. The two sets of ordinates differ by a scale factor of 7.5.

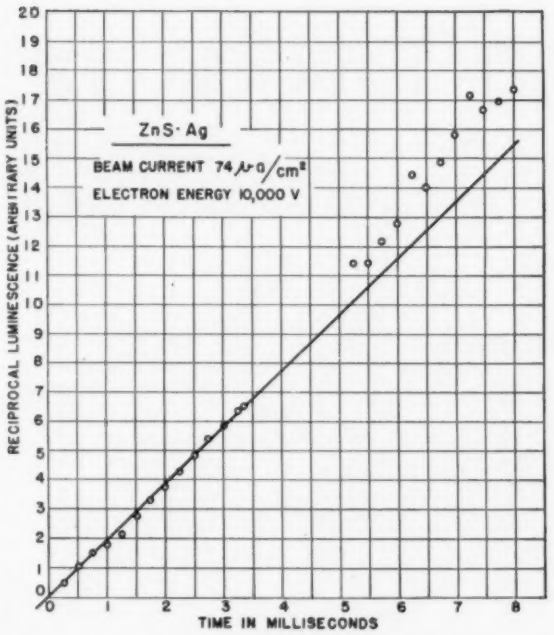


FIG. 11. Data of Fig. 9(B) plotted to show initial agreement with an empirical hyperbolic decay law.

as $E^{2.9}$, in the case of these samples.[1] It appears, then, that the excitation per unit path length of the primary electron within the phosphor is constant, while the total rate of loss of energy varies with residual energy in such a way as to give a penetration depth proportional to $E^{2.9}$.

The shape of the decay curves is of some interest. The simplest hypothesis for the sulphide phosphors, consistent with the fact that they are photoconducting, is that the excitation is an ionization process, and that light is emitted when an electron recombines with an ionized center.[8] If the electrons and ionized centers are equal in concentration and randomly distributed, the decay curve should then follow the same simple law as does the rate of a bimolecular gaseous reaction:

$$L=\frac{k}{((k/L_0)^{\frac{1}{2}}+t)^2},$$

where $L_0$ is the initial luminescence and $k$ is a constant of the material. Actually, all our decay curves for ZnS·Ag can be fitted, over the first five milliseconds where the photo-currents are

[8] This mechanism has recently been discussed by F. Seitz, J. Chem. Phys. 6, 454 (1938).

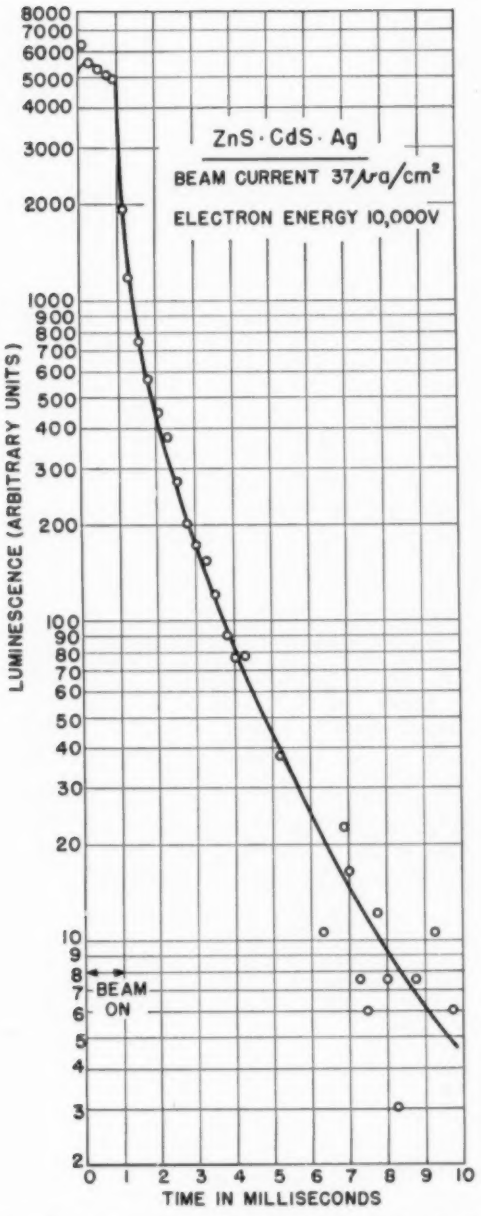


FIG. 12. Typical semi-log characteristic for mixed sulphide, ZnS·CdS·Ag.

most precisely measured,[9] by the empirical equation $L=a/(b+t)$. Fig. 11 shows the applicability of this formula. Unfortunately the curves could not be traced out far enough to tell whether the hyperbolic law, which of course cannot continue to hold, eventually yields place to a simple bimolecular law; neither could the initial decay be measured at current densities low enough to give useful precision to the intercept on the time axis.

An abnormally rapid initial rate in a bimolecular reaction can formally be explained on the basis of an initial non-uniform distribution of the reacting components. In the present case, a non-uniform excitation along the path of each primary electron is improbable for the reasons advanced above. It would conceivably be possible to invent an initial non-uniform distribution of excitation within a column surrounding the path of each primary electron which would yield an initial hyperbolic decay, and then to account for the dependence of the rate on current density by an overlapping of these columns. We are the more inclined to view any such hypothesis as *ad hoc*, since a number of investigators,[10] studying the decay of long-lived sulphide phosphors after optical excitation, have found empirical laws which may be approximated by the form

$$L=a/(b+t)^{\alpha},$$

with values of $\alpha$ ranging from 0.8 upward beyond 2.

The mixed sulphide sample, ZnS·CdS·Ag, is like the ZnS·Ag in that the decay curves are not affected in shape by a change in energy of the electrons, but are made initially more steep by increasing the current density. The shape of the curves, however, is markedly different from the hyperbolic course followed initially by the ZnS·Ag decay (Fig. 12). During the first four milliseconds the data is fitted reasonably well by the empirical formula

$$L=a/(b+t)^{2};$$

the deviation at longer times is in the direction of an exponent larger than two. It should perhaps be remarked that a formula of this type, in which the exponent exceeds two, cannot be explained by non-uniformity in the initial distribution of reactants in a bimolecular decay.

[9] The scattering of the observations after five milliseconds, which is somewhat greater than the experimental error, is perhaps caused by changes in the temperature of the samples. Several observers have reported that the decay of sulphide phosphors, optically excited, shows marked temperature dependence at longer times.

[10] E. Becquerel, Comptes rendus **51**, 921 (1860); A. Guntz, Ann. de Chimie **6**, 5 (1926); R. Coustal, J. Chim. Phys. **28**, 345 (1931); W. L. Lewchin and W. W. Antonov-Romanovsky, Comptes rendus (Doklady) de l'Acad. des Sciences, U. S. S. R. **17**, 95 (1937); P. J. Mulder, J. Frank. Inst. **225**, 527 (1938); W. H. Byler, J. Am. Chem. Soc. 60, 632 (1938).

# A HIGHLY EFFICIENT SOURCE OF ULTRA-VIOLET RADIATION

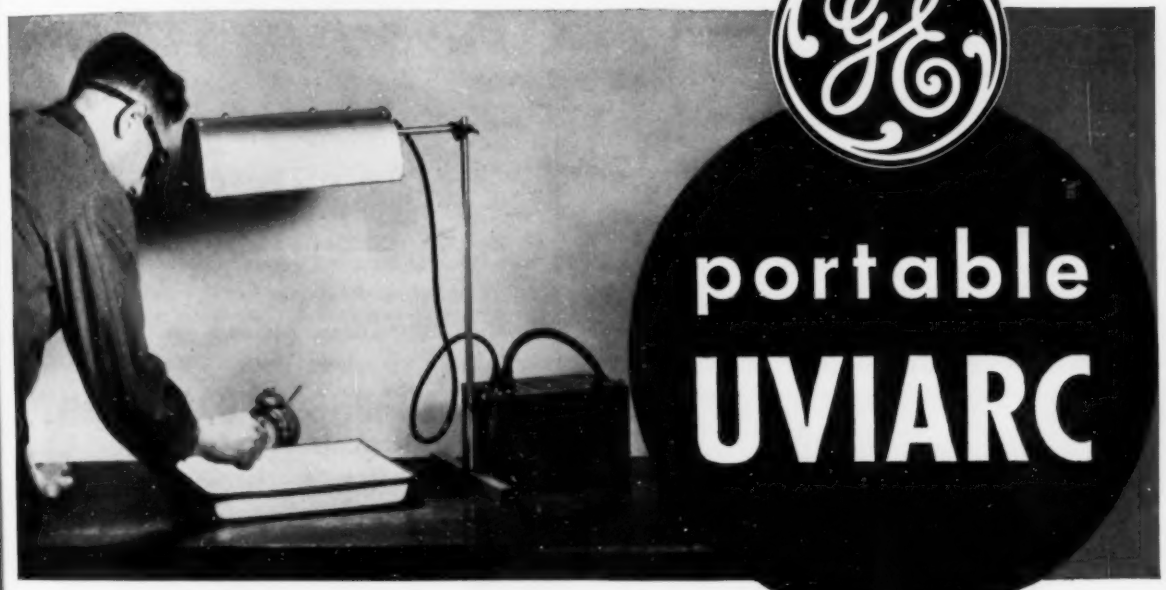


This portable self-starting A. C. outfit is the result of years of experience with mercury-pool cathode quartz lamps. The Uviarc utilizes the same "hot cathode" construction responsible for the efficiency and dependability of General Electric Type H lamps which are widely used throughout industry. » » » The reflector hood concentrates the radiation of the Uviarc within a 90° angle and is designed to accommodate standard 6½ x 6½ in. filters. The outfit draws 410 watts from 115 or 220 volt 60 cycle supply. Full efficiency is obtained in a vertical, horizontal or angular position. » » » Write for a copy of descriptive bulletin. General Electric Vapor Lamp Co., 835 Adams Street, Hoboken, New Jersey.

*Radiation characteristics, spectral analysis and other technical and mechanical data are contained in this Uviarc bulletin.*

**GENERAL ELECTRIC VAPOR LAMP COMPANY**

930U

## "JAGABI"
### HAND TACHOSCOPE

**This combined speed-counter and stop-watch gives the exact number of revolutions in the exact time in which they were made. Measures speed with "split-second accuracy" up to 20,000 r.p.m.**

**Write for Bulletin 1595-R describing these and other speed-measuring instruments.**

**JAMES G. BIDDLE CO.**
*ELECTRICAL AND SCIENTIFIC INSTRUMENTS*
1211-13 ARCH STREET PHILADELPHIA, PA.

## SHALLCROSS
### MULTI-RESISTANCE STANDARDS

**Five Different Standards in One Box**

**Range 1 ohm to 10 megohms**

Employing the high grade Shallcross non-reactive wire wound Manganin resistors, 0.1%.

The Standard Resistance Boxes provide resistance comparison standards for schools, colleges and industrial laboratories at minimum cost.

**Write for Bulletin No. 835AB**

**SHALLCROSS MFG. COMPANY**
COLLINGDALE, PA.

## PHOTOELASTIC POLARISCOPES
**With White and Monochromatic Light Sources (Up to 12 inches in diam.)**
**Equipped with POLAROID, Nicol Prisms, or Mark's Polarizers**

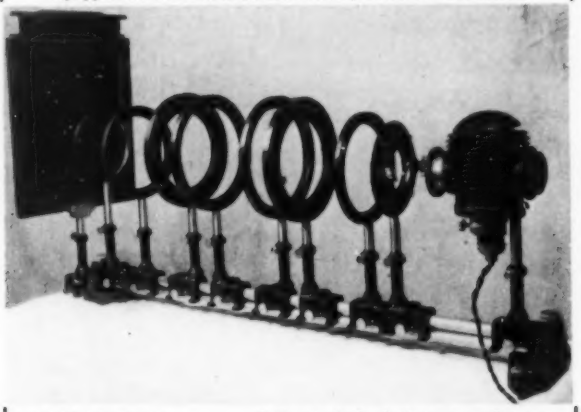

**POLAROID ***
**Mark's Polarizers**
**Mica 1/4 wave Plates**
} Cemented between glass discs, with fixed or rotating graduated (0° to 360°) mounts.

**White and Monochromatic Light Sources; Strain-free Lenses; Glass-strain Testers; Polarizing Attachments for Microscopes; Optical Beds, Riders, Lens Holders, etc.; Model Loading Frames; Photoelastic Model Materials (Bakelite, Marblette, etc.), Annealed strain-free and Polished; Photoelastic Stress Research; Photoelastic Journal, $2.00 Annually ($2.50 foreign).**

**POLARIZED LIGHT & PHOTOELASTIC CO.**
55 West 42d Street New York, N. Y.

** T.M. Reg. U. S. Pat. Office by Polaroid Corp.*

## HARSHAW SYNTHETIC CRYSTAL OPTICS

**. . . open new fields in ultraviolet and infrared spectroscopy. . . . Single crystals are synthetically grown from pure molten salts. . . . Harshaw's unique process makes available large crystals of Lithium Fluoride, Sodium Chloride (Rock Salt), and Potassium Bromide—and for polarizing optics, Sodium Nitrate. . . . Write for information.**

**THE HARSHAW CHEMICAL CO.**
SPECIAL PRODUCTS DIVISION
CLEVELAND, OHIO

# Class E Spectroscopic Plates

THIS RECENT ADDITION to the series of *Eastman Spectroscopic Plates* has its highest sensitivity through the region 6000Å. to 7000Å., with a maximum at 6500 Å. Class E sensitizing can be supplied with Types I, II, III, IV, V, and 144 emulsions.

Astronomers have found these plates valuable in the photography of faint red stars, and they have been successfully used by spectroscopists for photographing weak lines in the red region of the spectrum.

*Additional information concerning photography in the H-alpha region will be supplied on request.*

**EASTMAN KODAK COMPANY**

***Research Laboratories*** **ROCHESTER, N. Y.**



# *Two Successful Physics Texts*

## DUFF
## Physics
**8th EDITION**

***(For Students in Science and Engineering)***

This text presents a sound and substantial treatment of the fundamentals of general physics for students of science and engineering. Now in its eighth edition, it is the mature work of experienced teachers.

*627 Illus.* *715 Pages.*
*Washable Fabric $4.00.*

By A. W. Duff (Editor), Worcester; F. A. Jenkins (Calif.); L. R. Ingersoll (Wisc.) and R. J. Stephenson (Chicago).

## FOLEY
## College Physics
**2d EDITION**

***(For Students in Liberal Arts)***

This book is giving exceptional satisfaction in over 350 colleges. It is characterized by clarity and forcefulness of presentation, an abundance of original illustrations and a carefully selected list of problems. There is a teacher's handbook.

*466 Illus.* *777 Pages.*
*Washable Fabric $3.75.*

By Arthur L. Foley, Ph.D., Indiana University.

**P. Blakiston's Son & Co., Inc., Philadelphia**

*Standard or Experimental*

# RESISTORS

**ALL TYPES · ALL SHAPES · ALL SIZES**

Common resistor types made to uniformly high standards of quality . . . or special resistors for unusual applications . . . whatever the resistance units you need IRC can supply them. The following bulletins detailing various IRC resistance types are available upon request:

☐ BULLETIN No. 1—Volume Controls and Potentiometers.

☐ BULLETIN No. 2—Metallized Type Resistors. Insulated ½, 1 and 2 Watts; High Frequency; High Range; High Frequency Power and High Voltage Power Resistors.

☐ BULLETIN No. 3—Insulated Wire Wound Resistors. Type BW from ½ to 1 and 2 Watts. Type MW 5 to 20 Watts, 6 std. sizes, any needed combinations.

☐ BULLETIN No. 4—Power Wire Wound Resistors. Types from 10 to 200 Watts, fixed and adjustable types, all mountings. Precision units, 14 types, 1/10 of 1% accuracy.

☐ BULLETIN No. 5—Attenuators.

☐ BULLETIN No. 6—Power Rheostats.

**INTERNATIONAL RESISTANCE CO.**

419 N. Broad St., Philadelphia, Pa.

IRC

*New* **SENSITIVE ELECTRONIC AC VOLTMETER**

*Ideal for Research and Teaching*

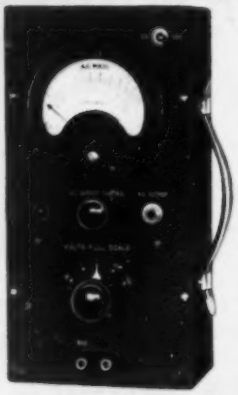

10 to 100,000 cycles

Range .001 to 100 volts

Logarithmic scale

AC or DC operated models

Stable calibration

Accurate and compact

Operating on a new principle—capable of reading down to one millivolt and up to 100 volts (or 1,000 volts with multiplier) over an extremely wide frequency range with an overall accuracy of 2 percent—single (logarithmic) scale to read for all ranges—unaffected by changes in line voltage or tubes—can also be used as an amplifier (70 DB gain), flat to 100,000 cycles.

*Send for Bulletin 2H*

Ballantine Laboratories, Inc.

BOONTON NEW JERSEY

**TYPE S POTENTIOMETER**

An accurate and inexpensive laboratory potentiometer suitable for all measurements of potential difference and for student instruction in the potentiometer method. Two ranges—1.6 volts and 16 M.V. Coils are accurate to within 1/20 per cent. Price seventy-five dollars.

ASK FOR BULLETIN 270.

**RUBICON COMPANY**

*Electrical Instrument Makers*

29 N. SIXTH STREET PHILADELPHIA, PA.